A Coupled Stress-Flow Numerical Modelling Methodology for Identifying Pore-pressure Changes due to Total Soil Moisture Loading

A Thesis
Submitted to the College of Graduate Studies and Research
in Partial Fulfilment of the Requirements
for the
Degree of Master of Science
in the Department of Civil and Geological Engineering
University of Saskatchewan
Saskatoon

by
Collins Ifeanyichukwu Anochikwa

PERMISSION TO USE

The author has agreed that the library, University of Saskatchewan, may make this thesis freely available for inspection. Moreover, the author has agreed that permission for extensive copying of this thesis for scholarly purposes may be granted by the professors who supervised the thesis work recorded herein or, in their absence, by the head of the Department or the Dean of the College in which the thesis work was done. It is understood that due recognition will be given to the author of this thesis and to the University of Saskatchewan in any use of the material in this thesis. Copying or publication or any other use of the thesis for financial gain without approval by the University of Saskatchewan and the author's written permission is prohibited.

Requests for permission to copy or to make any other use of material in this thesis in whole or part should be addressed to:

Head of Department of Civil and Geological Engineering
University of Saskatchewan
Engineering Building
57 Campus Drive
Saskatoon, Saskatchewan
Canada, S7N 5A9

ABSTRACT

This thesis describes a numerical modelling methodology to interpret dynamic fluctuations in pore-pressures to isolate the effects of loading associated with changes in total soil moisture (site water balance) alone. The methodology is required to enhance the data-interpretation and performance-assessment for potential applications of a novel piezometer-based, large-scale, geological weighing lysimeter. This interpretative methodology is based on a method of superimposing computer-based numerical analyses of independent causes of pore-pressure transients to separate the different pore-pressure responses. Finite element coupled load-deformation and seepage numerical models were used to simulate field-observed piezometric responses to water table fluctuations and loading induced by surface water balance (using meteorological data).

Transient pore-pressures in a deep clay-till-aquitard arising from variations in the water table within a surface-aquifer were modelled and removed from the measured pore-pressure record (corrected for earth tide and barometric effects) to isolate and identify pore-pressure fluctuations arising from loading associated with site water balance. These estimates were compared to simulated pore-pressure responses to an independently measured water balance using meteorological instrumentation. The simulations and observations of the pore-pressure responses to surface water balance were in good agreement over the "dry" years of a 9-year period. Some periods of significant differences did occur during "wet" years in which runoff, which is not accounted for in the current analyses, may have occurred.

The identification of pore-pressure response to total soil moisture loading using the developed numerical modelling methodology enhances the potential for the deployment of the piezometer-based geological weighing lysimeter for different applications which include real-time monitoring of site water balance and hydrological events such as precipitation and flooding. Interestingly, the disparity occurring during the "wet" years even suggests the potential to adapt the method to monitor runoff (net lateral flow).

The methodology also demonstrated the capability to accurately estimate in situ elastic and hydraulic parameters. Calibration of the model yielded "equivalent" properties of the aquitard (hydraulic conductivity, K_v, of 2.1 x 10^{-5} m/day and specific storage, S_s, of 1.36 x 10^{-5} m^{-1}) for a Skempton's $\bar{B}$ coefficient of 0.91 for an assumed porosity of 0.26. Sensitivity tests also provided insight into the consolidation and pressure propagation (swelling) behaviour of the aquitard under parametric variations. The parameters obtained are consistent with range of values reported for glacial clay till soil. Therefore, this work also provides a unique case history of a method for determining, large scale, in situ material properties for geo-engineers and scientists to explore by simply using piezometric and meteorological data.

ACKNOWLEDGEMENT

I am glad to acknowledge the people and organisations whose assistance and encouragement led to the successful completion of the research work reported in this thesis.

I proclaim my profound gratitude to Adjunct Professor (Doctor) Garth van der Kamp and Professor S. Lee Barbour, my supervisors, for the invaluable time and effort they invested in this work. This great pair provided such exemplary advisory and encouragement that I would gladly wish for a replay of our working together again. They provided freedom, cordial and intellectually stimulating atmosphere while providing direction and advice critical to the successful completion of this research work. Their advisory spanned through identification of the research problem, theory, conceptualisation, numerical modelling and concise technical writing. I am grateful to Doctor Garth van der Kamp for our discussions on the site data, theory, especially on the design of the boundary conditions and the associated assumptions, the hydrogeology and numerical modelling. I am also thankful to Professor S. Lee Barbour for shedding a lot light on "numerical modelling process" and the effective implementation of the numerical modelling of the hydrogeology problem with the geotechnical engineering analysis tool, coupled SIGMA/W and SEEP/W; in addition, his guest-lecture at the GEOSLOPE's Geotechnical Modelling Workshop – fundamentals, theory and application, at Banff in 2007, became beneficial in this work.

Constructive feedbacks provided by the members of my Graduate Advisory Committee contributed to the successful completion and quality of this work. I am therefore grateful to the members of my advisory committee: Professor Malcolm Reeves and Doctor Lal Samarasekera as well as Doctor Chris Hawkes, the Chairman of the committee. I am also thankful to Professor Moir Haug, the Chairman in the final session and Doctor Rashid Bashir, the external examiner.

The financial assistance provided by Dr. van der Kamp, through the Canadian Foundation for Climatic and Atmospheric Sciences' (CFCAS) support to the Prairie Drought Research Initiative (DRI) for the funding of the research, and by Prof. S. Lee Barbour through the support of Natural Sciences and Engineering Research Council of Canada (NSERC) Discovery Funds are highly appreciated. I am also grateful for other scholarship funds received from the College of Engineering in/and University of Saskatchewan.

I also express my gratitude to Randy Schmidt of Environment Canada for his technical support and maintenance of the installations at the study site. He also helped with site data gathering. I also appreciate the correspondence on meteorological data with Erin Thompson whose Environment Canada team provided the required cooperation.

I am also grateful to the staff of Engineering Computer Centre for providing me technical support on my simulation systems. I am also thankful to the Department of Civil and Geological Engineering and the College of Engineering in/and the University of Saskatchewan for providing me functional facilities and tools required for the research. The continuous and prompt help from the Library staff in the University of Saskatchewan is greatly appreciated.

The kind technical assistance of Professor John Krahn, Doctor Curtis Kelln and the staff of GEOSLOPE International Limited on effective implementation of hydrogeology simulation with the geotechnical engineering numerical modelling software is greatly appreciated. Prof. Barbour maintained this collaboration-corridor in this research work.

I am also thankful to my family, friends and colleagues whose kindness and continuous encouragement helped me keep focused on the target.

DEDICATION

My beloved parents: **Sir Cornelius O.N.** & **Lady Veronica N. Anochikwa**

TABLE OF CONTENTS

LIST OF TABLES

LIST OF FIGURES

LIST OF SYMBOLS AND ABBREVIATIONS

AET	Evapotranspiration (measured) expressed as accumulated height of water lost over a given period [LT^{-1}] (It is also interchanged with ET.)
AME	Absolute maximum error [L]
$\bar{B}$	Skempton's B-bar (pore-water pressure) coefficient [ ]
$\bar{B}\,\partial\sigma/\partial t$	Undrained pore-pressure response to the changes in surface mechanical loading [MLT^{-3}]
C_v	Terzaghi's coefficient of consolidation [L^2T^{-1}]
D	Hydraulic diffusivity [L^2T^{-1}]
Δz	Vertical displacement [L]
Δz_L	Vertical displacement in the case of load alone [L]
Δz_w	Vertical displacement in the case of water table fluctuation alone [L]
E	Drained Young's modulus [MLT^{-2}]
E_c	Drained constrained (or confined) elastic modulus [MLT^{-2}]
E_w	Elastic modulus of water [MLT^{-2}]
$1/E_w$	Compressibility of water [$M^{-1}L^{-1}T^2$]
g	Acceleration due to gravity [LT^{-2}]
h	Hydraulic head change [L] (It is used interchangeably with pore-pressure head change in piezometers, since piezometer are placed at fixed elevations.)
h_d	Longest drainage path of a domain (the same as the thickness of the aquitard domain of an impervious bottom and porous top boundaries) [L]
h_e,	Longest drainage path of typical elements close to the drainage boundary (also the element height) [L]
h_L	Hydraulic head change for the case of load alone [L] (It is used interchangeably with pore-pressure head change in piezometers, since piezometers are placed at fixed elevations.)
h_w	Hydraulic head change for the case of water table fluctuation alone [L] (It is used interchangeably with pore-pressure head change in piezometers, since piezometers are placed at fixed elevations.)

$h(t)$	Incremental hydraulic head changing with time [LT^{-1}]
K_v	Vertical hydraulic conductivity [LT^{-1}]
MAE	Mean absolute error [L]
m_v	Drained constrained (or confined) compressibility of the soil structure, also $1/E_c$, [$M^{-1}L^{-1}T^2$]
n	Porosity of the glacial till aquitard [ ]
v	Drained Poisson's ratio [ ]
OCR	Overconsolidation Ratio taken as the ratio of preconsolidation pressure to the existing effective overburden pressure (effective stress) [ ]
P	Precipitation expressed as height of water accumulated over a given period [LT^{-1}]
R	Runoff (net lateral flow gained or lost in the domain) expressed as cumulative height of water over a given period [LT^{-1}]
RMSE	Root mean squared error [L]
ρ_w	Density of water [ML^{-3}]
s_s	Specific storage [L^{-1}]
σ	Mechanical surface load (stress) [MLT^{-2}] or in terms of water head equivalent [L]
$\acute{\sigma}$	Effective stress [MLT^{-2}]
t	Time [T]
t_c	Characteristic time [T]
t_{ce}	Characteristic time of an element [T]
t_e	Initial "perceptible" drainage (reaction time) for an element [T]
t_i	Initial drainage time step applied in a simulation [T]
T_v	Dimensionless consolidation time factor [ ]
u	Incremental pore-pressure relative to a pre-existing background pore-pressure [MLT^{-2}] (In the case of aquitard piezometer (with sealed-in (non-vented) pressure transducer) it is the incremental pore-pressure corrected for barometric loading and earth tide. It is used interchangeably with hydraulic head change in piezometers, since piezometers are placed at fixed elevations.)

u_L	Incremental pore-pressure contributed by load changes relative to a pre-existing background pore-pressure [MLT^{-2}] (It is used interchangeably with hydraulic head change in piezometers, since piezometers are placed at fixed elevations.)
u_w	Incremental pore-pressure contributed by water table fluctuations relative to a pre-existing background pore-pressure [MLT^{-2}] (It is used interchangeably with hydraulic head change in piezometers, since piezometers are placed at fixed elevations.)
dP_a	Change in atmospheric pressure obtained from barometric data relative to a pre-existing reference atmospheric pressure [MLT^{-2}]
q_z	Water flux in the z-direction (i.e. volume of water flowing through cross a unit cross-sectional area perpendicular to the z-axis per unit time) [LT^{-1}]
q_{zL}	Water flux in the z-direction for the case of load alone (i.e. volume of water flowing through cross a unit cross-sectional area perpendicular to the z-axis per unit time) [LT^{-1}]
q_{zw}	Water flux in the z-direction for the case of water table fluctuation alone (i.e. volume of water flowing through cross a unit cross-sectional area perpendicular to the z-axis per unit time) [LT^{-1}]
du_{Pa}	Change in aquitard pore-pressure in response to barometric pressure change relative to a pre-existing background pore-pressure (also referred to as the barometric effect on the aquitard pore-pressure) [MLT^{-2}]
Y	Elevation measured as height above the base of the domain [L]
z	Depth below the top of the aquitard [L]
z_{max}	Depth of the bottom of the aquitard domain below the top of the aquitard [L]

1 CHAPTER 1 - INTRODUCTION

1.1 Background

Environment Canada is studying a new field technique for monitoring changes of total soil water balance by observing changes in pore-pressure that occur in response to the mechanical loading that is associated with the change in soil moisture. The ability to monitor soil water balance can provide uniquely useful information on climatic fluxes such as evapotranspiration. van der Kamp and Maathuis (1991) proposed this technique after observing water level fluctuations in deep confined aquifers induced by loading generated by changes of the overlying soil moisture. It is an advancement of the traditionally shallow installation of load cells beneath weighing lysimeters used to monitor small (m^2) scale soil water balance in hydrology. The innovation is the interpretation of observed pore-pressure dynamics in an aquitard to monitor water balance over much larger areas (hectare-scale) than the traditional weighing lysimeters and with minimal disturbance to site. Similar approaches of monitoring soil water balance using pore-pressure observations have been confirmed by a few other researchers around the globe (Bardsley and Campbell 1994; 2007; Sophocleous et al. 2006 and Marin et al. 2009).

This technique could be used to measure vertical moisture fluxes, precipitation and evapotranspiration; forecast floods in real time and verify hydrological models (van der Kamp and Maathuis 1991; Bardsley and Campbell 1994; Barr et al. 2000; van der Kamp et al. 2003; Marin et al. 2009). It could also be used for calibration of gravity.

measurements of soil water mass balance taken with satellites (Bardsley and Campbell 2000) and long-term climate-change studies. It could also provide continuous real-time monitoring of moisture-retention-performance of engineered soil covers over a large area from a single location.

In-situ measurements of pore-pressure made with highly sensitive piezometers have been used to monitor variations in the weight of water flowing into or out of the top zone of a soil profile at four sites in Canada for several years (van der Kamp et al. 2003). The pore-pressure responses of the piezometers at these sites were interpreted assuming that the whole geological formation responds as a large scale weighing lysimeter (van der Kamp and Schmidt 1997). The verification of this interpretation was obtained by measuring the pore-pressure response to a 39-tonne gravel-loaded truck used as a surface "point" load (Figure 1.1), using pressure transducer at the piezometer–tip.

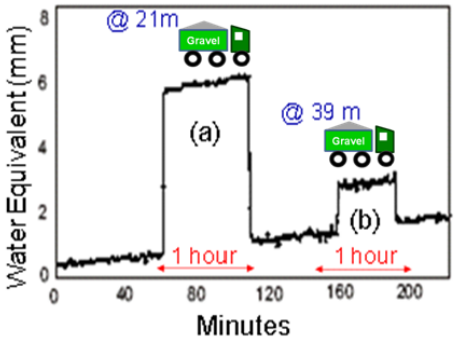

Figure 1.1. Observed Piezometric Response to 39-tonne Truck at: (a) 21m and (b) 39m distances (after van der Kamp and Schmidt (1997). Copyright 1997 by the American Geophysical Union. Modified by permission of American Geophysical Union)

The ideal geological setting for this "weighing lysimeter" method would be a thick, elastically compressible, low-permeability saturated formation (aquitard) in which there was insignificant drainage and no variations in pore-pressure as a result of changing groundwater flow conditions (van der Kamp and Schmidt 1997). This ideal condition, however, is not common and, therefore, the effects of transient groundwater flow due to dissipation of induced pore-pressures as well as changing boundary conditions (e.g.

water table fluctuations) must be considered in the interpretation of the measured pore-pressure (Barr et al. 2000).

Transient flow caused by changes in hydraulic head within a highly permeabile surface-units has been shown to complicate the interpretation of the "weighing lysimeter" pore-pressure responses (Barr et al. 2000). It was postulated that pore-pressure changes generated by water table fluctuations in an overlying aquifer contributed a significant part of the pore-pressure-changes observed in an underlying aquitard-piezometer.

The goal of this work is to establish a method of interpreting the pore-pressure dynamics for a geological weighing lysimeter when there are additional pore-pressure transients caused by groundwater flow transients. The general approach will be to superimpose numerical analyses of pore-pressure response due to surface mechanical loading cause by climatic fluxes and pore-pressure dynamics caused by water table fluctuations so as to allow the pore-pressure changes due to surface loading alone to be isolated. The stress and transient flow interaction in this problem was simulated using the coupled load-deformation and seepage finite element numerical models SIGMA/W and SEEP/W (GEOSLOPE 2007).

1.2 Objectives

The specific objectives of this study are as follows:

(i) Model the observed piezometric response in a confined aquitard due to total stress changes from mechanical surface loading and due to water table fluctuations using coupled finite element models of load-induced pore-pressure and transient flow;

(ii) Evaluate the contribution to observed pore-pressure changes that arise due to transient groundwater flow induced by water table fluctuation; and

(iii) Isolate the pore-pressure response in the aquitard due to mechanical surface loading alone, as associated with changes of total soil moisture.

1.3 Scope

This study involves geotechnical and hydrogeological numerical modelling and interpretation of piezometric data from a forest site in central Saskatchewan. The conceptual and numerical models are based on the following assumptions/considerations:

(i) The theory of one-dimensional consolidation with time-varying mechanical surface loading is applicable.
   - All stratigraphic units are assumed to be laterally extensive such that the one-dimensional analysis is applicable;

(ii) Infinitely extensive uniformly distributed mechanical surface loading in response to changes in soil moisture is occurring. This load type generates an instantaneous laterally uniform excess pore-pressure profile (e.g. Terzaghi and Frohlich 1936);

(iii) The soil can be described as a linear elastic isotropic fully-saturated soil ; and

(iv) The influence of the unsaturated soil that occurs near the ground surface (arising from rise and fall of the water table in an unconfined aquifer) can be excluded particularly as it relates to complex non-linear pore-pressure response and stress-strain behaviour which are both dependent on soil moisture content, as known in soil mechanics. This enables the use of method of superposition for the analysis of the fully saturated (linear elastic) underlying soil.

The limitations that may be important in the analysis and interpretation of results include:

(i.) Possible disparity between the estimate of mechanical loading due to meteorological water balance (model-input load) and observed soil water balance at the lysimeter-site; and

(ii.) Modelling the aquitard as an “equivalent” homogeneous material in spite of the potentially heterogeneous and possibly fractured nature of the formation.

A presentation and a paper in 2009 Canadian Geotechnical Conference Proceedings (Anochikwa et al. 2009) discussed some key preliminary results of this work.

2 CHAPTER 2 - LITERATURE REVIEW

2.1 Overview

Mechanical surface loading will produce an instantaneous change in pore water pressure at depths within a water-saturated soil profile, as known in soil mechanics and hydrogeology (e.g. Terzaghi and Frohlich 1936; Jacob 1940; Skempton 1954). The applied total stress is distributed to the water, as change in pore-pressure often referred to as excess pore-pressure, and to the soil skeleton, as the difference between the applied total stress and the pore-pressure, known as effective stress (Terzaghi 1923; Terzaghi 1925). Researchers have presented this phenomenon of pore-pressure response to mechanical loading of the soil profile (e.g. Terzaghi and Frohlich 1936; Jacob 1940; Skempton 1954; Bredehoeft 1967; van der Kamp and Gale 1983; Rojstaczer 1988; Rojstaczer and Agnew 1989).

Since soil is a compressible porous medium with interconnected pores linked to drainage boundaries, the instantaneous load-induced excess pore-pressures dissipate over time in a consolidation process (Terzaghi 1925). This transient flow process is also considered a form of pressure diffusion (van der Kamp and Gale 1983; Rojstaczer 1988) which controls both cases of transient pore-pressure propagation (e.g. van der Kamp and Maathuis 1991) and dissipation (Terzaghi 1925; Terzaghi and Frohlich 1936). Long term studies of pore-water-pressure and soil stress interaction have generally been carried out using transient flow analysis both in soil mechanics (e.g. Terzaghi 1925; Terzaghi and Frohlich 1936; Biot 1940; Vuez and Rahal 1998) and groundwater

hydraulics (e.g. van der Kamp and Gale 1983; Rojstaczer 1988; Rojstaczer and Agnew 1989). In order to successfully analyse a drained response to mechanical loading, the associated instantaneous excess pore-pressure needs to be accurately determined (Bishop 1954, 1973).

2.2 Instantaneous Pore-pressure Response to Surface Mechanical Load

Terzaghi and Frohlich (1936) presented initial (at time equal to zero) excess pore-pressure profiles, prior to consolidation, for various spatial distributions of surface load relative to soil thicknesses. They presented cases for excess pore-pressure profiles generated by laterally extensive (infinitely) distributed uniform surface loading and localised surface loads.

In the case of a laterally extensive uniform surface load Terzaghi and Frohlich (1936) considered the thickness of the loaded soil to be much smaller that the lateral extent of the distributed surface load resulting in the development of laterally uniform excess pore-pressures with depth. In a similar manner, hydrogeology researchers like Jacob (1940), van der Kamp and Gale (1983), Rojstaczer (1988), Rojstaczer and Agnew (1989) and Schulze et al. (2000) examined pore-pressure response to natural surface loading applying over large areas such as atmospheric pressure changes. In addition, pore-pressure has been observed to respond instantaneously to other natural aerially extensive loads such as that due to tidal straining of the ground due to earth tide (Bredehoeft 1967; van der Kamp and Gale 1983; Schulze et al. 2000). Recently, pore-pressure response to aerially extensive loading due to changes of soil moisture storage (water balance) has been investigated (van der Kamp and Maathuis 1991; van der Kamp and Schmidt 1997; van der Kamp et al. 2003; Bardsley and Campbell 1994, 2000, 2007; Sophocleous et al. 2006; Marin et al. 2009).

2.2.1 Mechanism and Observation of Instantaneous Pore-pressure Response

Skempton (1954) showed that undrained pore-pressure response to loading is generated in reaction to the straining of a saturated soil system. van der Kamp and Gale (1983) suggested that rapid drainage could still occur at the time of loading due to possible non-uniform excess pore-pressures induced at different locations arising from heterogeneous lithology or non-uniformly applied load. However, initial undrained pore-pressure response can be estimated in a given formation since the conditions of homogeneity (particularly of elastic properties) can often be assumed, even for a fractured heterogeneous formation, which has a permeable matrix, of low diffusivity (i.e. high consolidation reaction time) (van der Kamp and Gale 1983).

It is difficult to interpret pore-pressure response to loading using water levels in wells due to the numerous factors which might affect the magnitude and rate of the water level changes (e.g. Rojstaczer 1988). Rojstaczer (1988) investigated this option and noted the difficulties in observing undrained pore-pressure response due to complications associated with loading frequency, variable formation hydraulic properties and well-storage capacity. Sensitive (non-flow) piezometers, such as piezometers installed as sealed-in vibrating-wire transducers (e.g. Dunnicliff and Green 1993, p.128) are considered to be a better method of monitoring instantaneous pore-pressure response to loading (e.g. van der Kamp and Schmidt 1997; Barr et al. 2000) due to the rapid response and minimal flow volumes associated with these measurements.

2.2.2 Quantification of the Instantaneous Excess Pore-pressure

The magnitude of pore-pressure induced by surface loading has been estimated using a ratio of the pore-pressure response to applied surface load (Skempton 1954; Jacob 1940; van der Kamp and Gale 1983). That ratio is a constrained elastic pore-pressure coefficient known as Skempton's $\bar{B}$ (B-bar) coefficient (Skempton 1954) which is also

known as loading efficiency (van der Kamp and Gale 1983) or tidal efficiency (Jacob 1940). Skempton's observations were on laboratory soil samples while Jacob's and van der Kamp & Gale's formulations were for hydrogeological settings.

It is commonly assumed in geotechnical analyses, that the pore water pressure instantaneously bears the full loading pressures, as inferred from Terzaghi and Frohlich (1936) and Terzaghi (1943, p. 273). This is only true when the pore-water is considered incompressible relative to a more highly compressible soil structure and results in Skempton's $\bar{B}$ (Skempton 1954) of approximately 1. However, it has been demonstrated that for stiff, heavily overconsolidated formations Skempton's $\bar{B}$ (as well as unconstrained pore-pressure) coefficient drops below unity. This occurs when the stiffness of the soil skeleton becomes similar to that of water (e.g. van der Kamp and Gale 1983; Bishop 1973; Terzaghi 1996, pp 87-88).

2.3 Weighing Lysimeter-Interpretations of Pore-pressure Changes

The use of large scale weighing lysimeters using piezometers was pioneered by van der Kamp and Maathuis (1991). They theoretically proved that observed pore-pressure changes in deep confined aquifers were predominantly due to mechanical loading rather than seasonal recharge. Subsequently, similar monitoring of soil water balance using pore-pressure-observations have been reported by others: in aquitards (van der Kamp and Schmidt 1997; Barr et al. 2000; and van der Kamp et al. 2003) in Canada and in aquifers in New Zealand (Bardsley and Campbell 1994, 2006) and the USA (Sophocleous et al. 2006). Though response to soil moisture changes were observable in both aquitards and aquifers, aquitards were considered more suitable for the observation because of their relative hydraulic isolation from interference arising from changing groundwater flow conditions (van der Kamp and Schmidt 1997; Bardsley and Campbell 2000).

van der Kamp and Maathuis (1991) observed that confined aquifer formations behave like giant but complex weighing lysimeters when the pore-pressure response to surface loading was interpreted by considering stress, strain and pore-fluid pressure interaction. The surface load and formation were assumed to be laterally extensive such that the formation only deforms vertically with flow occurring only in the vertical direction. Elastic response to loading was assumed as in Jacob's (1940) work. In the analysis of piezometric measurements in aquitards earth tide determined by earth tide theory and barometric effects (van der Kamp and Gale 1983) had to be eliminated prior to the interpretation of the pore-pressure changes (van der Kamp and Schmidt 1997; Barr et al. 2000). They explicitly recognised the effect that transient flow induced by changes in boundary conditions, such as water table fluctuations, might have on the interpretation of the pore-pressure responses. However, these transient pore-pressure effects were not rigorously eliminated in the "weighing lysimeter" interpretation.

Bardsley and Campbell (1994, 2000, 2007) made observations of pore-pressure responses to changes of soil moisture storage in confined aquifers in New Zealand. They made their "weighing lysimeter" observations using a pair of laterally adjacent (nested) piezometers installed in two vertically separated aquifers. The changes of soil moisture storage was first interpreted by static (undrained) analysis of separate piezometric data set taken at hourly intervals, corrected only for barometric effects (Bardsley and Campbell 1994). Subsequently, they estimated changes of soil moisture assuming undrained conditions. They applied the analysis using a simultaneous expression for the duplicate piezometric data that corrected for barometric pressure fluctuations and earth tide (Bardsley and Campbell, 2007). They did not explicitly eliminate the contribution of transient pore-pressure phenomenon, ("dynamic effects"), but suggested that simultaneously obtaining similar piezometric responses from the different formations minimises the risk of misinterpreting the loading response in the presence of transient flow-induced pore-pressure changes. However, they did not provide any rigorous

approach for eliminating transient effects in geological settings which are not as ideal as their study site.

Sophocleous et al. (2006) observed pore-pressure responses to rainfall events in a 300 m deep well. The loading responses were interpreted using different methods of processing pore-pressure data as static response. They mainly considered undrained pore-pressure response of an elastic aquifer. Their data set was corrected for barometric effects and for earth tides using a wavelet filtering technique. Similar to Bardsley and Campbell's (1994, 2000, 2007) approach, they did not apply any rigorous approach for eliminating the effect of transient flow in the interpretation.

2.4 Treatment of Transient Flow Effects with Consolidation Theory

The phenomena of transient pore-water pressure change and effective stress change in saturated porous geological formations, known as consolidation, have been described by early researchers like Terzaghi (1925) and Biot (1941). Terzaghi (1925) developed consolidation theory for the case of a constant applied load (zero total stress change) on a laterally constrained saturated soil system allowing only one-dimensional vertical deformation and flow. Biot (1941) generalized the theory to include the case of arbitrarily time-varying load on unconstrained soil systems which permits free deformation and flow in three dimensions.

van der Kamp and Maathuis (1991) described observed pore-pressure responses to changes of total soil moisture with a one-dimensional consolidation equation with time-varying surface mechanical load, as presented by van der Kamp and Gale (1983). The mathematical model describing the physical problem is in the form of a partial differential equation. Observed pore-pressures in deep confined aquifers at any given time were assumed to be due to an undrained response to instantaneous loading, combined with overlapping transient pore-pressure changes due to earlier events such as

water table fluctuations and the drainage response to loading history. These latter events were assumed to precede the time of interest. They discussed the delay and attenuation of the water table fluctuation propagated downward while considering the effect of consolidation drainage from loading as negligible.

The magnitude of the vertically propagated transient pore-pressure associated with water table fluctuation due to recharge (or discharge), gets attenuated exponentially with depth (van der Kamp and Maathuis 1991). Due to this damping of the water table fluctuations within confining formations of high thickness and low diffusivity it was proposed that piezometric installations in deep confined formations be used for lysimeter observations (van der Kamp and Maathuis 1991; van der Kamp and Schmidt 1997). However, consolidation theory must be applied to explicitly deal with the effect of water table fluctuations on the "lysimeter" observation, especially where confining formations are less ideal (i.e. more permeable than the underlying formation) (Barr et al. 2000).

2.5 Numerical Modelling for Rigorous Analysis of the Transient Flow Effects

The need to rigorously treat the effects of transient flow of groundwater to refine the interpretation of the weighing–lysimeter-observations had been identified in an earlier attempt (Barr et.al. 2000). The use of numerical models is generally recommended for the analysis of potentially complex systems in hydrogeology (e.g. Mercer and Faust 1981, p.7). It offers flexibility and less restrictive assumptions than typical analytical approaches (Wang and Anderson 1982, p.3; Istok 1989, p.9). With the aid of a numerical model many simulations and sensitivity analyses can be carried out for different conceptual stratigraphic models with dynamic boundary conditions (e.g. Istok 1989, p.9) using a large amount (e.g. thousands) of time steps. Consequently, finite element numerical models (SIGMA/W and SEEP/W (Geoslope 2007, 2008)) were selected for the numerical modelling in this research.

3 CHAPTER 3 – SITE CONDITION AND FIELD OBSERVATIONS

3.1 Introduction

The field observations were gathered by Environment Canada, are not part of this project as such, but provide a basis for the numerical modelling. The location of the installations on the study site along with the description of the geology and hydrogeology of the site as well as the instrumentations and the key observed data are presented in this chapter.

3.2 Study Site Location

The measured pore-pressure responses were from a piezometer-based "geological weighing lysimeter" installation near the Old Aspen Fluxnet-Canada flux tower site of the Boreal Ecosystem Research and Monitoring Sites (BERMS) area, in the southern part of Prince Albert National Park, Saskatchewan, Canada, geographically located at 53.7^{o}N, 106.2^{o}W (Black et al. 1996; Barr et al. 2000). The piezometric installation (weighing lysimeter) site is located at 53.63^{o}N, 106.18^{o}W. The eddy flux tower and climate station are located 1.3km away from the weighing lysimeter site at 53.63^{o}N, 106.2^{o}W (Fluxnet-Canada website). The location of the piezometric installations used for "weighing lysimeter" observations are shown relative to the position of the Fluxnet-Canada's eddy flux tower in Figure 3.1.

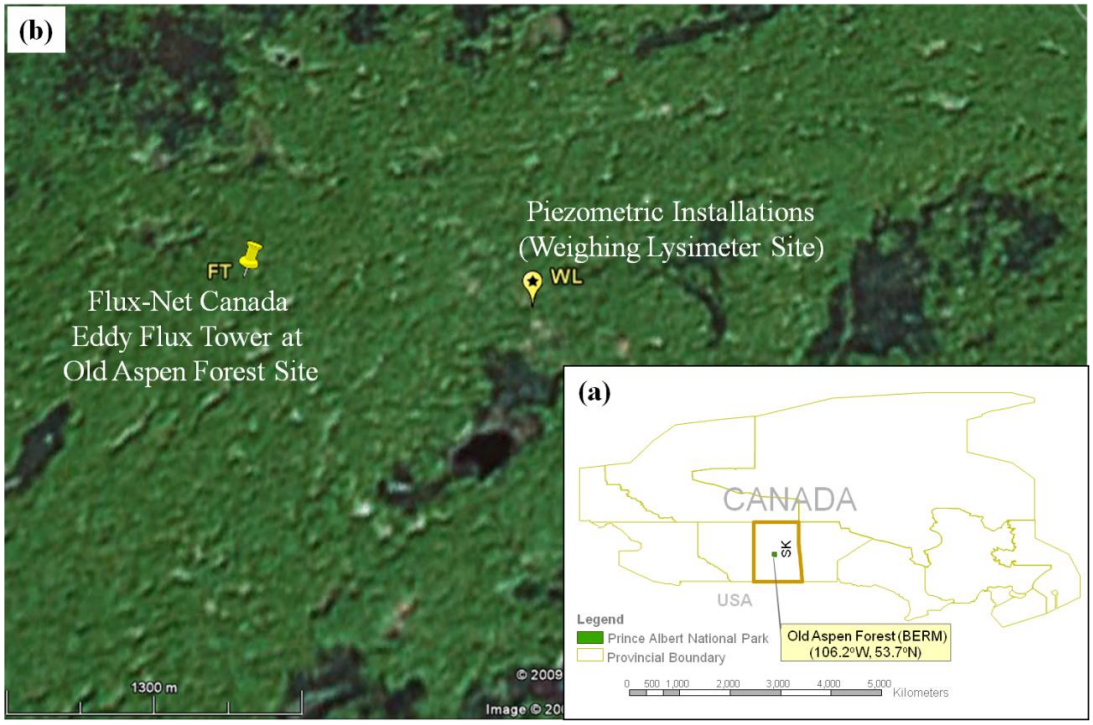

Figure 3.1. (a) Location of Old Aspen Forest at the Southern Prince Albert National Park, Saskatchewan (SK) (Source: Adapted from DMTI CanMap® Parks & Recreation v2008.3 – Saskatchewan, using ArcGis); and (b) Piezometric installations (geological weighing lysimeter) and Fluxnet-Canada's eddy flux tower sites (Google Earth: ©2009 Google, Image © 2009 TerraMetrics, © 2009 Tele Atlas, Image © 2009 DigitalGlobe)

3.3 Site Condition and Installations

3.3.1 Site Geology and Hydrogeology

The site-geological profile comprises a 20m-thick surface layer of gravel and sand with some layers of silt, which overlies a clay till extending to a depth of at least 42m (site construction information from Environment Canada; see Appendix A for the log of stratigraphic boreholes drilled at the site). On striking what might have been a boulder, drilling met with refusal around this depth. The glacial till deposit in the site is estimated to be up to 100m thick and comprises a Sutherland group till underlying a Saskatoon group till (Christiansen 1968, 1992; Millard 1994). The entire sequence of till deposits overlies Cretaceous shale (Millard 1994; Christiansen 1973). The depth to the water

table in the upper aquifer (sand and gravel with some silt) averages 3m to 4m below ground level (Barr et al. 2000). The water table elevation fluctuated by as much as 2.3m over a nine-year period.

The larger scale (regional) geologic context of the site was established by reviewing information on geological cross-sections and reports for the Shellbrook and Prince Albert areas. This information was obtained from the Saskatchewan Research Council's geology and groundwater resource maps and reports through Saskatchewan Watershed Authority (SWA) (www.swa.ca/WaterManagement/Groundwater.asp). On a regional scale, the glacial till is predominantly a Saskatoon group till overlying a Sutherland group till. In the Prince Albert area (73H) the Saskatoon group till and Sutherland group till may be as thick as 25m to 165m and 0 to 80m, respectively. In the Shellbrook area (73G) the thickness of these units may vary from 20m to 145m and 15m to 130m, respectively (Millard, 1990; Millard, 1994; Christiansen, E.A. 1973; Christiansen, E.A. 1975). Millard (1994) suggested that the till is generally underlain by Empress Group (stratified sand, gravel, silt and clay) at depths exceeding 120m or by the clay-rich bedrock (Lower Colorado group-Ashville formation and Upper Colorado group-Lea Park formation). The Saskatoon and Sutherland group tills could comprise other till formations in their stratigraphy (Christiansen 1968, 1992). The underlying Sutherland group till is generally stiffer and more clayey than the Saskatoon group till (Millard, 1994). There could also be some thin extensive intertill sand aquifers within 60m and beyond 75m depths (Millard, 1994).

Glacial till in Saskatchewan typically has a low hydraulic conductivity of about 10^{-11} to 10^{-8} m/s (Keller et al. 1986, 1988, 1989; Shaw and Hendry 1998). Fractures and oxidised (weathered) zones may be present in these tills and these increase the hydraulic conductivity by as much as two or more orders of magnitude over that of the unfractured matrix (Grisak and Cherry 1975; Keller et al. 1986, 1989; Shaw and Hendry 1998). Table 3.1 shows some reported values of properties of glacial till in some prairie areas of Canada.

Table 3.1. Reported Properties of Glacial Till in Saskatchewan Area (and Alberta)

#	Category of Geotechnical Property	Property	Value	Reference
1.	Composition[1]	Sand Content	39 ± 4.1%	Shaw and Hendry (1998)
		Silt Content	26.3 ± 1.9%	
		Clay Content	34.7 ± 3.7%	
2.	Some Index Properties	Dry Density	1870 kg/m^3	Shaw and Hendry (1998)
		Bulk Density	2170 kg/m^3	
3.	Mechanical Properties	Pre-consolidation Pressure	Average 1800±200 kPa (Range 1200 - 2300kPa)	Sauer et al. (1993)
		OCR[2]	4 – 7 (Floral Till) 7 – 8 (Warman till)	Sauer et al. (1993)
		In situ Modulus of Elasticity, E	496 – 1475MPa (72,000 – 214,000 psi)	Klohn (1965)
			100 – 1387MPa	Matheson et al. (1987)
			207 – 723MPa	DeJong and Harris (1971)[3]
		Porosity	0.26 – 0.36	Keller et al. (1986; 1988)
			0.29 – 0.32	Shaw and Hendry (1998); Sauer et al. (1993)
4.	Hydraulic Properties	Hydraulic Conductivity (generally for glacial till in Saskatchewan)	10^{-11} – 10^{-8} m/s	Keller et al. (1986,1988,1989); Shaw and Hendry (1998)
		Hydraulic Conductivity (fractured till – weathered or unweathered)	10^{-8} m/s ($5x10^{-9}$ m/s)	Keller et al. (1988)
		Hydraulic Conductivity (unoxidised/ unweathered, unfractured till)	10^{-10} m/s ($5x10^{-11}$ m/s)	Keller et al. (1986, 1988)
		Hydraulic Conductivity (fractured weathered till in Alberta)	10^{-9} – 10^{-7} m/s ($5x10^{-9}$ – $2x10^{-7}$ m/s)	Hendry (1982)

[1] The till, for which sample composition was presented, was reported to be of plastic behaviour
[2] Obtained using effective stress and preconsolidation pressure profiles in the source literature
[3] Determined from observation of settlement of building-foundation over a range of contact pressures at a site in Alberta

3.3.2 Field Instrumentation and Operation

3.3.2.1 Piezometer-Installations

Two sensitive non-vented, 50psi, Geokon 4500H vibrating-wire pressure transducers were installed in the piezometers in this research (Figure 3.2). The pressure transducers have a resolution of less than 1 mm-water (Table 3.2). A rotary drilling rig was used to drill to a depth of 34.6 m where the deep (aquitard) transducer was placed within a meter-long cavity filled with saturated sand. The second pressure transducer was hung in an open standpipe piezometer completed at the depth of 6.26m, within the surficial sand and gravel aquifer, to monitor water table fluctuations. Figure 3.3 shows the site profile and piezometric installations. Two other pressure transducers were placed in an accessible shallow (9m deep) pit and each connected to an oil-filled tube tapping into deep sand cavity at the depth of 34.6m (Barr et al. 2000).

Figure 3.2. Sample of Geokon pressure transducer (Source: *http://www.geokon.com/products/datasheets/4500.pdf*)

Table 3.2. Key Specifications of the pressure transducers installed in the Old Aspen Forest Site (adapted from: Barr et al. (2000), information from van der Kamp (2009) and Geokon (2008) http://www.geokon.com/products/datasheets/4500.pdf)

Transducer	Model	Full Scale Range	Quoted Resolution	Observed[4] Resolution	Temperature Range	Thermal Zero Drift	Length x Diameter
		(kPa)	(kPa)	(kPa)	(^{o}C)	(kPa/^{o}C)	(mm)
Aquitard Piezometer	Geokon 4500H	350	0.086 (8.8mm)[5]	< 0.001 (<1mm)	-20 to 80	0.18	140 x 25.4
Water table (aquifer) Piezometer	Geokon 4500H	350	0.086 (8.8mm)	< 0.001 (<1mm)	-20 to 80	0.18	140 x 25.4

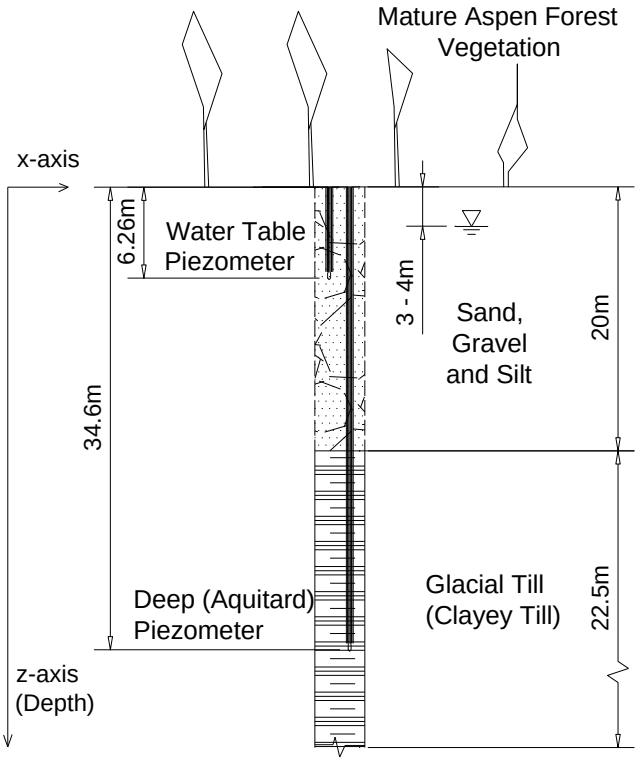

Figure 3.3: Profile of geology and hydrogeology and the two piezometric installations in the Old Aspen Forest Site up to depth where drilling met refusal on a boulder

Sealed-in transducers are preferred for real-time "lysimeter" observations over open stand-pipe piezometers since the latter are subject to pipe-geometry related hydrodynamic time-lag, particularly when used in such low permeability formations

[4] Observed response of the installed piezometer by van der Kamp
[5] Linear dimensions (mm) for pressure resolutions are water head equivalents of the pressure

(e.g. glacial till) (Dunnicliff and Green 1993, p 139). The sensitive of the vibrating-wire pressure transducers derive from the sensitively flexible diaphragms which deform under the applied pore water pressure and this deformation changes the tension in a vibrating wire. The frequency of vibration of this wire is then captured electronically to produce an equivalent pressure signal (Geokon Inc. 1996; Dunnicliff and Green 1993, pp 102, 127).

In long term observations, vibrating wire pressure transducers may experience creep of the tensioned vibrating wire termed "zero-drift", which may adversely affect the consistency and accuracy of the measurements taken with the pressure transducer (Dunnicliff and Green 1993, pp 104, 128). Multiple transducers for the same elevation would allow long term "zero-drift" errors to be monitored under the assumption that drift would not occur uniformly in all piezometers. Consistent long-term adjacent measurements of pore-pressure would mean that the vibrating wire transducers are stable. Two additional near-surface (9.6m-deep) vibrating wire pressure transducers were installed with oil-filled tubes connecting them to the completion depth (34.6m) of the aquitard piezometer. These piezometers were installed to provide higher resolutions of pore-pressure measurements (Barr et al. 2000), but also served as a check of zero-drift. The buried aquitard pressure transducer was assumed to be stable over the study period. The other two near-surface pressure transducers, which may be slightly subject to weather conditions, will have to be re-calibrated to validate the stability of the buried pressure transducer.

3.3.2.2 Meteorological Installations (Eddy Correlation Instrument, Precipitation Gauges and Barometer)

The presence of a flux tower and climate station located 1.3km away from the piezometric installations was the key attraction for selecting the study area (Barr et al. 2000). Precipitation (P) and actual evapotranspiration (AET) measured at this station

provided the data for the site water balance used for model comparison. The data from the following meteorological instruments were used in this study:

i. *Precipitation Gauges:* P was measured using a Belfort 5915 accumulation gauge for year round measurement and a Texas Electronics TE525M tipping bucket rain gauge for spring and summer rainfall (Barr et al. 2000). In order to ensure accuracy of the precipitation measurements, motor oil (film) was used in the accumulation gauge to minimise water losses to evaporation and optimal snow catch efficiency was achieved by placing the gauges in the centre of an open space in the forest with a diameter of approximately one tree height (Barr et al. 2000). Figure 3.4 shows a climate station bearing a precipitation gauge at Old Aspen Forest site.

Figure 3.4. Climate station bearing a precipitation gauge at Old Aspen Forest site

ii. *Eddy Correlation Instruments:* AET was measured using an eddy correlation instrument mounted on an eddy flux tower (Figure 3.5) 39.5m above ground level over the 21m-tall Aspen forest stand (Black et al. 1996). This device uses a three-dimensional sonic anemometer-thermometer device to capture the fluxes (Black et al. 1996). Closed-path infra-red gas (IRGA) analysers measured fluctuations in water vapour (and CO_2) (Black et al. 1996). This technique of monitoring water vapour fluxes (ET) operates by measuring wind speed, temperature and humidity and

correlating the water vapour transport to the vertical covariant (eddy) wind velocity transporting them (Fluxnet-Canada 2005). Other supplementary instruments such as hygrometer, and air-temperature thermocouples and thermometers were also installed at the site and the details can be found in Black et al. (1996).

Figure 3.5. Fluxnet-Canada's eddy flux tower bearing the eddy correlation instrument at Old Aspen Forest Site Prince Albert National Park, Saskatchewan

iii. *Barometer:* A Setra barometer was also installed in a temperature-regulated shelter near the flux tower (Barr et al. 2000). It measures barometric (atmospheric) pressure which is used to evaluate barometric response within the deep piezometer (Jacob 1940; van der Kamp 2001). These were used to correct the barometric pressure-change effects in the piezometric data and determine the elastic pore-pressure coefficient (elastic properties) of the aquitard simultaneously (van der Kamp 2001).

Measurements from each of the piezometers and meteorological instruments at the site were continuously logged at high frequency, in every 30 minutes. The data logger for the piezometer samples every 30seconds and then averages the reading every 30minutes (Barr et al. 2000). Data was then accumulated to a daily time scale over a 9-year period (1998-2006) for this study. Piezometric and meteorological data logged over the same time was required for the numerical modelling. However, the time stamp for the piezometric data was Central Standard Time (CST) while meteorological data were

collected on a Universal Standard Time (UST). This introduced a 6-hour lag between the two daily data sets taken at midnight but it did not have significant effects on the results.

3.4 Precipitation- and Evapotranspiration-Observations

The daily accumulation of precipitation and evapotranspiration monitored at the site were used to generate the daily meteorological water balance (P – AET). The 9-year accumulation of the daily water balance (Figure 3.6) served as input for generating stress boundary condition in the numerical modelling discussed in the subsequent chapters.

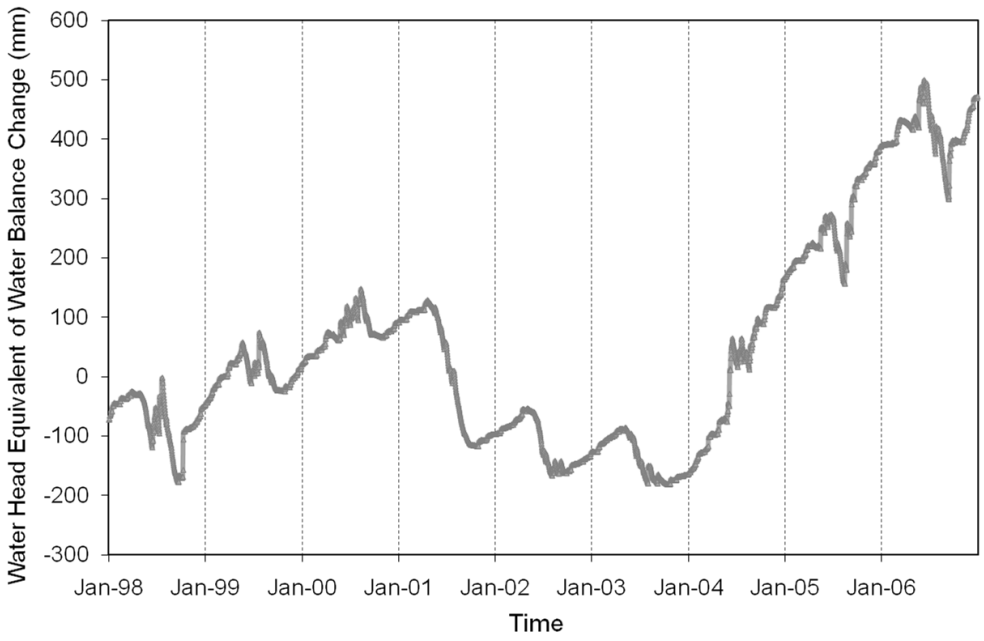

Figure 3.6. Observed cumulative meteorological water balance (P–AET) for generating a stress boundary condition for numerical modelling of Old Aspen Site (1998 – 2006)

3.5 Observed Water Table Fluctuations

The daily fluctuations of water table elevation observed with the water table (aquifer) piezometer were corrected for barometric effect by deducting the full barometric

pressure variations sensed by the non-vented vibrating wire pressure transducer hung in the open piezometer. The 9-year daily fluctuations in water table elevation cleaned of barometric effects are shown in Figure 3.7. This data set served as input for generating a hydraulic boundary conditions in the numerical modelling explained in the subsequent chapters.

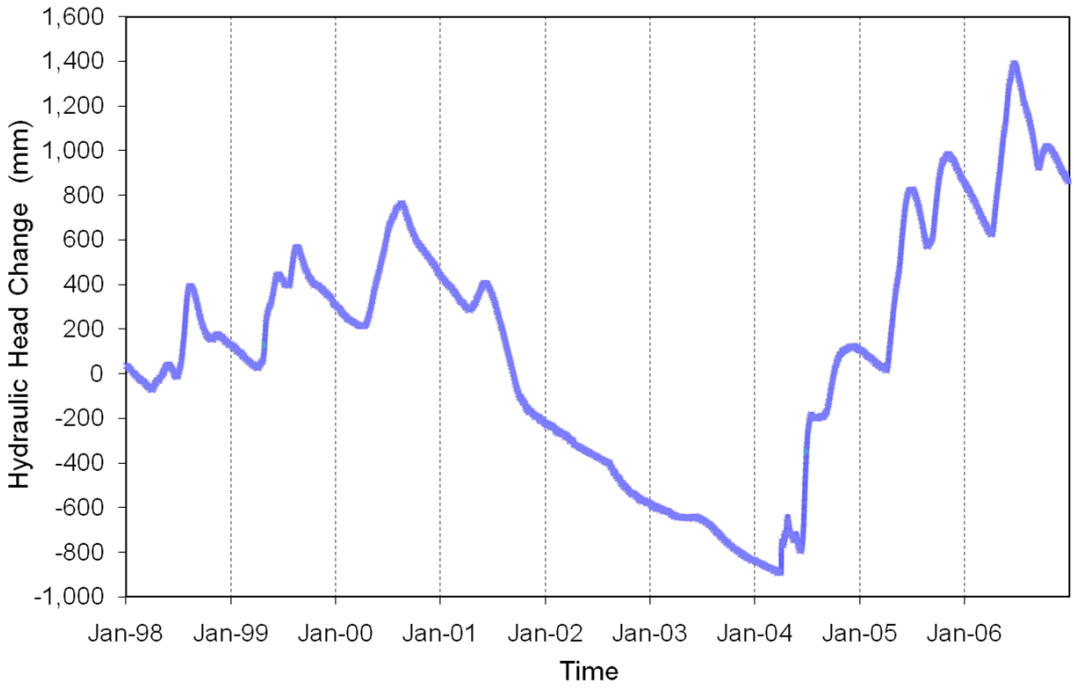

Figure 3.7. Observed water table fluctuations for generating hydraulic boundary condition for the numerical modelling Old Aspen Site problem (1998 – 2006)

3.6 Aquitard-Piezometer-Observations

3.6.1 Observed Elastic Response and Processing of Site Pore-pressure Data

The pore-pressure-time records from the aquitard-piezometer also include responses to barometric pressure fluctuations and periodic earth-tide-dilation of the earth-crust (Jacob 1940; Bredehoeft 1967; van der Kamp and Gale 1983; Rojstacjer and Agnew 1989). Skempton's $\bar{B}$ elastic pore-pressure coefficient was determined through the correction

for effect of the barometric loading after correcting for earth tide (e.g. Barr et al. 2000). Figure 3.8 illustrates the barometric correction on the data set (see Appendix B for details of the barometric correction).

Before using the piezometric data for modelling, some identified data gaps and abnormal spikes at various short time periods were filled and smoothed, respectively. Simple linear functions were used to bridge the gaps and spikes at the various spots they occurred. A total of 145 days of data gap spread throughout the 9-year- (3,286 day-) period were filled. These adjustments were made on both the aquifer- and aquitard-piezometric data to ensure realistic data trends and continuous time stepping for the 9-year modelling period to minimise data related errors in the modelling and calibration.

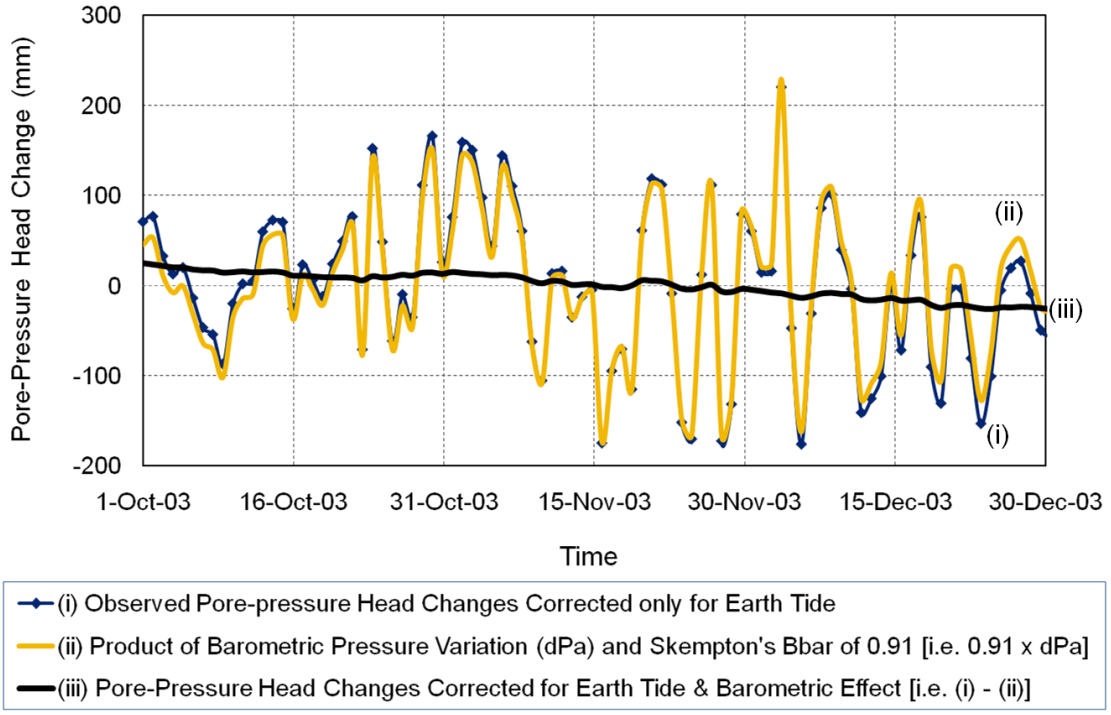

Figure 3.8. Barometric effect and its correction on pore-pressure head changes from which Skempton's $\bar{B}$ (B-bar) of 0.91 was determined (at the depth of 34.6m for Old Aspen Site): (i) Observed pore-pressure head changes corrected only for earth tide; (ii) Observed barometric pressure head change x 0.91; and (iii) Pore-pressure head changes corrected for earth tide minus observed barometric pressure head change x 0.91 [i.e. (i) – (ii)]

3.6.2 Observed Aquitard-Piezometer Hydraulic Head Changes

The 9-year daily hydraulic (pore-pressure) head changes observed with the aquitard-piezometer which were corrected for earth tide and barometric loading are shown in Figure 3.9. It is also represents the response of the aquitard-piezometer to fluctuations in water table elevation and loading by variation in site water balance (total soil moisture). A comparison of the trend and magnitude of these aquitard piezometric observations (Figure 3.9) and the proposed input signals (i.e. accumulation of meteorological water balance (Figure 3.6) and water table fluctuations (Figure 3.7)), combined as Figure 3.10, suggests that the influence of the water table appears to dominate the hydraulic head changes recorded in the deep aquitard-piezometer. This observation served as a basis for postulating that the contribution of the transient flow propagated to the aquitard by the water table fluctuation had a significant effect on the measured head changes in aquitard-piezometer. This data set (Figure 3.9) served for calibration of the model and the calculation of the key research variable, response of aquitard-piezometer to the change in total soil moisture (site water balance).

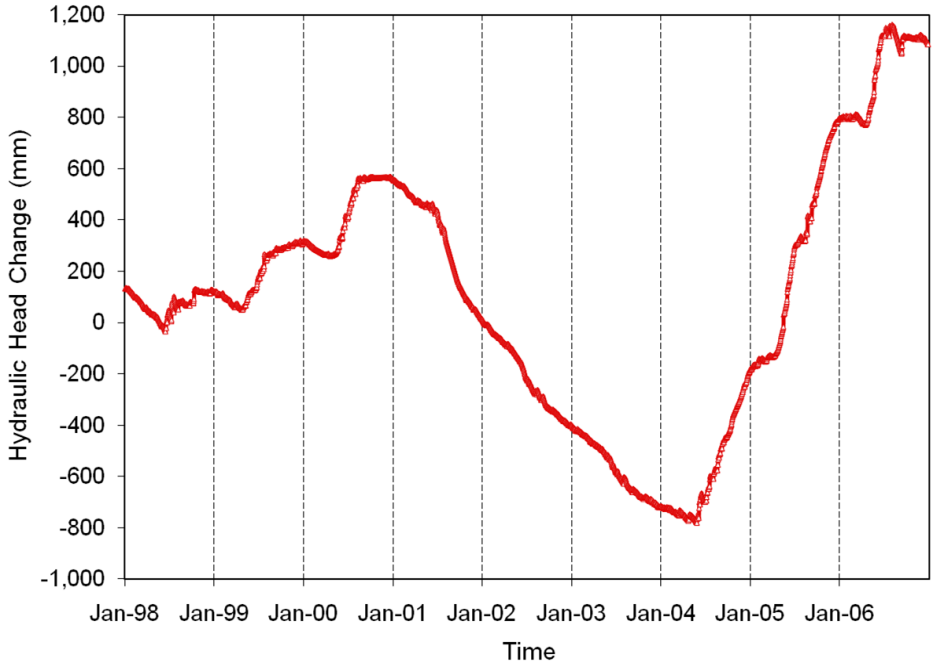

Figure 3.9. Observed aquitard piezometer hydraulic head changes for the Old Aspen Site (1998 – 2006)

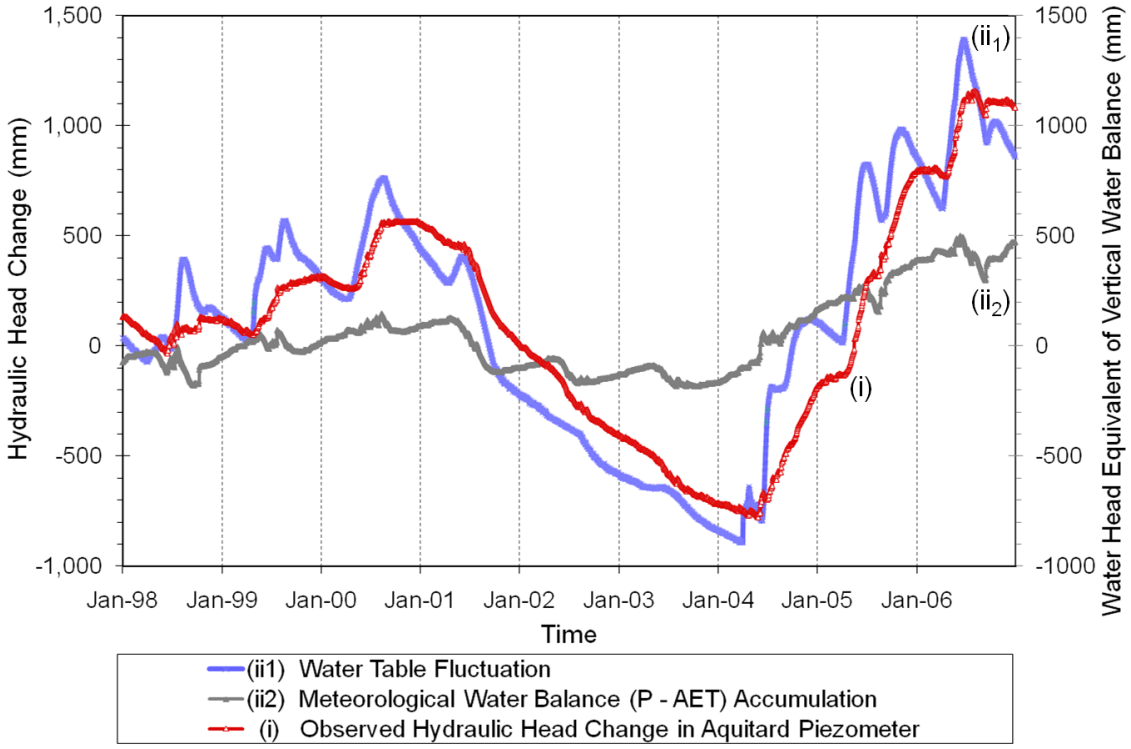

Figure 3.10. A Comparison of the (i) observed hydraulic head changes in aquitard piezometer with the contributing input signals: (ii_1) water table fluctuation; and (ii_2) meteorological water balance (P –AET) accumulation

4 CHAPTER 4 – THE NUMERICAL MODELLING PROCESS

4.1 The Modelling Framework

The process adopted in the numerical modelling of the problem is the simplified scientific methods as discussed by Barbour and Krahn (2004). The four major iterative steps/procedures include: observe (i.e. define objectives and develop conceptual model for the problem using site information), measure (i.e. define theoretical model and obtain input data), explain (i.e. verify numerical modelling/analytic tool) and verify (i.e. interpret results, calibrate model to formation properties and critically validate results to real physical behaviour). The various steps of the modelling process were not carried out in isolation, but required iterative "feedback" (e.g. Mercer and Faust 1981, p.4) connecting the modelling steps, however, the steps were discussed separately below only for clarity.

The modelling-objective of refining the interpretation of the piezometer-based lysimeter was first defined. A conceptual model of the site was then developed which incorporated all available information on site geology, hydrogeology, and hydrology as well as details of the field installations. The physical processes to be simulated were then described by a set of partial differential equations which were solved over the domain of the model, using appropriate initial and boundary conditions.

The developed numerical model was verified and sensitivity studies were undertaken to evaluate the influence of various model parameters. Finally, after the verification of the numerical modelling tool, simulations of the actual problem using specified initial and boundary condition were carried out.

The results of each simulation were interpreted and checked for accuracy. Subsequently, calibration to the field-measured response of the formation was carried out. In getting the "best-fit" calibrated (hydraulic and elastic) properties, the model results and fitting errors were evaluated taking into account the physical reality and the associated simplifying assumptions used in the theoretical modelling.

In the final stage, the fully calibrated model was used to simulate and isolate the influence of water table fluctuation on the piezometeric observations. These pore-pressure variations arising from water table fluctuations were subtracted from the observed pore-pressure changes to assess whether the remaining pore-pressure variations would provide a reasonable estimate of the modelled pore-pressure response to net water balance for the site obtained from meteorological observations. This was done using the principle of superposition of solutions for linear differential equations which allows two separate solutions of the equations to be added together to obtain the solution of both equations being solved simultaneously.

Precautions were taken in the modelling process to minimise error sources: "conceptual errors", "truncation errors" and "data errors" (Mercer and Faust 1981, p.7). A detailed review of site information and testing of the numerical modelling tool were done prior to conceptualization in order to minimise "conceptual errors". Appropriate discretisation and time stepping were applied to minimise the "truncating error" of the numerical solution; and understanding of operation and limitations of field instrumentation, data processing, smoothing of abnormal data spikes and gap-filling minimised "data errors".

4.2 Conceptual Model

The model-domain was delineated as a one-dimensional soil column from the top of the aquitard (bottom of the overlying unconfined aquifer) extending to depth of 42.5m (Figure 4.1). The domain excluded the unconfined aquifer to avoid complications with non-linearity resulting from fluctuations in saturation within the aquifer accompanying the rise and fall of the water table. Therefore, this allows only the response of the fully saturated aquitard to be modelled using the hydraulic and stress boundary conditions that act within the top of the unconfined aquifer. The key assumptions required for this simplification are that the hydraulic conductivity of the unconfined aquifer is assumed to be several orders of magnitude higher than that of the underlying clayey glacial till aquitard, the stiffness of the aquifer is significantly higher than that of the aquitard, and there are no changes in storage within the unconfined aquifer as a result of lateral flow.

The hydraulic conductivity of the silty sand, clean sand and gravel ranges from the order of 10^{-5} to 10^{-2} m/s based on typical ranges of hydraulic conductivity as presented by Freeze and Cherry (1979, p.29). This is much higher than the hydraulic conductivity of the glacial till in Saskatchewan-area (10^{-11} to 10^{-8} m/s) (Keller et al. 1986, 1988, 1989; Shaw and Hendry 1998).

The influence of the relative stiffness and hydraulic conductivity of the unconfined aquifer and the aquitard can be evaluated by estimating the time for consolidation for both units. The time for consolidation is the ratio of the square of the longest drainage path, h_d^2, to diffusivity, D (i.e. h_d^2/D (e.g. van der Kamp and Maathuis 1985)). Assuming a value of $\bar{B}$ of 0.75 and 0.91 for the (sand and gravel) aquifer and the (clayey till) aquitard, respectively, for a common porosity of 0.26 and for a typical range of hydraulic conductivity, the diffusivity for the unconfined aquifer and aquitard are about $4x10^6 m^2$/day and 1.5 m^2/day, respectively. Given the thicknesses, which are also drainage path lengths, h_d, of the unconfined aquifer and aquitard as 20m and 22.5m,

respectively, then the consolidation times for the unconfined aquifer is $1x10^{-4}$ days while the consolidation time for the aquitard is 3×10^{2} days. This highlights that the surficial aquifer will reach equilibrium with any induced pore-pressure change over a million times faster than the underlying aquitard.

This assumption is further supported by the "drainage factor" of a multi-layer soil system with incompressible impeded drainage boundary type discussed by Gray (1945) and Mesri (1973). They showed that the consolidation response of a consolidating layer bounded by a relatively stiffer "impeded" drainage boundary-layer is close to the consolidation response of the same consolidating layer with freely-draining boundary, if the drainage factor of the system is more than 100. That is, for instance, where the hydraulic conductivity, K_v, of the impeded-boundary-layer is more than 100 times more than the K_v of the consolidating layer, given about the same thicknesses. Since the hydraulic conductivity of the overlying aquifer may be as much as 1,000, 000 times more than that of the underlying aquitard, which is far more than the limiting drainage factor of 100 (Gray 1945; Mesri 1973; Terzaghi 1996, p.229), then excluding the surficial aquifer and assuming a freely-draining top for the aquitard is justified.

Since the full stratigraphic depth of the till aquitard was not confirmed by drilling, sensitivity analyses were carried out to assess the significance of both thickness of the aquitard and varying aquitard properties (such as elastic modulus) with depth. The finally adopted model was an "equivalent" single layer aquitard of 22.5m thickness, extending to the refusal depth, with free-draining top and impervious bottom boundaries. This assumes that the boulder marks the transition from the unoxidised till to another formation with a significantly lower hydraulic conductivity. Figure 4.1 shows the conceptual model and the assignment of the surficial boundary conditions to the top of the glacial till aqitard.

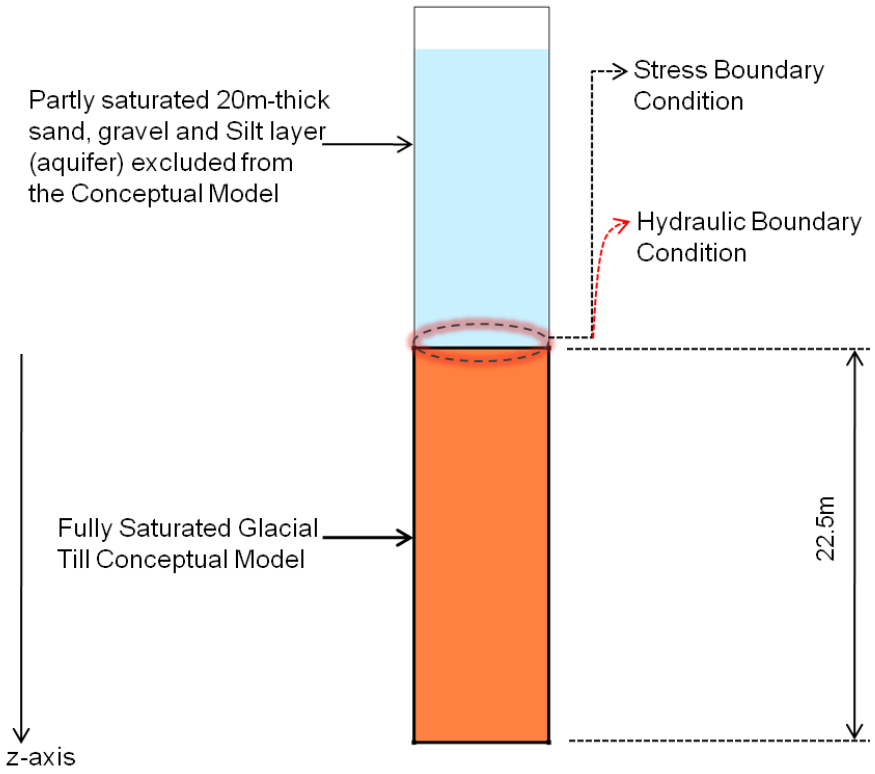

Figure 4.1. Conceptual model of fully saturated glacial till excluding unconfined aquifer material and placing surficial boundary conditions on top of the till-domain

4.3 Theory and the Mathematical Models

The one-dimensional system of a fully-saturated soil used to describe the mathematical model is shown in Figure 4.2. The governing partial differential equation together with the associated boundary and initial conditions for the "geological weighing lysimeter" problem were first presented. Subsequently, the method of superposition required to decompose the pore-pressure responses was discussed and proven to be applicable under specific boundary conditions. Finally, the assumptions made on boundary conditions and constitutive behaviour of the formation for the site that enabled the use of method of superposition were rationalised.

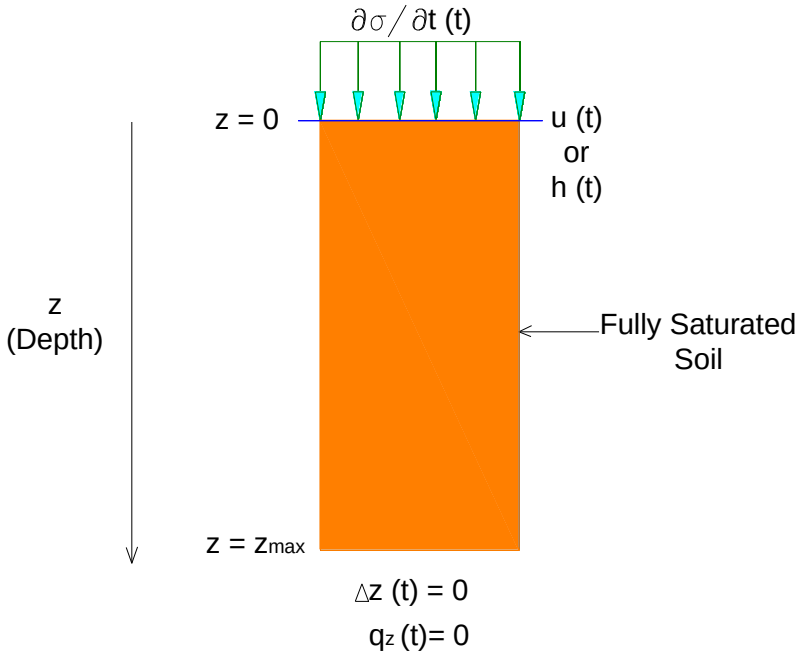

Figure 4.2. One-dimensional system of fully saturated soil

4.3.1 The Governing Partial Differential Equations

The governing one-dimensional partial differential equation describing transient changes in pore-pressure arising from loading and drainage was presented by van der Kamp and Gale (1983), Domenico and Schwartz (1998), and Vuez and Rahal (1994, 1998):

$$\frac{\partial u}{\partial t} = \bar{B}\frac{\partial \sigma}{\partial t} + D\frac{\partial^2 u}{\partial z^2} \qquad [4.1]$$

where u is the incremental pore-pressure relative to the pre-existing reference (background) pore-pressure at any depth, z, with time, t, which is expressed as unit of pressure [$ML^{-1}T^{-2}$] but also interchanged with the unit of water pressure-head (water head equivalent) [L] in the plots for convenience; $\bar{B}\,\partial\sigma/\partial t$ is the undrained pore-pressure response to the changes in surface mechanical loading; $\bar{B}$ is the (constrained) elastic pore-pressure coefficient which is dimensionless [ ]; σ is the mechanical load in units of pressure [$ML^{-1}T^{-2}$]; $D\,\partial^2 u/\partial z^2$, represents vertical transient groundwater flow;

and D is the hydraulic diffusivity in unit of diffusion coefficient [L^2T^{-1}]. $\bar{B}$ is often referred to as the Skempton's B-bar coefficient (Skempton 1954), and is also known as loading efficiency or tidal efficiency, defined as the ratio of the pore-pressure response to the applied load (Skempton 1954; Jacob 1940; van der Kamp and Gale 1983). D is the ratio of vertical hydraulic conductivity, K_v, to specific storage, S_s, (K_v/S_s) and is equivalent to Terzaghi's coefficient of consolidation, C_v.

The associated hydraulic and stress-strain boundary conditions mathematically required at the two ends, top (z = 0) and bottom (z = z_{max}), of the one-dimensional-response domain are:

- incremental pore-pressure at the top due to water table fluctuation, $u_w(t)$:

$$u(0,t) = u_w(t) \qquad [4.1a(i)]$$

  – which can also be expressed as hydraulic head changes due to water table fluctuations, $h_w(t)$:

$$h(0,t) = h_w(t) \qquad [4.1a(ii)]$$

- incrementally applied stress at the top due to change of water balance:

$$\frac{\partial\sigma(0,t)}{\partial t} = \rho_w g(P - AET - R) \qquad [4.1b]$$

  where the loading applied at surface (z = 0) corresponds to the change in total stress arising from the changes in stress associated with changes of total soil moisture, $\partial\sigma/\partial t$, with time [$ML^{-1}T^{-3}$] (e.g. van der Kamp and Schmidt 1997; Barr et al. 2000). The symbol ρ_w is the density of water [ML^{-3}]; g is the acceleration due to gravity [LT^{-2}]; P is precipitation; AET is the evapotranspiration; and R is the runoff (net lateral flow). The latter term is assumed to be negligible for the site considered

in this work given its semi-arid climate (e.g. Conly and van der Kamp 2001) with average annual precipitation of less than 500mm, but runoff from the area was observed to occur in exceptionally wet years. P, AET and R are each expressed as height of water accumulated over a given period [LT^{-1}]. This loading due to changes of soil moisture is controlled by meteorological events, which can be assumed extensive relative to the installation depths of piezometers. Therefore it was assumed that the loading generated a uniform undrained excess pore-pressure profile in the ground water similar to the case of the uniform consolidation stress profile illustrated by Terzaghi and Frohlich (1936);

- impervious (zero water flux) bottom hydraulic boundary condition:

$$q_z(z_{max}, t) = 0 \qquad [4.1c]$$

where q_z is water flux in the z-direction (i.e. volume of water flowing through a unit cross-sectional area perpendicular to the z-axis per unit time) [LT^{-1}];

- and no displacement (fixed) bottom stress-strain boundary condition:

$$\Delta z(z_{max}, t) = 0 \qquad [4.1d]$$

where Δz is the vertical displacement [L];

The accompanying initial stress-strain and hydraulic (pore-pressure) conditions throughout the domain (z) are:

- zero stress change (or constant stress):

$$\frac{\partial \sigma(z,0)}{\partial t} = 0 \qquad [4.1e]$$

- zero incremental pore-pressure (though unknown "residual" pore-pressure changes typically exist (e.g. Schiffman and Stein 1972)):

$$u(z,0) = 0 \qquad [4.1f].$$

4.3.2 Method of Superposition

The governing equation is a linear (second order) partial differential equation, therefore the equation, as well as each of the primary variables (e.g. u) and the boundary conditions can be decomposed and its components can also be superimposed. Therefore, the incremental pore-pressure, u, can be broken into the components of change of pore-pressure contributed from load changes, u_L and from water table fluctuations, u_w, all varying in time, t, and space, z,:

$$u(z,t) = u_L(z,t) + u_w(z,t) \qquad [4.2]$$

The general governing equation (Equation [4.1]) is then re-written as:

$$\frac{\partial(u_L + u_w)}{\partial t} = \bar{B}\frac{\partial \sigma}{\partial t} + D\frac{\partial^2(u_L + u_w)}{\partial z^2} \qquad [4.3].$$

The governing equation for the case of change of pore-pressure, u_L, produced by only mechanical surface loading due to changes in total soil moisture (water balance) and its associated dissipation can be written as follows:

$$\frac{\partial u_L}{\partial t} = \bar{B}\frac{\partial \sigma}{\partial t} + D\frac{\partial^2 u_L}{\partial z^2} \qquad [4.4]$$

The hydraulic and stress-strain boundary conditions at the surface (z=0) and at the bottom (z = z_{max}) of the domain include:

- incrementally applied stress at the top due to change of water balance as stress-strain boundary condition:

$$\left.\frac{\partial\sigma(0,t)}{\partial t}\right|_{Loading\ alone} = \rho_w g(P - AET - R) \qquad [4.4a]$$

where $\left.\frac{\partial\sigma(0,t)}{\partial t}\right|_{Loading\ alone}$ is the change in (top) total stress arising from the changes in stress associated with changes in total soil moisture, with time [$ML^{-1}T^{-3}$] in the case of loading alone;

- top drainage hydraulic boundary condition, (i.e. constant water table):

$$u_L(0,t) = 0 \qquad [4.4b(i)]$$

  - which can also be expressed as zero change in surface total hydraulic head with time:

$$h_L(0,t) = 0 \qquad [4.4b(ii)]$$

- impervious bottom hydraulic boundary condition:

$$q_{zL}(z_{max},t) = 0 \qquad [4.4c]$$

where q_{zL} is water flux in the z-direction for the case of loading alone [LT^{-1}];

- no-displacement (fixed) stress-strain bottom boundary:

$$\Delta z_L(z_{max},t) = 0 \qquad [4.4d]$$

where Δz_L is the vertical displacement in the case of loading alone [L];

The initial stress and hydraulic (pore-pressure) conditions everywhere in the domain are:

- zero stress change (or constant stress):

$$\left.\frac{\partial \sigma(z,0)}{\partial t}\right|_{Loading\ alone} = 0 \qquad [4.4e]$$

- zero incremental pore-pressure due to loading:

$$u_L(z,0) = 0 \qquad [4.4f].$$

Fluctuations in the water table elevation within the surface-aquifer overlying the aquitard will propagate pore-pressures into the aquitard. The governing equation describing these pore-pressure transients is similar to that form expressed by Terzaghi (1925) for consolidation:

$$\frac{\partial u_w}{\partial t} = D\frac{\partial^2 u_w}{\partial z^2} \qquad [4.5].$$

This governing equation can be solved purely as a transient seepage problem requiring only hydraulic boundaries. The hydraulic and the null stress-strain boundary conditions at the surface (z = 0) and at the bottom (z = z_{max}) of the aquitard used to solve the Equation [4.5] as a coupled stress-flow problem include:

- the incremental pore-pressure at the top due to water table fluctuations, $u_w(t)$ as hydraulic boundary condition:

$$u_w(0,t) = u_w(t) \qquad [4.5a(i)]$$

– alternatively expressed as hydraulic head changes due to water table fluctuations, $h_w(t)$:

$$h_w(0,t) = h_w(t) \qquad [4.5a(ii)]$$

- zero stress change (or constant stress) as stress-strain boundary condition at the top:

$$\frac{\partial\sigma(0,t)}{\partial t}\Big|_{Water\ table} = 0 \qquad [4.5b]$$

where $\frac{\partial\sigma(0,t)}{\partial t}\Big|_{Water\ table}$ is the change in (top) total stress in the aquitard arising from the changes in stress associated with changes in water table elevation, with time [$ML^{-1}T^{-3}$] in the case of water table fluctuation alone;

- no-flow hydraulic boundary condition at the bottom:

$$q_{zw}(z_{max},t) = 0 \qquad [4.5c]$$

where q_{zw} is water flux in the z-direction for the case of water table fluctuation alone [LT^{-1}];

- no-displacement stress-strain boundary condition at the bottom:

$$\Delta z_w(z_{max},t) = 0 \qquad [4.5d]$$

where Δz_w is vertical displacement in the case of water table fluctuation alone [L];

The initial stress and hydraulic (pore-pressure) conditions everywhere in the domain are:

- zero stress change (or constant stress):

$$\left.\frac{\partial \sigma(z,0)}{\partial t}\right|_{Water\ table} = 0 \qquad [4.5e]$$

- zero pore-pressure change due to water table fluctuations (i.e. constant water table):

$$u_w(z,0) = 0 \qquad [4.5f].$$

Given that the principle of superposition is permissible in this problem (from Equation 4.2), it then follows that the components of the change of pore-pressure, u_L and u_w, can be separately solved for and superimposed to produce the same incremental pore-pressure of the coupled effects. That is, combining the solutions to both Equations [4.4] and [4.5] should result in the same solution as that of Equation [4.3], as long as their initial and boundary conditions also satisfy both Equation [4.3] and its initial and boundary conditions. Adding the two equations (Equation [4.4] + Equation [4.5]):

$$\left(\frac{\partial u_L}{\partial t}\right) + \left(\frac{\partial u_W}{\partial t}\right) = \left(\bar{B}\frac{\partial \sigma}{\partial t} + D\frac{\partial^2 u_L}{\partial z^2}\right) + \left(D\frac{\partial^2 u_W}{\partial z^2}\right) \qquad [4.6]$$

- produces Equation [4.3], which is the same as Equation [4.1]:

$$\frac{\partial (u_L + u_W)}{\partial t} = \bar{B}\frac{\partial \sigma}{\partial t} + D\frac{\partial^2 (u_L + u_W)}{\partial z^2} \qquad [4.6*].$$

Similarly, adding the corresponding stress-strain and hydraulic boundary, and initial conditions for the two equations (Equations [4.4a] to [4.4f] and Equations [4.5a] to [4.5f]) produces the same boundary and initial conditions as those required to solve Equation [4.1] or [4.3]) as follows:

$$\left.\frac{\partial \sigma(0,t)}{\partial t}\right|_{Loading\ alone} + \left.\frac{\partial \sigma(0,t)}{\partial t}\right|_{Water\ table} = \rho_w g(P - AET - R) + 0 \qquad [4.6a]$$

- which reduces to the top stress boundary for Equation [4.1] or [4.3]:

$$\frac{\partial \sigma(0,t)}{\partial t} = \rho_w g(P - AET - R)$$ [4.6a*];

$$u_L(0,t) + u_w(0,t) = 0 + u_w(t)$$ [4.6b(i)]

- simplifies to observed changes in pore-pressure, *u*, with reference to Equation [4.2]:

$$u(0,t) = u_w(t)$$ [4.6b(i)*]

  - which can also be expressed in terms of hydraulic head changes:

$$h_L(0,t) + h_w(0,t) = 0 + h_w(t)$$ [4.6b(ii)]

$$h(0,t) = h_w(t)$$ [4.6b(ii)*].

Also adding the hydraulic and displacement boundary conditions at the bottom ($z=z_{max}$): The sum of the no-flow bottom boundaries:

$$q_{zL}(z_{max},t) + q_{zw}(z_{max},t) = 0 + 0$$ [4.6c]

- with reference to similar operation in Equation [4.2], then q_{zL} and q_{zw} combine to simplify q_z, which is the same no-flow bottom hydraulic boundary for Equation [4.1] or [4.3]:

$$q_z(z_{max},t) = 0$$ [4.6c*];

The sum of the zero displacement boundary conditions at the bottom of the domain, ($z=z_{max}$):

$$\Delta z_w(z_{max},t) + \Delta z_L(z_{max},t) = 0 + 0$$ [4.6d]

- also simplifies, through similar operation in Equation [4.2], by combining Δz_w and Δz_L to produce Δz below, which is the same as the bottom displacement boundary for Equation [4.1] or [4.3]:

$$\Delta z(z_{max}, t) = 0 \qquad [4.6d^*]$$

Similarly and finally, adding initial conditions everywhere in the domain:
The summation of zero initial incremental stress conditions:

$$\frac{\partial \sigma(z,0)}{\partial t}\Big|_{Loading\ alone} + \frac{\partial \sigma(z,0)}{\partial t}\Big|_{Water\ table} = 0 + 0 \qquad [4.6e]$$

- combines the two stresses in a similar approach as used for pore-pressure change in Equation [4.2] and simplifies to the same initial stress condition as for Equation [4.1] or [4.3]:

$$\frac{\partial \sigma(z,0)}{\partial t} = 0 \qquad [4.6e^*];$$

Adding the zero initial incremental pore-pressure conditions:

$$u_L(z,0) + u_w(z,0) = 0 + 0 \qquad [4.6f]$$

- with reference to the approach used in Equation [4.2], simplifies to the initial hydraulic condition for Equation [4.1] or [4.3]:

$$u(z,0) = 0 \qquad [4.6f^*].$$

The summary and the proof of the superposition of the equations and the associated surface boundary and initial domain-wide conditions for the cases of loading alone and

water table fluctuation alone to produce the case of coupled effect of loading and water table fluctuation are shown in the Table 4.1 below.

Table 4.1. Summary of surface boundary and initial (entire-domain) conditions associated with the governing equations simulated or superposed for the aquitard

Modelled Equation	**Boundary Description**	**Initial (t =0)**		**Transient (t>0)**	
		Hydraulic, u (kPa)	Stress, $\Delta\sigma(t)$[6] (kPa)	Hydraulic, u (kPa)	Stress, $\Delta\sigma(t)$ (kPa)
Equation [4.5]	Water table fluctuation [$h_w(t)$]	0	0	$u_w(t)$	0
Equation [4.4]	(P-AET) Load [Stress(t)]	0	0	0	$\Delta\sigma(t)$
Equation [4.3] (also Equation [4.1])	Water fluctuation and (P-AET) Load [coupled $h_w(t)$ & Stress(t)]	0	0	$u_w(t)$	$\Delta\sigma(t)$
Equations: ([4.4]+[4.5])	Superposition of $h_w(t)$ & Stress (t) for Equations [4.4]&[4.5]	0	0	$u_w(t)$	$\Delta\sigma(t)$

4.3.3 Key Assumptions Enabling the Superposition

In order to solve the governing differential equations and successfully apply the method of superposition some important realistic and enabling assumptions have been made. Assumptions were made on the top boundary conditions that were adopted, the constitutive behaviour of the formation and the long term behaviour of material properties.

[6] $\Delta\sigma(t)$ refers to stress changes over time due to changes in water balance [e.g. $\frac{\partial\sigma(0,t)}{\partial t} = \rho_w g(P - AET - R)$]

4.3.3.1 Boundary Conditions

Two critical assumptions of top boundary conditions on the aquitard were made in the solution of the partial differential equations to enable superposition. They are:

i. The constant hydraulic head boundary condition in the case of loading alone (Equation [4.4]); and
ii. The constant-stress (zero-stress change) boundary condition in the case of water table fluctuation alone (Equation [4.5]).

These assumptions are realistic for the site setting because of the high stiffness of the aquitard.

The constant hydraulic head boundary (Equation [4.4b(i)] or [4.4b(ii)]) enables simulation of the free consolidation drainage of the load-induced pore-pressure from the aquitard to the overlying aquifer (Equation [4.4]). This may appear to be rather contradictory since the aim of the decomposition is to treat the effect of water table fluctuations on the aquitard-pore-pressure response. Deformation and drainage associated with surface mechanical loading of the aquitard would lead to seepage or absorption of pore-water to or from an overlying unconfined aquifer, therefore, contributing to the overall water table fluctuation (i.e. adding to the fluctuation due to seasonal recharge/discharge). However, for a highly stiff aquitard, the changes in water volume stored within the pores of the aquitard as a result of pressure changes generated by the surface mechanical loading from changes in soil moisture (water balance) are very small and are unlikely to make any significant changes to the weight (density) of the aquitard or the volume of pore-water released or absorbed from the overlying aquifer. It is conservatively estimated that this change in water table elevation would be less than 1% of the water pressure head equivalent of an applied surface load associated with changes in soil moisture storage, given the high stiffness of the formation and the large effective (potential) storage at the water table. Since this fluctuation in water table (in millimetre-scale) created by mechanical loading is small compared to the annual fluctuation (in metre-scale), the water table elevation can be assumed constant in the

simulation of loading alone (Equation [4.4]). The same constant hydraulic head and constant stress (zero-stress change) apply in the entire aquitard as initial conditions.

The constant stress (zero stress change) boundary enables the separate analysis of the effect of water table fluctuation (Equation [4.5]). The temporal water table fluctuation applies as a varying hydraulic head boundary at the top of the aquitard alongside the constant stress as stress-strain boundary condition. The change of pore-pressure within the aquitard generated by a change of hydraulic head above the aquitard will lead to small changes of total water mass (weight) within the pores of the (elastic) domain and, thereby, result to small changes of total stress. However, if the soil is highly stiff, these changes of water mass, which generate total stress changes, are so small (less than 1% of applied hydraulic head in water pressure head equivalent) compared to stress changes due to mechanical surface loading (over 100 times higher) that they can be ignored. Therefore the use of constant stress boundary condition on top of the glacial till aquitard for the case of water table fluctuation alone remains valid. The same constant stress and constant hydraulic head apply everywhere in the aquitard-domain as initial conditions.

4.3.3.2 Linear Elastic Constitutive Model

The aquitard-material was assumed to be of linearly elastic isotropic behaviour. This is in agreement with the linear elastic constitutive model implied in the governing equation (van der Kamp and Gale 1983) and as assumed by Terzaghi (1925) and Biot (1941). The linear elastic constitutive model assumption was made for the following three reasons:

i. This constitutive behaviour is appropriate for the heavily overconsolidated deposits found in Saskatchewan area (Klohn 1965; Sauer et al. 1993). The over consolidation ratio (OCR) of the glacial till in the study site was roughly estimate as between 5 and 6.8 which is considered overconsolidated. The OCR value was obtained as a ratio of preconsolidation pressure of 1800 to 2200kPa (glacial till

deposits in some Saskatchewan sites (Sauer et al. 1993)) to the effective stress profile around the piezometric elevation in the aquitard;

ii. The typical daily and seasonal mechanical loading arising from total moisture changes would be less than 100mm and 400mm of water pressure (about 1kPa and 4kPa), respectively. These are not only well below the typical preconsolidation pressure (yield stress) of glacial till in some Saskatchewan sites 1800 $\pm$ 200 kPa (Sauer et al. 1993) but would also result in very small strains, consistent with an elastic behaviour; and

iii. The water table fluctuations through the geological life of the glacial till induce many effective stress cycles of rebound and recompression in the elastic range. For instance, the site data indicate about 1m of annual fluctuation and about 2.3m of fluctuation over 9 years which would exert effective stress cycles of, conservatively, less than 10kPa and 23kPa, respectively, all within the elastic range. These multiple load-rebound cycles are likely to minimise any potential non-linear behaviour, such as hysteresis, of the glacial till formation when subjected to such stress ranges.

The assumption that the glacial till is isotropic is somewhat controversial as noted by Biot (1941). In hydrogeology, it is generally conceived that anisotropic (mechanical and hydraulic) behaviour of hydrostratigraphic deposits may exist due to their complex genesis, particularly layered deposition (e.g. Domenico and Schwartz 1998, p.39). Recent studies even suggest investigation into the possible occurrence of "multiple" anisotropy in the horizontal plane due to glacial shearing movements (Huang 2005). However, isotropic elastic properties were assumed in this work. The support for this assumption is based on:

i. Deductions made from Terzaghi et al. (1996, p.90) which suggests that clay soil of OCR near 6 to 8 exhibit an isotropic (and linear elastic) behaviour as implied in the zero shear-induced pore-pressure response likely to be observed in such deposits. Woods (2007, p.42) shows expression to illustrate that isotropic materials do not exhibit shear-volume coupling. Since the OCR of 6 is roughly estimated for the glacial till in this study, it was assumed elastically isotropic.

Given that the problem is analysed as a one-dimensional problem, this isotropy may appear redundant since material properties in only one direction (vertical) z-direction are used (e.g. Freeze and Cherry 1979, p.56).

4.3.3.3 Constant Material Properties (Elastic and Hydraulic Parameters)

The elastic and hydraulic parameters of the glacial till were assumed constant for the entire period of simulation (9 years). This assumption was based on the small strain and the linear elastic behaviour discussed in the previous section.

4.3.4 Defining Material Properties

4.3.4.1 Elastic Parameters

The elastic parameters required to solve the differential equation are related to the Skempton's $\overline{B}$ (pore-pressure) coefficient, and were determined from the correction for evaluated barometric response. The relationship between the confined elastic pore-pressure coefficient (Skempton's $\overline{B}$) and the drained confined elastic modulus of soil structure, E_c, expressed by van der Kamp and Gale (1983) is as follows:

$$\overline{B} = \frac{1/E_c}{1/E_c + n/E_w} \qquad [4.11]$$

where n is the porosity of the formation; $1/E_c$ is the drained constrained compressibility of the soil structure, m_v; and E_w is the elastic modulus of water, such that $1/E_w$ is the compressibility of water. The porosity was assumed to be 0.26 in this research based on a range of reported *n* values for similar tills of 0.26 – 0.36 in Saskatchewan (Keller et al.

1986, 1988). The confined elastic modulus of the clay till formation at the depth of the deep piezometer is easily derived from Equation [4.11] as:

$$E_c = \frac{E_w - \bar{B}E_w}{\bar{B}n} \quad [4.12]$$

Elastic storage (specific storage) of laterally constrained soil, S_s, can be reliably obtained from barometric response of its pore-pressure (van der Kamp 2001). Once E_c is determined and a value of porosity is selected, the value of S_s can be obtained. Specific storage was presented by Jacob (1940):

$$S_s = \rho_w g\left(\frac{1}{E_c} + \frac{n}{E_w}\right) \quad [4.13]$$

The specific storage coefficient S_s of the glacial till formation at the depth of the deep piezometer was obtained from Skempton's $\bar{B}$ coefficient through the use of Equations [4.12] and [4.13].

The drained Young's modulus, E, used as input in the numerical model was established from the relationship with the drained constrained elastic modulus, E_c, and drained Poisson's ratio, ν (Poulos and Davis 1974; van der Kamp and Gale 1983):

$$E = \frac{E_c(1+\nu)(1-2\upsilon)}{(1-\nu)} \quad [4.14]$$

which becomes:

$$E = \frac{2}{3}E_c \quad [4.15]$$

if ν is assumed to be 1/3 (i.e. E becomes $0.67E_c$).

4.3.4.2 Hydraulic Conductivity

The vertical hydraulic conductivity is determined by adjusting the hydraulic conductivity, K_v, by "trial-and-error" in the simulation to get the best-fit to the required field-observed piezometric response. In other words, the model attains the "best-fit" diffusivity, D:

$$D = \frac{K_v}{S_s} \qquad [4.16]$$

such that the corresponding K_v (in Equation [4.16]) is the "equivalent" hydraulic conductivity of the formation.

4.4 Numerical Solution Approach

The stress and transient flow problems (the governing equations) were simulated using the coupled load-deformation and seepage finite element numerical models, SIGMA/W and SEEP/W, respectively, (GEO-SLOPE 2008). The commercially available software was operated from high speed personal computer(s) operating on Microsoft's Windows XP and Windows Vista operating systems, in some cases. The use of the former appeared to run the model faster for the heavy time-stepping involved in solving the current problem. The coupled stress and pore-pressure (coupled Sigma/W and Seep/W) mode is used for the analysis of consolidation type problems (all on Sigma/W interface) (GEOSLOPE 2008). The coupled analysis simultaneously solves two groups of nodal equations, equilibrium (stress-deformation) and continuity (flow) equations, across the finite element mesh (GEOSLOPE 2008). The basic material-parameters required for such analysis on fully saturated linear elastic systems are: the effective (drained) Young's Modulus, E; drained Poisson's ratio, υ; Skempon's $\bar{B}$ coefficient (i.e. equal in magnitude with a Load Response Ratio), porosity, n; and saturated hydraulic conductivity, K.

The numerical models can simulate two-dimensional or axi-symmetric domains and their corresponding element types (GEOSLOPE 2008). A two-dimensional model domain, one element wide, was used to represent the one-dimensional regime described by the governing equations. The model was constrained laterally (hydraulically and mechanically) with the appropriate boundary conditions to achieve the one-dimensional behaviour (e.g. Istok 1989, p.14). These included zero deflection in the stress-deformation analyses and zero water flux boundary conditions for the hydraulic analyses placed along the sides and base of the domain. The top boundary had specified stress and total head (hydraulic) boundary conditions. The model set up showing most of the typical boundary conditions are shown in Figure 4.3.

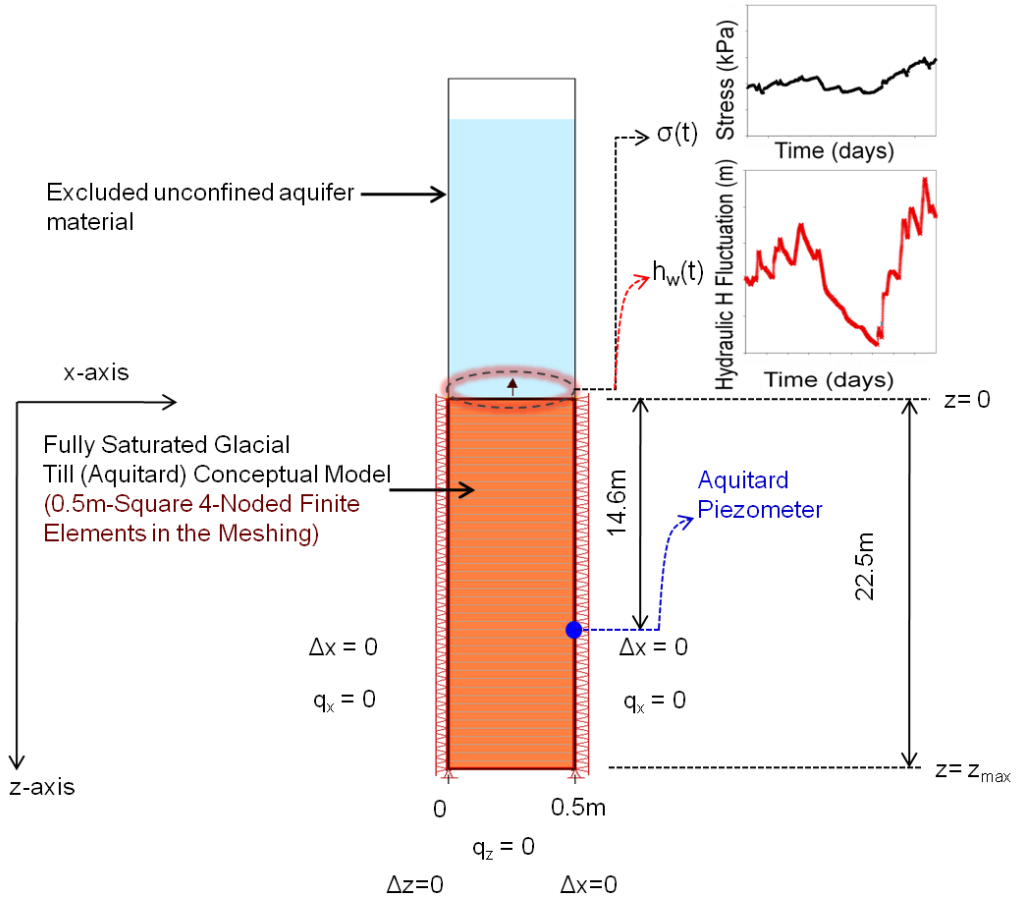

Figure 4.3. A set-up of the numerical modelling domain for the aquitard showing typical stress-strain ($\sigma(t)$, or Δz (or Δx)) and hydraulic ($h_w(t)$ or q_z (or q_x)) boundary conditions

Different combinations of hydraulic and stress boundary conditions were applied at the upper boundary to simulate the three cases (Equations [4.3] (or [4.1]), [4.4] and [4.5]). In the simulation of Equation [4.3] for calibration of the model against all available observed field-data, the incremental total stress obtained from the meteorologically monitored daily water balance, $\rho_w g(P - AET)$, was utilised as the top stress boundary condition together with the measured total (hydraulic) head from the water table fluctuation. In the simulation of the pore-pressure transients generated by water table fluctuations alone (Equation [4.5]), a constant stress (zero stress change) boundary condition was applied together with the measured changes in hydraulic head from the water table fluctuations. The daily 9-year (1998 – 2006) observed data set for the cumulative meteorological water balance (P – AET) and changes in water table elevation (Figures 3.6 and 3.7) were used to generate the upper stress-strain and hydraulic boundary conditions shown in Figures 4.5 and 4.6.

The stress boundary condition, applied at the top boundary, was generated from water balance (P – ET) to represent the continuous cumulative loading on the aquitard. In the field, the applied total stress due to daily incremental water balance accumulates (positive or negative) until drainage occurs. It is unlike short lived atmospheric loading (Jacob 1940; van der Kamp and Gale 1983; Domenico and Schwartz 1998) which may just be considered to generate only an undrained response.

Numerical stress-deformation models are generally based on an incremental formulation in which all stress boundary conditions represent a change in boundary conditions over the specified time interval (e.g. GEOSLOPE 2008, p.62). Therefore, the incremental form of the continuously accumulating surface loading from water balance (at z=0) was derived by cumulatively adding the stress due to daily water balance accumulation (P – ET) from start (i.e. an initial time step *t*, leading to day 1) to any given time step, t_i:

$$\frac{\partial \sigma(0,t_i)}{\partial t} = \rho_w g \sum_0^i (P - AET) \qquad [4.16]$$

where *i* is the daily time step counter. The daily-time-step incremental loading is then applied as the difference between the cumulative load for the given time at the end of the time step and that of the time preceding the step (GEOSLOPE 2008).

The top hydraulic head boundary condition, for cases of water table fluctuation alone (Equation [4.5]) and the case of coupled effects (Equation [4.3]), was derived from the water table measurements. The hydraulic head fluctuations at the top boundary generate transient vertical flow in the system driven by the changes in the hydraulic head relative to a specified initial hydrostatic condition. An initial head was assumed for the aquifer-aquitard system to which changes in water table elevation were represented as change in total head (as in Equation [4.1a(ii)]). Any convenient initial water table was chosen as long as it did not create de-saturation and an associated non-linear behaviour in the aquitard at the lowest point of the cycles of water table fluctuation.

4.4.1 Model Verification by Undrained, Drained and Linearity Tests

The numerical modelling tools selected for the modelling are SEEP/W and SIGMA/W both coupled in a SIGMA/W interface. The model was tested to ascertain that it correctly solves the partial differential equations described previously including: undrained pore-pressure response, consolidation drainage and the method of superposition. Documented results of one–dimensional consolidation using SIGMA/W coupled stress and seepage model can be found in GEO-SLOPE (2008). In addition preliminary modelling exercises for simple problems checked with simple hand-calculations were carried out at the early stage of the research. These were to further build confidence in the use and results of the modelling tools. The detailed preliminary model-testing is not reported here but they indeed did verify the capability of the modelling tools.

4.4.1.1 Verification of Undrained Pore-pressure Load-Response

It was important to test the model to confirm that it captures undrained responses in stiff overconsolidated soil of low Skempton's $\bar{B}$. The same Sigma/W analysis mode of coupled stress and pore-pressure (coupled stress/pwp) used for drained simulations was used for this undrained test. The test was set up using a single-step load and impervious (null) hydraulic boundaries. The modelled undrained pore-pressure was verified by hand-calculation of the product of load and pore-pressure coefficient (i.e. load x Skempton's $\bar{B}$). The result of the undrained response of the model agreed exactly with the product of load and Skempton's $\bar{B}$. Similarly, the initial excess pore-pressure values (at first time step) of consolidation drainage also verify the same undrained response (Figure 4.4(a)).

4.4.1.2 Verification of Drained Response (Consolidation or Transient Pore-pressure)

Simple cases of consolidation drainage following load-response and downward pore-pressure propagation due to change of water table elevation were modelled using coupled seepage and load-deformation analysis. Two different simulations were set up. First was the case of a simple arbitrary single-step-load (100mm water pressure-head equivalent) applied and sustained for an entire 9-year duration (i.e. assumed to infinity) as the stress boundary condition together with a constant head boundary condition at the top of the aquitard. This was used to test the simulation of the creation and dissipation of excess pore-pressure. The second simulation was done using a simple arbitrary single-step increment of water table (100mm water head) applied and sustained for the entire 9-year duration as hydraulic boundary condition while constant stress (zero stress change) was applied as the stress top boundary condition. The results of pore-pressure changes in the aquitard obtained from the second simulation were used to verify the use of the model to simulate pore-pressure propagation from water table fluctuations. Any material parameter (elastic properties and hydraulic conductivity) were sufficient for this test.

Hand (analytical) calculations of consolidation time (dimensionless time factor T_v) and a computation of the degree of consolidation with respect to excess pore-pressure dissipation (or pore-pressure build up from pressure propagated from the water table) at the aquitard piezometer were made. The plots of the degree of dissipation and propagated pore-pressure against time (T_v) were compared with similar plots from solution of the one-dimensional consolidation of a fully saturated single soil layer with one-way drainage (Lee et al. 1992) and with analytical solutions of Terzaghi (1943, p.274).

A convenient benchmark for this comparison was the degree of consolidation for T_v of unity (1); the actual time, t_c, corresponding to this T_v of 1 is termed the characteristic time (e.g. van der Kamp 1985) which is when consolidation should nearly be complete:

$$t_c = \frac{{h_d}^2}{D} \qquad [4.17]$$

where h_d is the longest drainage path (the same as the thickness of the aquitard domain) and D is hydraulic diffusivity. In the case of a domain with only top drainage, the degree of consolidation for T_v of 1 (at characteristic time) was about 90% which agrees with the results of the corresponding degree of consolidation for one-way draining single layer soil using Terzaghi's (1925) consolidation theory presented by Lee et al. (1992). The degree of pore-pressure dissipation at T_v of 1 in the the piezometer was close to 90% (specifically 90.8%) which agreed with the analytically determined rate of pore-pressure dissipation for the piezometer (90.8%) using the appropriate initial excess pore-pressure ($\bar{B}\Delta\sigma$) in Terzaghi's solutions (Terzaghi 1943, p.274; Terzaghi et al. 1996, p.228) (Figure 4.4(a)). Similar results were also obtained for rate of propagation of water table change to the piezometer, as a case of swelling (Figure 4.4(b)). The model was therefore considered satisfactory for the simulation of the consolidation and the propagation of pore-pressure involved in this research work.

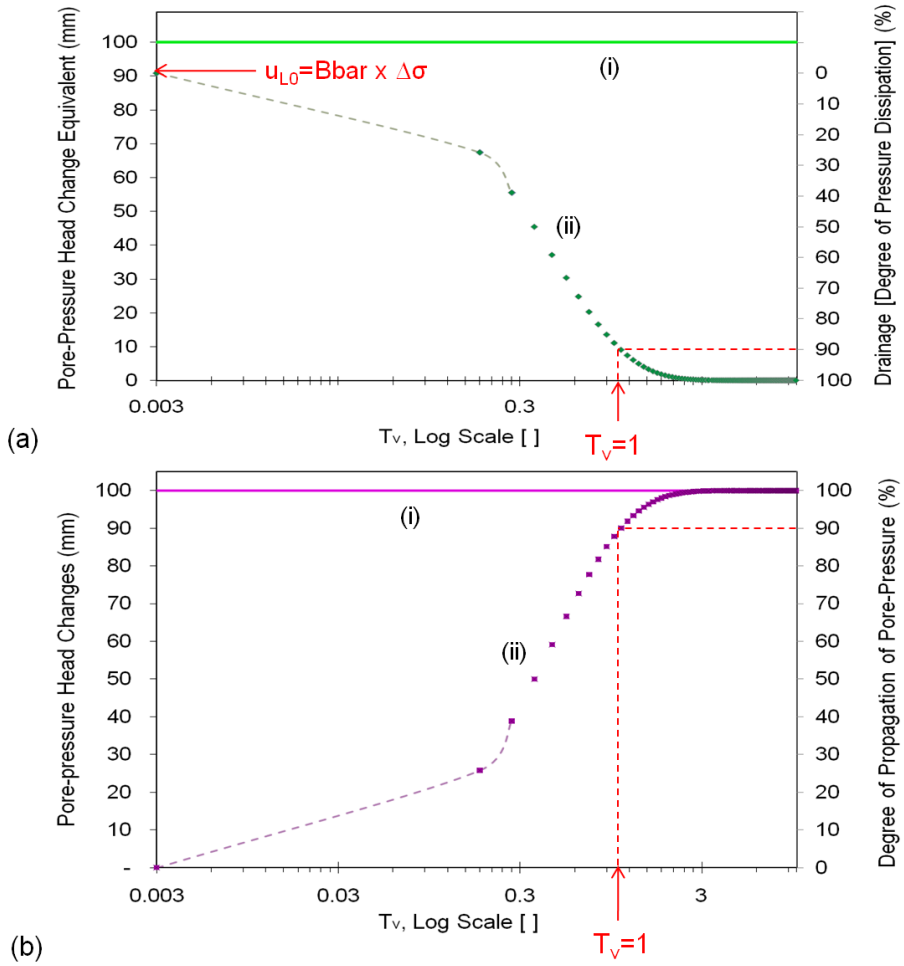

Figure 4.4. Modelled Pore-pressure change (degree)-time (T_v) of a one-way-draining saturated soil domain showing a benchmark (T_v and degree of change of pore-pressure) for model verification of (a) consolidation drainage also showing verification of initial undrained excess pore-pressure, u_{L0}: a(i) applied surface single-step load in terms of pore-pressure head equivalent; and a(ii) degree of pressure-dissipation against T_v; and (b) pore-pressure propagation to aquitard from change in water table elevation: b(i) single-step change in water table elevation; and b(ii) degree of pore-pressure accumulation in response to pore-pressure propagation from one-step change in water table elevation of an overlying aquifer

4.4.1.3 Linearity Test on Drained Response to Loading and Water Table Fluctuation

Finally, the modelling system was tested to verify its capability to solve the linear governing partial differential equations (Equations [4.3], [4.4] and [4.5]) such that it

permits the use of method of superposition. Coupled seepage and load-deformation analyses were carried out to confirm that for a given set of typical conditions, the addition of the simulated changing pore-pressures for Equations [4.4] and [4.5] produced the same result as a simulation of Equation [4.3] or [4.1]. The simulations and superposition of changing pore-pressures for Equations [4.4] (the case of the load alone) and [4.5] (the case of water table fluctuation alone) provided the same result as the changing pore-pressures simulated for Equation [4.3] or [4.1] (case of coupling of loading and water table fluctuations).

The same domain and boundary conditions as discussed previously in Section 4.4 were used. The initial conditions were constant hydraulic head (hydrostatic) by specifying the arbitrary initial water table elevation, Y, (assumed 39m) and zero-stress change achieved by applying no load. The only distinguishing conditions for the three cases were the hydraulic and stress boundary conditions applied at the top of the domain.

In simulating the pore-pressure changes for Equation [4.4] (the case of the load alone) the typical stress top boundary condition (Figure 4.5) generated with the soil water balance was applied as shown in Figure 3.6. A constant hydraulic head boundary condition representing a constant water table elevation (39 m) was also applied at the top of the aquitard.

Equations [4.5] (the case of water table fluctuation alone) was simulated using the typical hydraulic head boundary condition (Figure 4.6) applied at the top of the aquitard. A zero-stress change boundary condition at the top of the aquitard was achieved by applying no load.

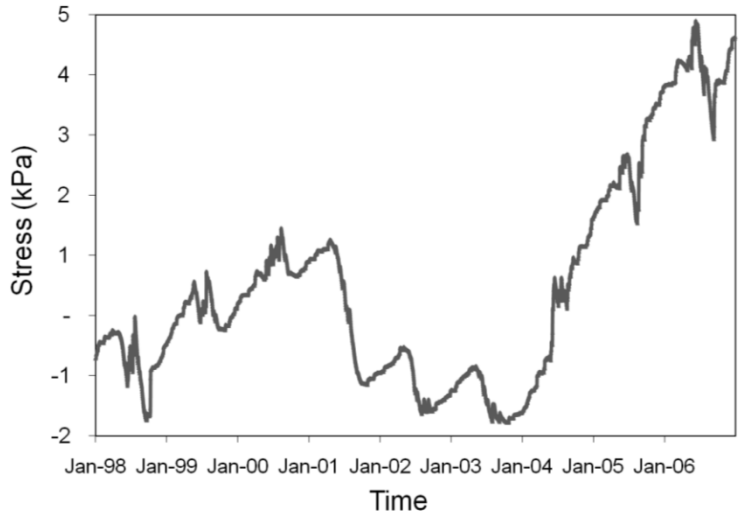

Figure 4.5. Top stress boundary condition due to mechanical loading pressure generated from meteorological measurements surface water balance

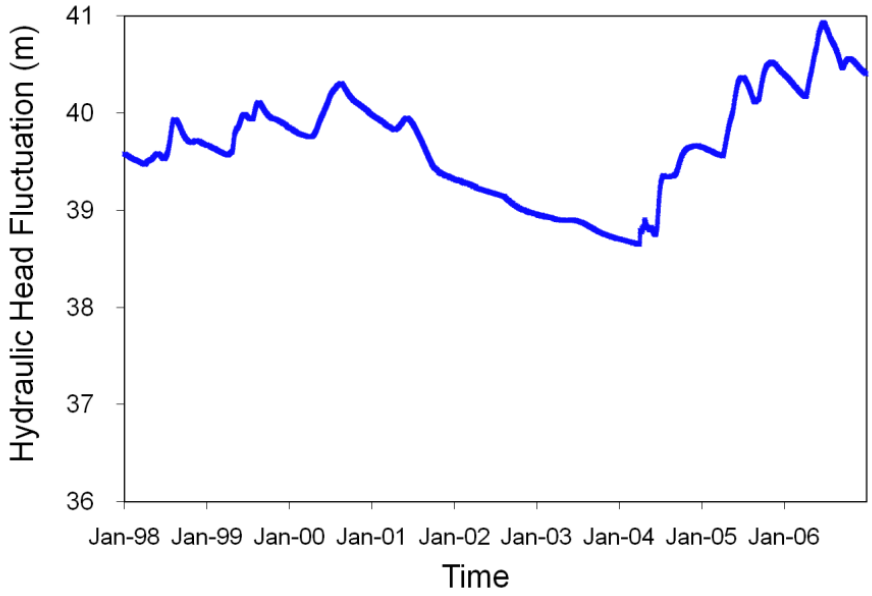

Figure 4.6. Top hydraulic head boundary condition from water table fluctation monitored with an aquifer piezometer (taking the elevation of the bottom of aquitard as zero-reference)

Simulation of Equation [4.3] (case of coupled response to loading and water table fluctuations) was carried out by applying both the stress change function (as in Figure 4.5) and the hydraulic head fluctuation function (as in Figure 4.6). All boundary conditions were set on monthly (30-day) time stepping rather than daily time stepping to

save modeling time. Since the stress and the hydraulic boundary conditions are cumulative, the larger time interval still captures the accumulation reasonably.

Linear response of pore-pressure in the saturated glacial till formation was achieved by using linear elastic constitutive materials in the model. An arbitrarily chosen hydraulic conductivity of 1×10^{-9} m/s (8.64×10^{-5} m/day) was used. A value of Young's modulus, E, of 528MPa was selected based on value derived from barometric response along with an assumed porosity of 0.26 and a Poisson's ratio of 1/3 (Equations [4.11] to [4.15]).

The results of pore-pressure changes for the simulations of Equations [4.4], [4.5] and [4.3] are shown in Figures 4.7, 4.8 and 4.9, respectively. The results of pore-pressure changes for the Equation [4.4] were added to results for Equation [4.5]. The pore-pressure changes resulting from superposition of Equations [4.4] and [4.5] were compared with the results of pore-pressure changes for Equation [4.3]. There was total (100%) agreement of the two model results thereby verifying the suitability of the model for solving the linear partial differential equations by the method of superposition. This gives confidence that the numerical model and method of superposition could be applied to obtain the key unknown field variable in this research, the observed pore-pressure responses to loading.

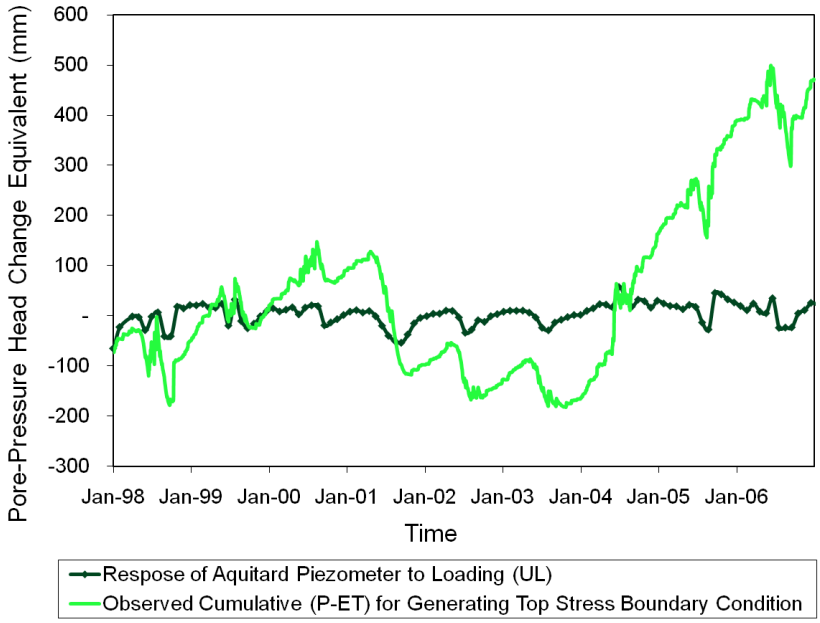

Figure 4.7. Modelled response of Aquitard Piezometer to Mechanical Surface Loading (also showing the water equivalent of the input top boundary load)

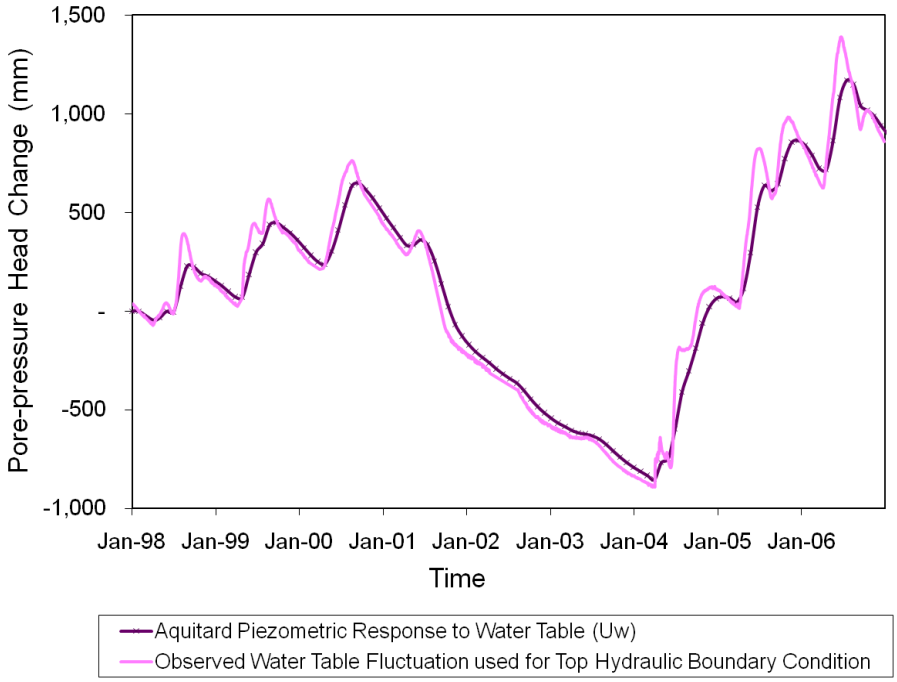

Figure 4.8. Modelled response of aquitard piezometer to the overlying aquifer water table fluctuation (and also showing the aquifer-piezometer-observed water table fluctuation used to produce the top hydraulic boundry condition)

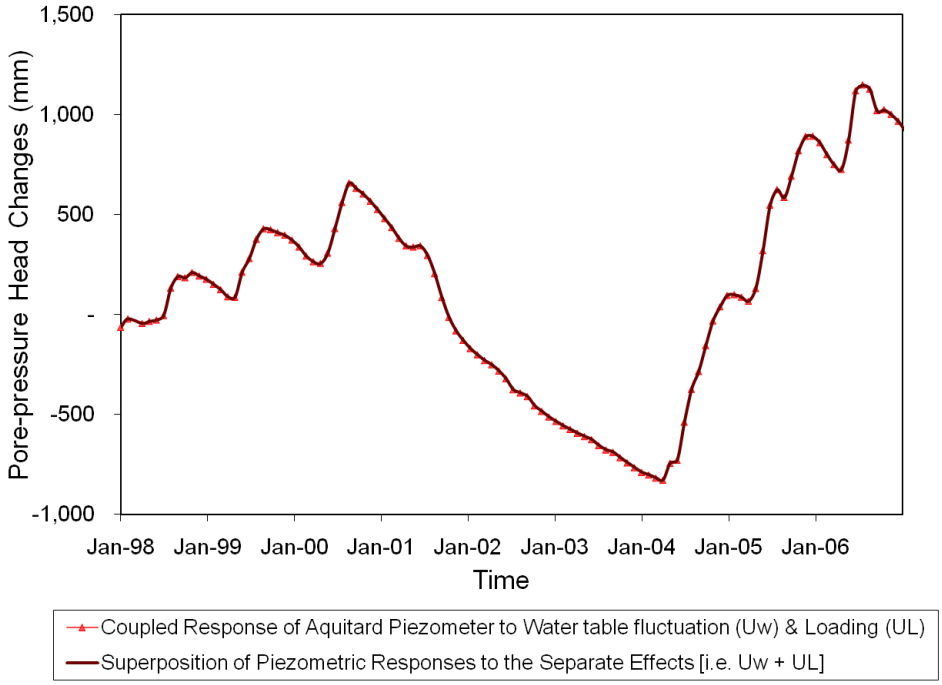

Figure 4.9. Comparison of the modelled coupled response of aquitard piezometer to water table fluctuation and loading, and Superposition of separate aquitard piezometric responses to water table fluctuation and loading showing a perfect (100%) agreement (a proof of linearity of solutions with the model)

4.4.2 Numerical Simulations and the Applied Superposition Steps

After the model verification, the next step was to determine the equivalent formation properties (especially the hydraulic conductivity) using the model. Numerical simulations of the incremental pore-pressure for Equation [4.3] were carried out using a set of daily field data for stress and hydraulic boundary conditions at the top of the aquitard as discussed in the previous section. The result was matched to the measured pore-pressure response of the aquitard piezometer corrected for both earth tide and barometric effects. This process of generating the equivalent formation properties for the model by achieving the best-fit simulation of the corresponding field measurement (observed aquitard piezometric response) is the model calibration (e.g. Barbour and Krahn 2004; Mercer and Faust 1981, p.4), which is discussed in the next section. Sensitivity of fitting (e.g. root mean square error (RMSE)) of simulations to the field measurements was tested for cases of varying depth (geometry) and cases of

correspondingly varying stiffness with depth. These sensitivity tests are discussed in subsequent sections of this chapter and the outcome of the tests are presented in Chapter 5.

The material properties from the calibrated model were then used to simulate the case of pore-pressure variations due to water table fluctuations as in the previous section. Subtracting these water table effects from the total measured changes of pore-pressure is theoretically expected to yield the responses to loading alone. These responses to loading isolated in this manner were compared to the response to loading represented by the water balance variations for the site as obtained from meteorological monitoring.

In modelling the "geological weighing lysimeter" problem discussed in this section, daily time steps were used rather than the monthly (30-day) time step used in preceding model verification. This is imperative in order to be able to calibrate model effectively as well as superpose results from water table fluctuations and aquitard piezometric response data, which were accumulated on a daily time scale. That also implied ensuring that all boundary conditions generated from water table fluctuation and loading were daily data as in Figures 4.5 and 4.6.

4.5 Model Calibration to Define the "Equivalent" Site Geology and Hydrogeology

The conceptual models developed prior to the development of a numerical model are idealised and simplified such that the potentially complex nature of the formation (e.g. heterogeneity) may not be fully captured. Therefore, the term "equivalent" was preferably used to qualify the subsequent parameters and conceptual geology obtained in this numerical modelling work. The assumption was that the properties obtained were large-scale, average values rather than specific localised properties. The conceptual models were also made simple to correspond to the available field data (e.g. borehole

logs and two piezometric installations) for a start (Barbour and Krahn 2004; Mercer and Faust 1981, p.6).

Even with the calibrated model parameters, it is difficult to tag any solution as "unique" since they are obtained by trial and error (Wang and Andersen 1982, p 110). This was evident in the way similar levels of fitting could be obtained for various sets of calibrated hydraulic and elastic parameters for different stratigraphic (single- and multi-layer) and geometric configurations. Karvonen (1997) also noted this lack of "unique" solution while calibrating a groundwater model by trial-and-error. This reason also contributes to the use of the term "equivalent" for any parameter determined through this numerical modelling.

4.5.1 Calibration Process

Calibration of the model was carried out using simulations of aquitard-pore-pressure changes arising from coupled water table fluctuation and loading from meteorological water balance (P – ET), and matching these to observed changes in aquitard pore-pressures, corrected for barometric effects and earth tide. The "best-fit" matching of model properties to the glacial till aquitard using the aquitard piezometric data was obtained by a trial-and-error process as commonly practiced in groundwater modelling (Mercer and Faust 1981, pp. 4, 55; Wang and Andersen 1982, p.109; Barbour and Krahn 2004). It was therefore important to carefully plan the process noting potential sources of fitting error from the understanding of the field conditions, limitations of measurement (data gathering) techniques and modelling assumption (e.g. Karvonen 1997). Though the ideal statistical best-fits should be very close to zero-error, in reality certain errors will remain. Therefore, in order not to allow the calibration process to last "indefinitely" in pursuit of "unrealistic" and "elusive" perfection in best-fit, it is important, before or at the early stage, of the calibration to determine:

i. The controlling parameters;

ii. The period for effective calibration; and
iii. The best-fit criteria relative to expected possible-errors.

Various sensitivity tests were carried out to evaluate the influence of till thickness and varying till stiffness with depth for single- and multilayer- profiles. In each case the best-fit K_v values were obtained by trial-and-error. K_v was considered the controlling variable out of the two major variables (S_s and K_v) and the explanation for this is given in the subsequent section.

4.5.1.1 The Controlling Parameter (K_v)

Given the large potential range (possibly orders of magnitude) of the value of K_v (Keller et al. 1986; Keller et al. 1988; Shaw and Hendry 1998) across the formation, it was decided to allow it to vary while assuming a constant value for the elastic (specific) storage, S_s, as derived from Skempton's $\bar{B}$ and porosity. Elastic properties (S_s or E) likely vary by less than a factor of 2 (far below even an order of magnitude) across the till thickness and were, therefore, assumed uniform for the entire domain. The effect of varying elastic parameters on pore-pressure response did not appear as significant as that arising from variations in K_v.

4.5.1.2 The Period for Effective Calibration

Transient residual (excess) pore-pressures (Schiffman and Stein 1970) due to historic water table fluctuation or loading disturbance that precede the simulation period would typically pre-exist in the pore-pressure profile (Keller et al. 1989). In order to avoid difficulties with some unknown "residual" pore-pressure transients appearing in the data set due to "forcing" that occurred before the onset of monitoring, it was decided that the results for the first 3 years be excluded from the calibration. This was based on

preliminary numerical modelling of the time for over 99.9% pore-pressure dissipation of a typical daily surface load applied for the entire period.

4.5.1.3 Best-fit Criteria Relative to the Potential Fitting-Errors

A curve-fit target of 70mm of root mean square error (RMSE), 200mm of absolute maximum error (AME) and 50mm mean absolute error (MAE), (e.g. description in Dawson et al (2007)), have been set for the fitness of the modelled 9-year drained response of aquitard-pore-pressure to the observed aquitard-piezometer response to daily moisture loading and water table fluctuation.

Though the calibration targets were arbitrarily set, they were chosen to reasonably accommodate "residual" fitting errors that could occur as a result of the assumptions made in measurement and modelling. Factors and possible sources of errors considered in choosing the calibration targets include: (i) the spatial variability in precipitation even in such a small catchment area; (ii) possible misrepresentation of evapotranspiration; and (iii) unaccounted mechanical surface loading or pressure changes (e.g. runoff losses and precipitation not captured in the model-input mechanical load, leakages in the formation).

i. Spatial Variability of Precipitation and Errors in Precipitation Measurement: Conditions of uniform precipitation were assumed to occur over the lysimeter site. This is contrary to observable spatial variability of the distribution of precipitation which could be up to 4% -14% even over as short as 100m distance for convection storm events (Goodrich et al. 1995). Faures et al. (1995) also observed variability in convective precipitation in modelling sensitivity of runoff to input precipitation from different gauge densities for a small catchment area of less than 4.4hectares. Consequently, the location of the climate station 1.3km (Barr et al. 2000) away from the "lysimeter" installation could also aggravate the

possible disparity between the meteorological water balance and the water balance observed at the lysimeter site. As a result of the spatial variability in precipitation, differences are expected between the modelled and actual piezometric responses in the calibration fitting. The precipitation gauge is also likely subject to undercatch during intense rain events. As high as 28mm to 38mm difference was found between an estimated 265mm-cumulative precipitation inferred from the lysimeter record and gauge measurements at the Old Aspen site (Barr et al. 2000). Therefore model calibration errors of up to tens of millimetres of water head equivalent could occur due to discrepancies between the precipitation measured at the flux tower and the actual precipitation at the lysimeter site.

ii. Possible Misrepresentation of Evapotranspiration: There could be disparity between the evapotranspiration (AET) occurring at the lysimeter site and the AET measured at a flux tower at the climate station located 1.3km apart due to variation in site top soil conditions.

iii. Lateral Flow into or out of the Site and Other Unaccounted Mechanical Surface Loading: The net lateral flow (runoff of groundwater) over the site was considered negligible in the estimation of vertical water balance used for generating the input load in the model. The semi-arid site climate (Conly and van der Kamp 2001) (as well as fairly flat topography, permeable top soil (Barr et al. 2000) and relatively low water table position) favours this assumption. However, this assumption could become invalid under "highly wet" conditions when runoff due to snow melt and rainfall may become significant. Surface runoff from the watershed in which the site is located was observed but not measured at a location about 2 km north of the site during the wet summers of 2005 and 2006. Independent measurement of runoff to account for the net lateral losses or gains could improve the modelled site water balance for such wet periods. Finally, the risk of other surface loading sources is low since the site is on a reserved national park area with minimal human disturbance, such as pumping or surface-forcing, (Barr et al. 2000; van der Kamp et al. 2003) that could affect the ground water pressure.

4.5.2 Sensitivity Tests and Numerical Considerations

Sensitivity-analyses were carried out in which one parameter of interest was varied while keeping others constant to understand and apply the effects (e.g. Barbour and Krahn 2004) to obtaining the best-fit modelled pore-pressure response of the aquitard piezometer. This was necessary because of insufficient site data. Simulations were conducted to test the sensitivity of the modelled "lysimeter" pore-pressure response to: (i) discretisation of space and time; (ii) initial offset of the boundary conditions; (iii) geometry (thickness) of aquitard; (iv) variation of elastic properties (E or Ss) with depth; and (v) hydraulic conductivity.

In order to ensure high accuracy of simulation-results with minimal numerical approximation (truncation) errors, oscillation "noise" and numerical convergence, optimisation of model discretisation was carried out (e.g. GEOSLOPE 2008). Sensitivity analyses of simulation-results to time-step and element mesh discretisation were also carried out. Subsequently, appropriate mesh for selected time stepping was ensured in all simulations in this work.

4.5.2.1 Sensitivity of Results to Discretisation of Space and Time

Inherent in the finite element method is the discretisation of time and space to represent what are "continuous" partial differential equations. Consequently, it is necessary to check the accuracy and stability (convergence) of the solution obtained for the chosen level of discretisation (Mercer and Faust 1981, p.32; Barbour and Krahn 2004). Therefore the sensitivity of solutions to various spatial and temporal refinements of the discrete approximation was considered (Zienkiewicz and Taylor 2000, p.402). Time stepping was already fixed to (i.e. not finer than) daily time step in this research. This

was to conform to the daily water balance and piezometric data used as input in the model.

Consequently, the only other discretisation option was to test the refinement of the spatial discretisation as approximated by either p-refinement (interpolating polynomial integration order) or h-refinement (mesh size) (Zienkiewicz and Taylor 2000, p.402). It was decided to leave the element type as 4-noded (square) quadrilateral but vary the mesh sizes. Since the problem being solved is transient, the mesh sizes (close to the drainage face) were selected to suite the initial time stepping (GEOSLOPE 2007) to avoid numerical oscillations in results (Barbour 2007).

The relationship between the consolidation dimensionless time factor, T_v, diffusivity, D, (K_v/S_s), initial "perceptible" drainage time (reaction time) for an element, t_e, and (the longest) drainage path, h_e, for typical elements close to the drainage boundary were applied in making initial guesstimates of appropriate pair of element size and initial time steps (Barbour 2007):

$$t_e = \frac{{h_e}^2 T_v}{D} \qquad [4.18]$$

where h_e was taken as the height of the one-way draining square element (assumed pervious top and impervious bottom); a reasonable estimate of D was used (1.5 m^2/day); and T_v for about 30% initial consolidation was recommended (Barbour 2007) which has to be referenced from degree of consolidation-T_v charts for the given drainage condition and loading (usually from 0.1; e.g. from Figure 3.9). For convenience, T_v of 1 for significant consolidation (about 90%) was used; this is similar to the calculation of a "characteristic time", t_c, by van der Kamp and Maathuis (1985). Therefore, t_e is taken as the characteristic time of the element, t_{ce}.

The initial drainage time step, t_i, was then assumed as time for drainage through the first few, N number of (e.g. at least 2 to 3) elements near the boundary, for any chosen element size (Barbour 2007):

$$t_i = Nt_{ce} \quad [4.19]$$

Substituting t_e (i.e. t_{ce}) in terms of t_i from Equation [4.19] and T_v of unity in Equation [4.18] then element size:

$$h_e = \sqrt{\left(\frac{t_i D}{N}\right)} \quad [4.20]$$

which becomes:

$$h_e = \sqrt{\left(\frac{D}{2}\right)} \quad [4.21]$$

given that time step t_i is fixed to 1-day, D in m^2/day and the number of elements considered near the boundary, N, of 2. Guided by the use of Equations [4.20] and [4.21], simulations were run using different meshing, h_e, choices with 0.5m- and 2.5m-square elements, respectively. In addition, 0.25m-square-element meshing was also applied for curiosity. The different mesh sizes (e.g. Barbour and Krahn 2004; GEOSLOPE 2007) (0.25m-, 0.5m-, and 2.5m-square meshes) were used to run simulations (of Equation [4.3]) for the calibration while retaining the same hydraulic and elastic properties and then comparing their "best" fitting statistical parameters.

4.5.2.2 Sensitivity to Initial Offset of Boundary Conditions

Historic site data (e.g. pore-pressure measurements) are required to make realistic estimates of the initial offset(s) of the model input data. However, there are insufficient

historic data preceding the modelling period to guide in specifying representative initial offsets of the boundary conditions for both water table fluctuation and the applied load at the top of aquitard. Therefore, sensitivity analyses were conducted to evaluate the effect of variation of the initial offset on the modelled aquitard pore-pressure response. These analyses were required, particularly to assess how long-lasting the transient pore-pressures resulting from the initial offset (step change) of boundary conditions would be and how they impact the selection of the effective calibration period. Getting the right setting of the boundary conditions could also be a critical part of the solution (e.g. GEOSLOPE 2007). The associated sensitivity tests could also provide further insight on the behaviour of the model relative to the physical system.

First, simple simulations of the separate cases of loading (Equation [4.4]) and water table fluctuation (Equation [4.5]) were generated using sustained one-step changes of the respective key boundary conditions. Superposition of the results of these simple simulations produced the coupled response to the combined simple one-step boundary conditions. These simple cases were generated to facilitate understanding of the trends and effect of the separate initial offsets on the "residual" pore-pressure changes discussed previously (section 4.5.1.2).

Next, Equation [4.3] was simulated. Three coupled simulations involving different initial offsets of the top hydraulic boundary condition combined with a stress boundary of zero-initial offset were used to study the effect of offsetting the hydraulic head at the water table. The initial offsets of top hydraulic boundary considered are: (i) zero-initial offset; (ii) 100mm-initial offset; and (iii) 36mm-initial offset of water table. Similarly, to study the effect of initial offset of loading, three simulations of coupled response to different initial offsets of top stress boundary conditions and hydraulic boundary of zero-initial offset were carried out. The initial offsets of the top stress boundary were: (i) zero-initial offset; (ii) 100mm-initial offset; and (iii) -72mm- initial offset of water head equivalent of applied load. Simulations with 50mm- and -50mm-initial offsets of the boundary conditions were only included in the sensitivity analyses of the isolated cases of water

table and loading effects, respectively. The durations for the dissipation and/or full propagation of each case of initial offset were noted. The trends of the modelled pore-pressure-responses were studied as valuable information for the calibration.

4.5.2.3 Sensitivity to Geometry of Glacial Till

The available site bore-hole logs (Appendix A) do not give sufficient information on the site profile to the basement rock as discussed previously. Consequently, simulations of Equation [4.3] (coupled water table fluctuation and loading) were generated for the same material properties but using various thicknesses of the glacial till aquitard domain. Thicknesses of 22.5m, 40m and 60m were used. Simple top boundary conditions of one-step (100mm-water equivalent) loading and similar (100mm) water table change were applied to the first set of simulations to examine their consolidation (or pore-pressure propagation) rates. Finally, the same types of coupled simulations were run for all three geometries using the typical boundary conditions from field measurements; the procedure applied to obtain their respective optimum material property (K_v) is discussed in the subsequent section 4.5.2.5.

4.5.2.4 Sensitivity to Variation of Stiffness in Strata with Geometric Depth

The elastic properties of soils are known to often vary with depth and effective stress profile (e.g. Santucci de Magistris et al. 1998). Elastic properties (Skempton's $\bar{B}$, E and S_s) were only determined for one location in the aquitard profile (34.6m depth) using the available piezometric measurements. In the absence of any additional piezometric data to derive the profile of elastic parameters in the aquitard, a simple linear extrapolation of elastic properties with effective stress profile was applied.

The sensitivity of the aquitard piezometric response to degrees of variation of elastic properties with depth was evaluated. The linearly varying elastic Young's modulus, E, with effective stress, $\acute{\sigma}$, profile used for the aquitard was approximately E of 1000 times $\acute{\sigma}$ (i.e. a slope of 1000 for E-$\acute{\sigma}$ graph). Different degrees of (refinement of) the linear variation of elastic properties were achieved by using different multi-layer- (multi-region-) systems on a given domain with differently specified elastic property on each region. Constant hydraulic conductivity was, however, applied to the entire domain. Elastic properties of about the mid-point of each stratum were applied as the average elastic property of each layer to achieve the linear profile of elastic properties. Two geometries were used, a 22.5m thick aquitard and a 60m thick aquitard. First, measured elastic properties (at 14.6m below top of aquitard) were applied as average properties in the respective single region model for each of the two geometries.

The three stratified cases of the 22.5m-thick domain were: (i) single (undivided) region-, (ii) 3-region-, and (iii) 5-region-models. The fitting (RMSE) of modelled aquitard piezometric response (simulation of Equation [4.3]) relative to observed data were compared for the three cases, as a basis for evaluating the sensitivity to the degree of variation of elastic properties. The degree of disparity or close agreement of the their fit (RMSE) would be the basis for deciding whether to model the 22.5m-thick domain as a single region (assumed homogenous stiffness) or multi-region (assumed heterogeneous stiffness profile), respectively.

The 60m-thick aquitard domain was similarly simulated and evaluated using three cases of: (i) single (undivided) region, (ii) 2-region, and (iii) 6-region models. This geometry was included to examine the effect of variation of elastic properties across the depth of a high thickness formation. It was chosen as a continuous aquitard after it was confirmed, from preliminary simulation of the multilayer systems, that laterally extensive intertill sand aquifers do not exist at such depths.

The lowest RMSE between modelled to observed aquitard piezometric responses to water table and loading for the two geometric cases was used to evaluate and select the better fit. The best-fit and simplest stratigraphic case was then considered for use in the final calibration process.

4.5.2.5 Sensitivity to Variation of Hydraulic Conductivity (Kv)

The hydraulic conductivity had been identified as a controlling parameter in the calibration process due to its potentially larger variation across the aquitard profile (could be in orders of magnitude) compared to the elastic properties. However, to test this hypothesis, sensitivity-simulations and assessment of the effect of varying K_v on the aquitard piezometric response (to water table and loading due to change of water balance) were carried out.

Several simulations of coupled water table fluctuation and loading (Equation [4.3]) were generated trying different values of K_v, while keeping the elastic properties constant. The fitting parameters (RMSE, MAE and AME) of the modelled to the observed aquitard piezometric response were compared. These were done for three conceptual geometries: 22.5m-, 40m- and 60m-thick aquitard models. Therefore, the final calibration exercise was based on selecting the hydraulic conductivity and the associated conceptual model-geometry that produced the best fit (lowest combination of fitting errors) as the "equivalent hydraulic conductivity" of the aquitard.

4.6 Application of Modelling to "Weighing Lysimeter" Interpretation

The essence of the calibration was to obtain the best parameters defining the aquitard behaviour. Subsequently, these material properties were applied in generating specific

simulations which were used to eliminate most of the overlapping transient pore-pressure (flow) interfering with the "lysimeter" observations.

4.6.1 Modelled Aquitard-Piezometer Response to Water Table Fluctuations

The response of the piezometer in the aquitard formation to the water table fluctuation alone (Equation [4.5]) was modelled using the best-fit values of elastic and hydraulic parameters (S_s and K_v) from the model calibration. This simulation was made using the hydraulic boundary conditions generated with the daily measurements from the aquifer piezometer (as shown in Figure 4.6) for the top of the aquitard. Since the simulation was run on the same coupled stress and seepage model, a constant stress (zero stress change) boundary condition also applied at the top of the aquitard. Daily time steps were also used in order to enable superposition with the daily aquitard piezometer observation cleaned of atmospheric and earth tide "noise".

4.6.2 Observed Aquitard Pore-pressure Response to Total Soil Moisture Changes

Pore-pressure response to the water table fluctuation was then subtracted from the observed pore-pressure response, since superposition is admissible, to obtain the long term pore-pressure response due to loading by changes in total soil moisture (site water balance) alone and the associated consolidation drainage. The yardstick for assessing the performance of the results of the "lysimeter-" measurements of change in total soil moisture relative to the changes in measured meteorological water balance was the comparison of the modelled pore-pressure response to the change in meteorological water balance and the corresponding observed pore-pressure response of the "lysimeter".

5 CHAPTER 5 - DISCUSSION OF RESULTS

5.1 Overview of the Calibration, Sensitivity and the Key Results

The outcome of matching the observed and modelled aquitard pore-pressure responses to calibrate the model is presented in this chapter along with a series of sensitivity studies on discretisation, domain geometry, spatially dependent properties and boundary conditions. The implications of these insights into model behaviour relative to field conditions are also discussed in the light of the limited site data. The aquitard pore-pressure responses to water table fluctuations simulated using calibrated model parameters are also presented. The pore-pressure responses to the site water balance is then isolated and compared to the meteorological water balance for the site. The significance of the key results and their potential applications are also discussed.

5.2 Outcome of Calibration (S_s and K_v)

The results of the final model calibration are presented in Figure 5.1. The large fitting error in 2006 (a wet year like 2005) was possibly due to errors in under-catchment by the precipitation gauge (Barr et al. 2000) or the result of increased total moisture arising as a result of lateral flow within the aquifer. Similar changes in water storage at the water table of an aquifer were suggested by Bardsley and Campbell (1994, 2000) in a related "geological weighing lysimeter" study. The large fitting error in spring 2005 may be due to runoff losses.

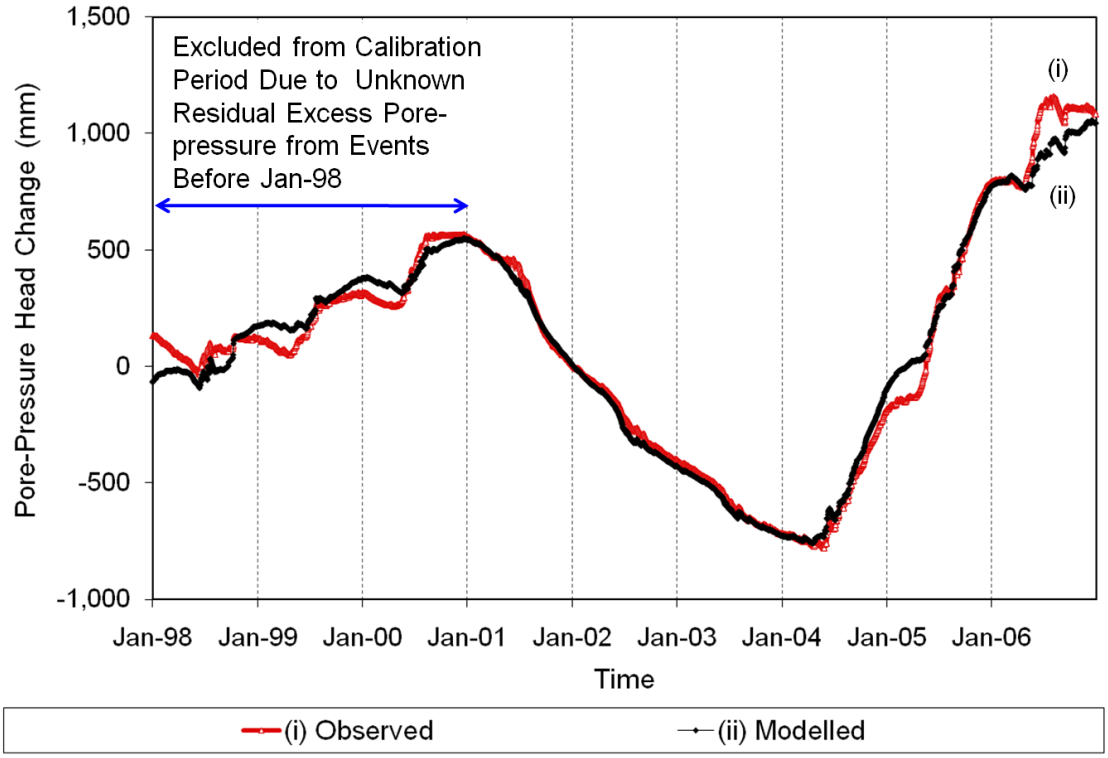

Figure 5.1. Calibration "best fit" of (i) Observed; and (ii) Modelled pore-pressure responses for Old Aspen Site (considering 2001 – 2006 as effective calibration period)

The calibration produced a diffusivity of 1.52 m^2/day (1.8 x 10^{-5} m^2/s) for the till. The field-calibrated-geotechnical parameters defining the "equivalent" geology and hydrogeology of the formation are shown in Table 5.1.

Table 5.1. Summary of Field-Calibrated Properties[7] of the 22.5m-thick Glacial Till

Vertical Hydraulic Conductivity,	Elastic (Storage) Parameters						Hydraulic Diffusivity (C_v, equivalent),
K_v	$\bar{B}$	E	m_v	υ	n	**S_s**	**D** or **K_v/S_s**
(m/day)	[ ]	(MPa)	(kPa^{-1})	[ ]	[ ]	(m^{-1})	(m^2/day)
2.1x10^{-5} (2.4x10^{-10})	0.91	528.318	1.26x10^{-6}	0.33	0.26	1.36x10^{-5}	1.52 (1.8x10^{-5})

The vertical hydraulic conductivity, K_v, was estimated at 2.1 x 10^{-5} m/day (2.4 x 10^{-10} m/s) with specific storage, S_s, of 1.36 x 10^{-5} m^{-1} (using drained confined compressibility, m_v, of 1.26 x 10^{-6} kPa^{-1} or the inverse of confined elastic modulus, E_c, of 793MPa). The

[7] The values in bracket are K_v and D values in the units of (m/s) and (m^2/s), respectively.

calibrated K_v of the model agrees with the reported range for glacial till in Saskatchewan (Keller et al. 1986; Keller et al. 1988; Keller et al. 1989; Shaw and Hendry 1998). The other properties of the till include the measured Skempton's $\bar{B}$ coefficient of 0.91, the assumed porosity, n, of 0.26 and the drained Young's modulus, E, of 528MPa assuming a Poisson's ratio, υ, of 1/3. The E value, obtained from piezometric measurements, falls within the reported range of values of in situ modulus of elasticity of 496MPa to 1475MPa (72,000 – 214,000 psi) for dense, overconsolidated glacial till in a site in northern Saskatchewan obtained through in situ plate loading tests, rebound gauge and settlement observations (Klohn 1965), as well as the other reported values on Table 3.1.

Although porosity of 0.26 was assumed, the use of any other value of porosity out of the reported range of 0.26 to 0.36 would be satisfactory since the elastic parameters for clay till of Skempton's $\bar{B}$ of 0.91 is not significantly sensitive to porosity (Appendix C). Consequently, the elastic parameters obtained for glacial clay till at the level of the aquitard piezometer could potentially vary with the porosity value selected; for instance, Young's modulus, E, may vary between approximately 380MPa and 530MPa (by less than a factor of 1.4) for porosity values of 0.36 and 0.26, respectively, using Equations [4.12] and [4.15].

5.3 Outcome of Sensitivity Analyses

5.3.1 Effect of Discretisation

The results of the sensitivity studies of mesh refinement are shown in Table 5.2. They were analysed using the fitting error of modelled to observed aquitard piezometric responses. The results for 2.5m-, 0.5m- and 0.25m-square element meshing were almost identical with the last two results showing (an almost insignificant) marginally better calibration fit. The 0.5m-square element meshing was used for all the simulations.

Table 5.2. Sensitivity of model-results to mesh-size refinement with 1-day time step

Square-Element Size (m)	Calibration "Best-fit" RMSE (mm)	MAE (mm)	AME (mm)
0.25	63.1	42.7	222.1
0.50	63.1	42.6	222.5
2.50	63.1	42.7	222.9

5.3.2 Effect of Initial Offset of Boundary Conditions

The simulation of a single-step loading sustained through the modelling period defined the time required for near full dissipation (over 99.9%), of the generated excess pore-pressure. Not surprisingly, a similar time was obtained for full propagation of a single-step water table change to the aquitard-piezometer. Figure 5.2 shows the characteristic time, t_c, as 333days and times for near full dissipation or propagation, $t_{99.9\%,}$ of approximately 3 years for both the drained load response and transient pore-pressure accumulation due the simple offsets of loading and water table, respectively. These time estimates were considered in evaluating an effective model calibration period that would be influenced by minimal unknown pore-pressure dynamics.

The initial 3 years of monitoring data were ultimately excluded from the calibration data set. The convergence of various initial excess pore-pressures arising from different initial load offsets (in Figure 5.3) is evidence that the discounted period correctly eliminates effects of unknown "residual" pore-pressure responses to loading history of any magnitude. Similarly, Figure 5.4 shows convergence of results of different modelled aquitard-piezometric responses to observed water table fluctuations and water-balance-loading, for stress boundary conditions having initial offsets of 0mm-, 72mm- and 100mm-water head equivalent.

The combined response of the aquitard piezometer to the sustained single-step offset of loading and change in water table elevation (Figure 5.2 (c)) clearly show that the effect

of change in water table dominates in the long term. This trend is as anticipated since load-induced pore-pressure change decays at the same rate as the water-table induced aquitard-pore-pressure grows, although in an inverse manner. For the case of an isolated single-step change in the water table elevation (Figure 5.5(i), (ii) and (iii)), the pore-pressure propagated to the piezometer comes close to equilibration at approximately 3years ($t_{99.9\%}$), irrespective of magnitude of the initial water-table-offset. This is the same as the approximate equilibration time in the load-response shown in Figure 5.3.

The modelled piezometric response to measured stress and hydraulic boundary conditions used to study the influence of offsetting the hydraulic boundaries (by 36mm and 100mm) (Figure 5.6(ii) and (iii)) were obtained by superposition. These results were compared with the case of simulation of piezometric response to zero (0mm) initial offsets of observed hydraulic and stress boundary conditions (Figure 5.6(i)). As expected, the magnitude of the pore-pressure change separating each of the results of the offset cases (Figure 5.6) remained constant after the 3-year equilibration time, thereby producing identical trends in all results within the modelling period that followed.

Given that the equilibration time of the model is easily discounted from the available data set (3 out of 9 years), offsetting the boundary conditions (particularly water table elevation) is, therefore, not critical to the calibration. Offsetting the boundary conditions would have been critical to the solution if the aquitard were to have a characteristic (or equilibration) time larger than the duration of available data. The post-equilibration identical trends (Figures 5.4 and, particularly, 5.6) provide insight and evidence that during the calibration more emphasis should be laid on matching the trends first rather than matching the exact points (e.g. by minimising the RMSE). This implies that if the trend of the observed pore-pressure is correctly modelled, any existing constant separation of the modelled and the observed responses could then be bridged by offsetting.

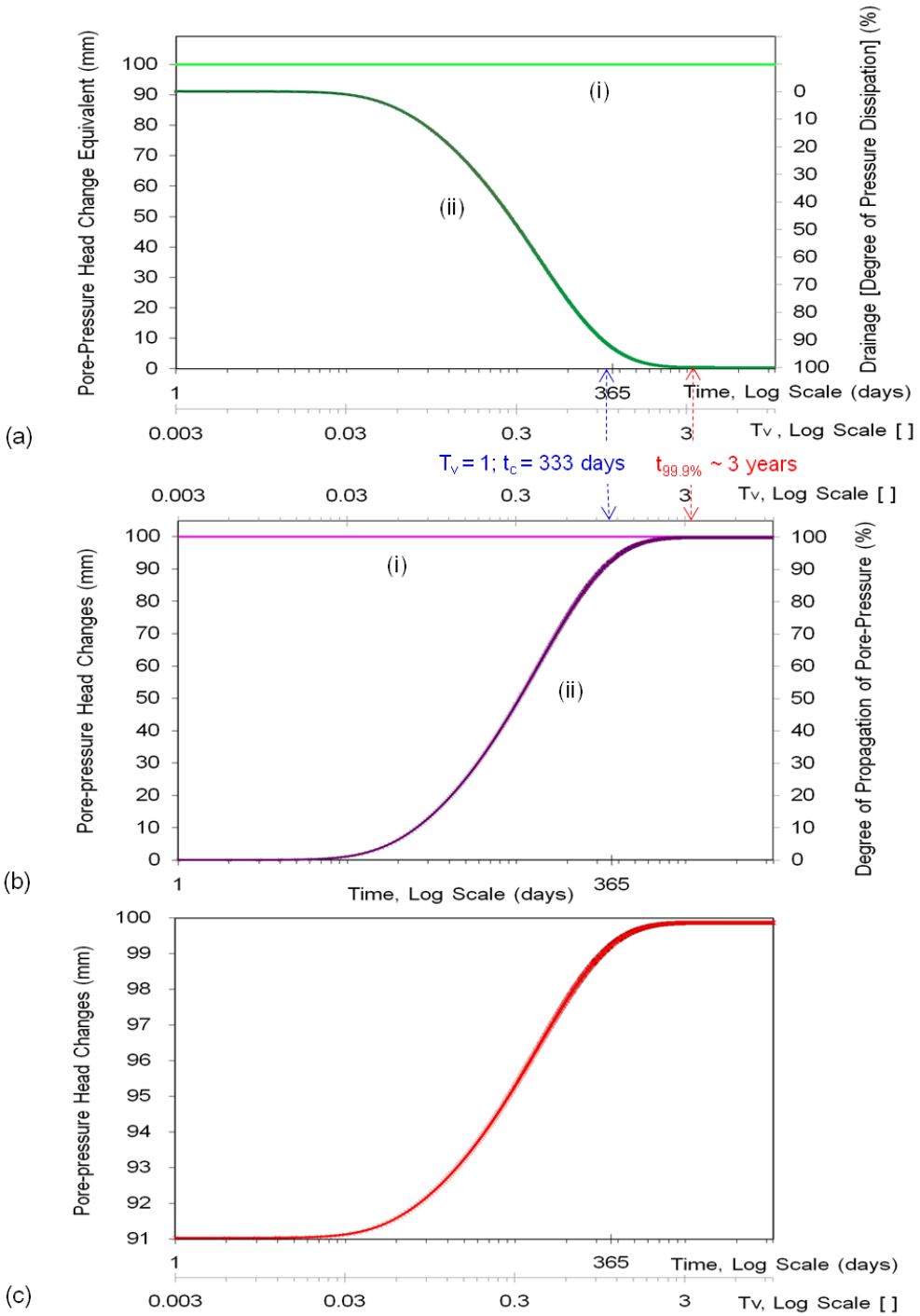

Figure 5.2. Aquitard-piezometer-response to (a) single-step loading and (b) water table change, and (c) the coupled or superposed responses [i.e. (a) + (b)] showing characteristic time, t_c, and time for near full dissipation ($t_{99.9\%}$) or propagation; [in detail: a(i) single-step load sustained to infinity; a(ii) drained aquitard-piezometer-response to load; b(i) single-step water table change; b(ii) transient pore-pressure propagation to the aquitard piezometer; and (c) aquitard-piezometer response to both load and water table change]

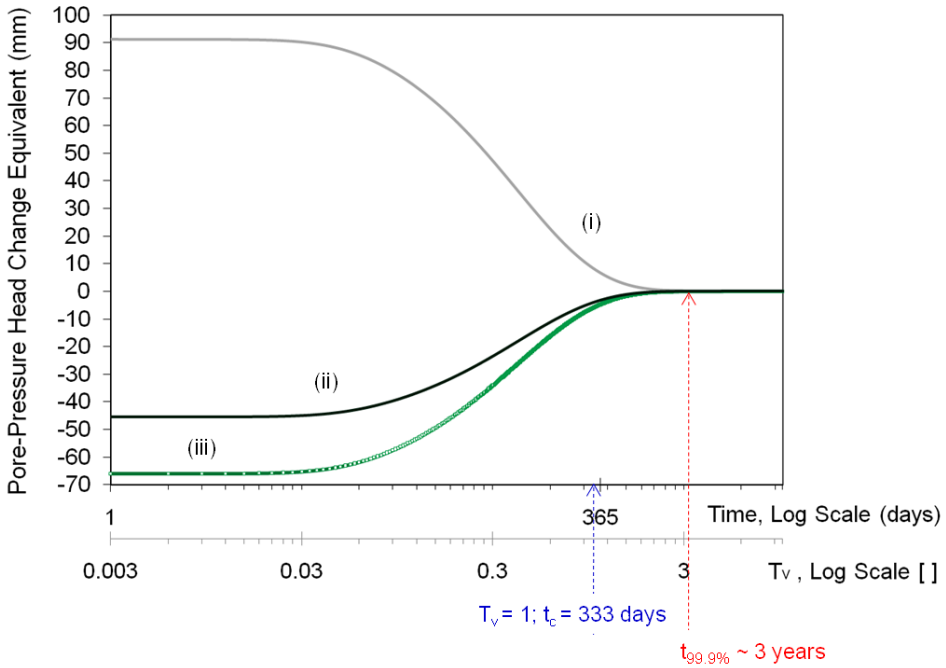

Figure 5.3. Effect of offsetting the measured load showing modelled drained response of aquitard-piezometer to: (i) 100mm-, (ii) -50mm- and (iii) -72mm-water-head equivalent of applied initial load offsets showing close convergence (equilibration) of the drainage at approximately 3 years ($t_{99.9\%}$)

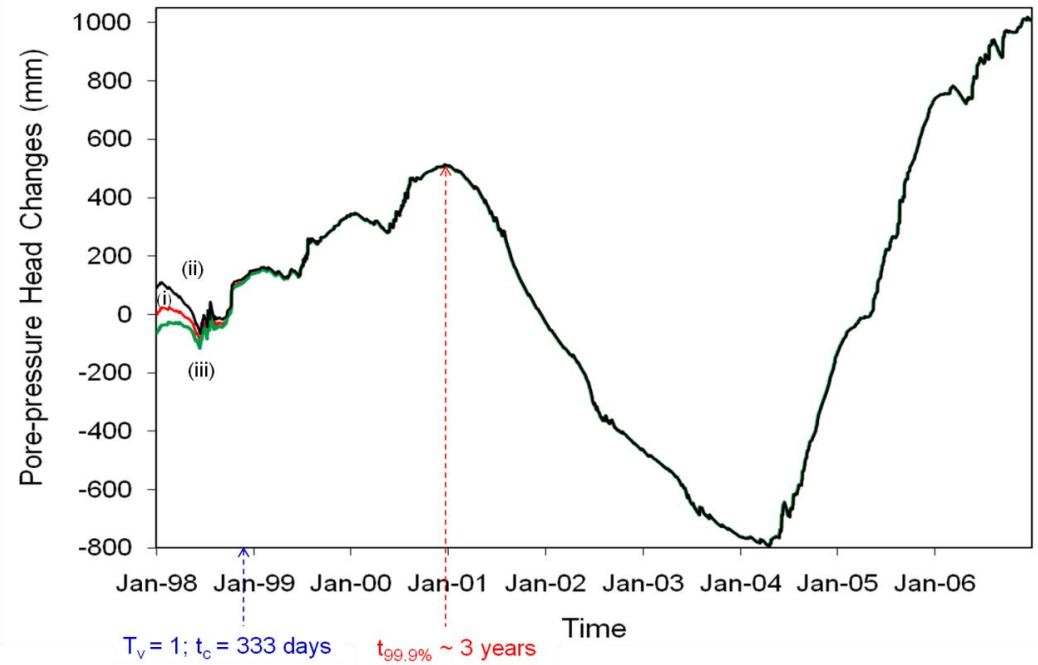

Figure 5.4. Effect of offsetting the measured load showing modelled response of aquitard piezometer to observed water table fluctuation and (P – ET) water balance load with initial offsets of: (i) Zero-, (ii) 100mm- and (iii) -72mm-water head equivalent load

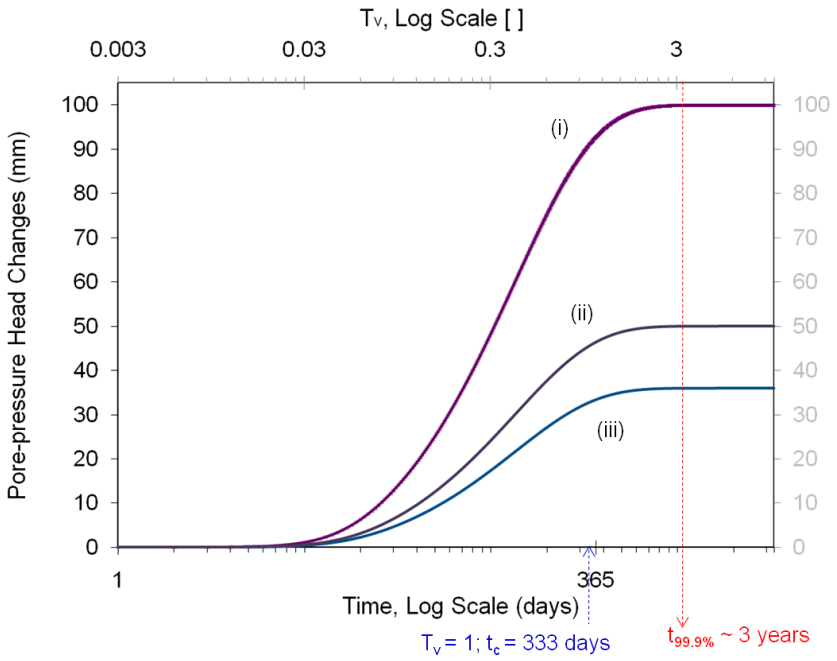

Figure 5.5. Effect of offsetting the changing water table: Modelled drained response of aquitard-piezometer to single-step water table changes with initial offsets of: (i) 100mm, (ii) 50mm and (iii) 36mm, respectively, showing time for near full propagation of the water table change to the aquitard-piezometer ($t_{99.9\%}$) common to all the offset cases

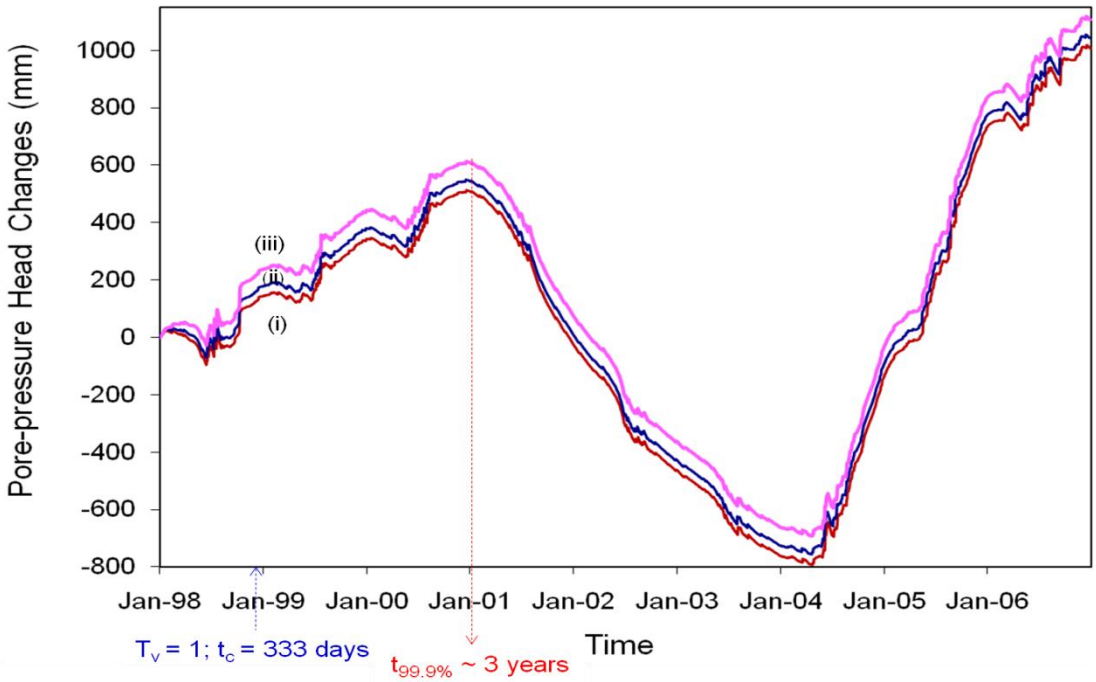

Figure 5.6. Effect of offsetting the observed changing water table: Modelled response of aquitard piezometer to measured (P – ET) stress and water table fluctuation with initial offsets of: (i) zero (0mm-), (ii) 36mm- and (iii) 100mm- change in water table elevation

5.3.3 Effect of Varying Geometry of Aquitard

The results of the sensitivity study for aquitard thickness are shown in Figure 5.7. The results indicate that drainage and propagation of pore-pressure changes to the piezometer are sensitive to the thickness of the domain. The 60m-thick glacial till aquitard had the longest consolidation time (t_c or $t_{99.9\%}$) followed by that of the 40m-thick geometry and the 22.5m-thick, which had the fastest drainage. This was as anticipated from the direct proportion of consolidation time with the square of the drainage path, that is, the square of domain thickness, (h_d^2) (Terzaghi 1925) similar to Equation [4.17].

The implication of these trends for conceptualising the domain geometry of the model and the calibration is that poorer fitting (RMSE) of the model results to the observations occurred with increasing aquitard-thickness. Though the thickness of the whole glacial till deposit may be up to 100m, the simple single-region (layer) conceptual model (of assumed uniform "equivalent" properties) fails to match the aquitard piezometric response for the case of a high thickness aquitard. That is, the "best-fit" of the high thickness models (e.g. 60m thick aquitard) show a wider fitting error than that of the low thickness aquitard models (e.g. 22.5m thick aquitard). This may be attributed to potentially wider variations in properties due to heterogeneity of hydraulic conductivity (e.g. Keller et al. 1986, 1988; Shaw and Hendry 1998) and elastic properties with depth which "equivalent" properties could not fully represent.

Consequently, modelling with a thicker model domain would demand more information to incorporate the heterogeneity of material properties with depth, which, unfortunately, is not available given the limited drilled depth and the single piezometric installation in the aquitard. Therefore, in applying the prudential modelling approach of starting simple and keeping model complexity commensurate with available data (Barbour and Krahn 2004; Mercer and Faust, 1981, p.6) as well as considering the overall "best-fit", the 22.5m-thick aquitard conceptual model was then adopted.

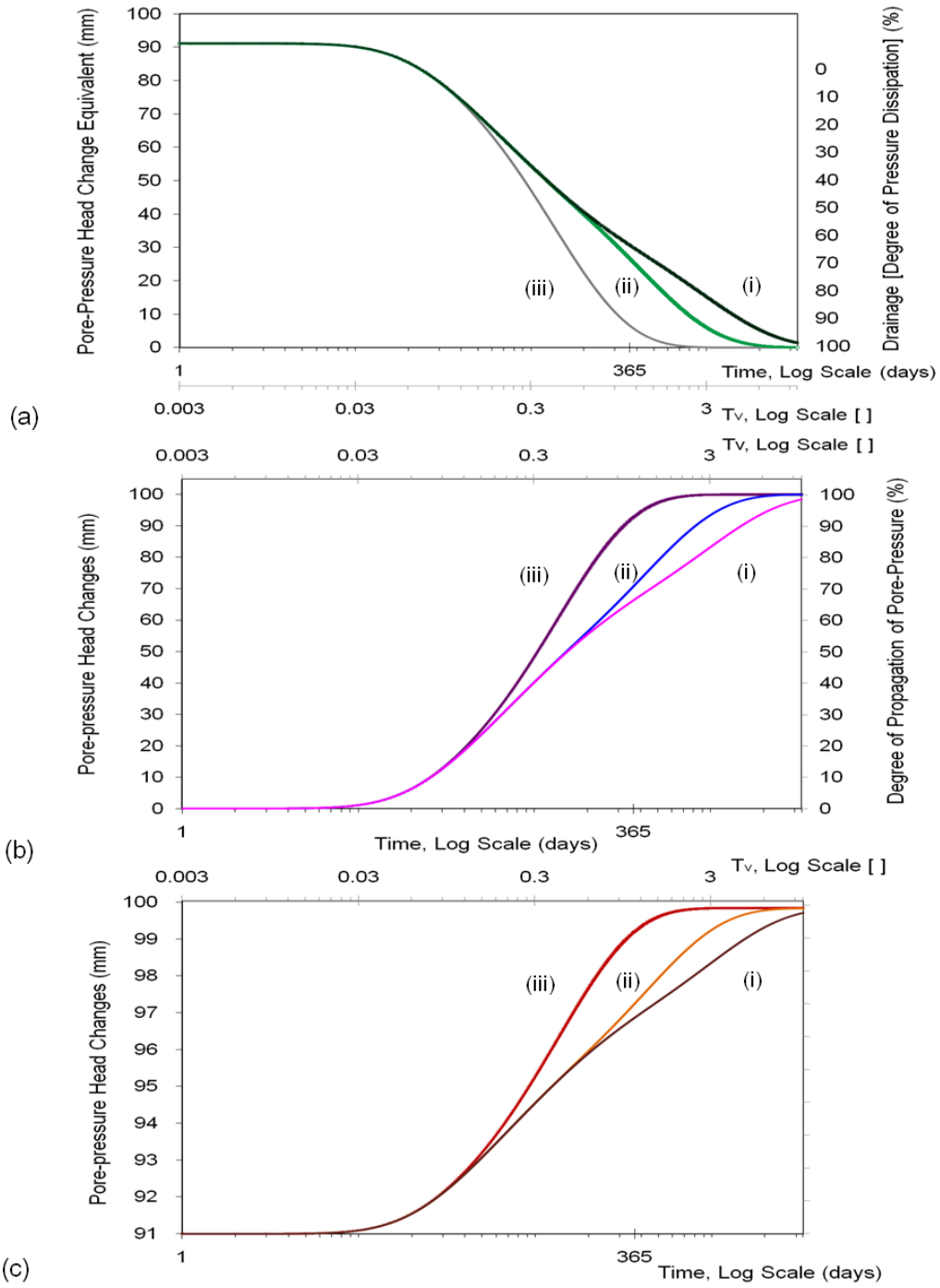

Figure 5.7. Effect of geometry: (i) 60m-, (ii) 40m- and (iii) 22.5m-thick glacial till on modelled response of aquitard-piezometer to (a) sustained 100mm-water pressure head equivalent one-step load; (b) 100mm change in water table elevation; and (c) combined effects of water table and loading [i.e.(a) + (b) for corresponding (i),(ii) & (iii)] (see section 5.3.5 for optimal K_v and associated RMSE for the 3 geometries)

5.3.4 Effect of Varying Elastic Parameters (S_s or E) with Depth

The results of the sensitivity study into the influence of varying elastic properties with depth are presented in Figures 5.8 and 5.9 for simple single-step changes in water table and loading for 22.5m- and 60m-thick aquitard models respectively. The thicker model (60m-thickness) was included in order to evaluate the sensitivity of the degree of variation of elastic properties over a greater depth.

The cases of 1-, 3- and 5-elastic-region-models of the 22.5m-thick aquitard model, were roughly identical for the aquitard-piezometer response to simple (single-step) water table and load changes separately as well as their combined effect (Figure 5.8 (a), (b) and (c)). The three cases were not even easily distinguishable for labelling in the plot. The fitting of the observations with the model results for the three cases (1-, 3- and 5-layer-models) were approximately the same with less than 1mm difference in their RMSE. Therefore, it was inferred that the variation of elastic properties with depth is not critical to the solution of the 22.5m thick conceptual model, which justified the adoption of the 1-region model.

Contrary to the trends for the 22.5m-thick model, the modelled piezometric responses for 60m-thick model showed some sensitivity to the degrees of variation of elastic properties (in 1-, 2- and 6-layer-models) with depth (the (i), (ii) and (iii) plots in Figure 5.9 (a)-(c)). They indicate that drainage was faster for the multi-layer systems (of higher overall stiffness) than the single-layer model. The results and calibration fitting of modelled to observed aquitard pore-pressures indicate that even a simple variation of elastic properties using 2-elastic-regions resulted in about 20% reduction in fitting error (RSME) relative to that of the 1-layer (uniform property) model. In summary, variation of elastic parameters with depth is critical for only thick domains. However, in order to continue to keep models as simple as the available data (Barbour and Krahn 2004; Mercer and Faust 1981, p.6) and due to poorer fit of the “best-fit” of the 60-m-thick model relative to the fit of the 22.5m-model, the 60m-thick model was discarded.

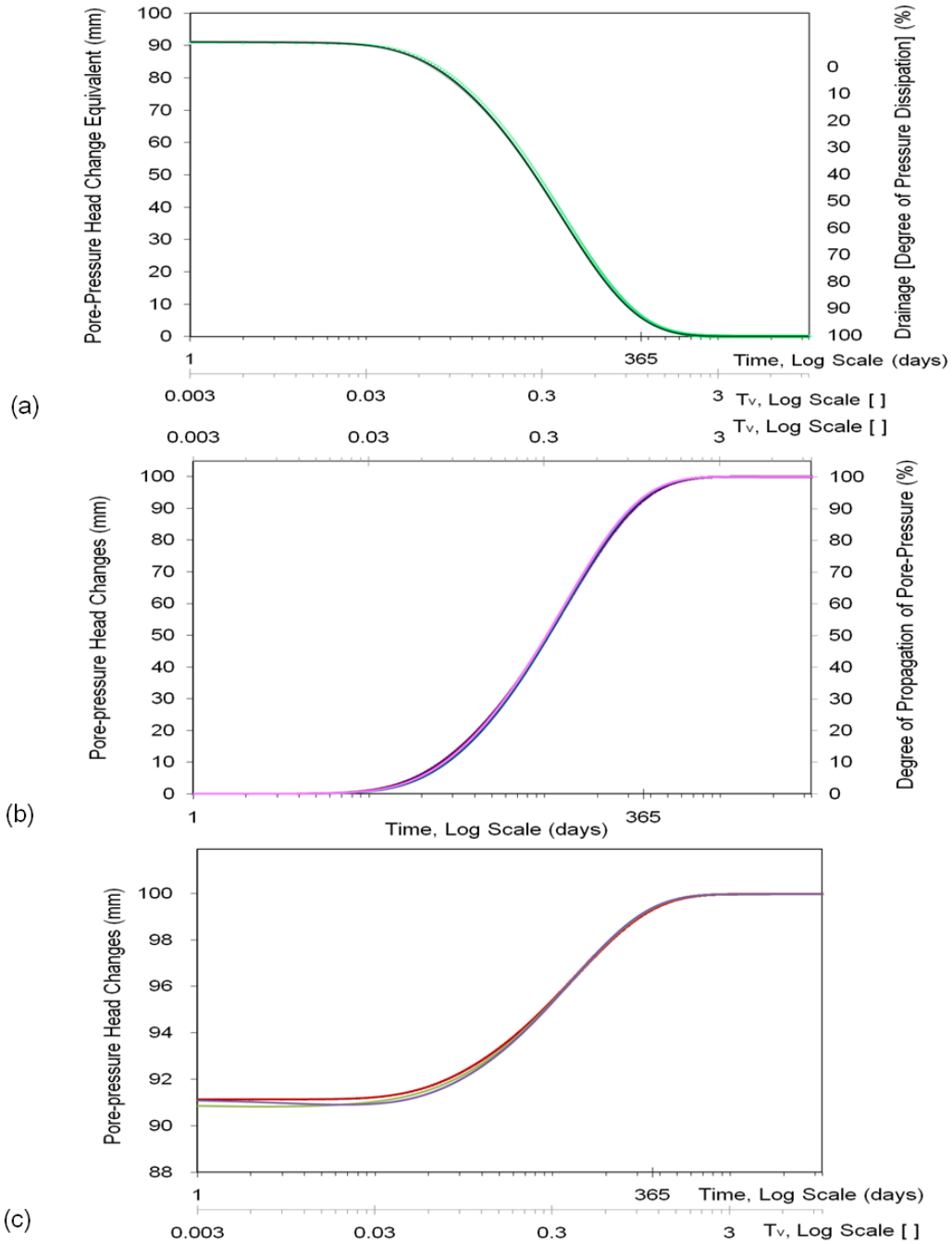

Figure 5.8. Effect of degree of linear variation of elastic properties with depth on a 22.5m-thick glacial till conceptual model using (i) 1-(uniform)-elastic-region-, (ii) 3-elastic-region- and (iii) 5-elastic-region-models (all nearly indistinguishable due to insesnsitivity) showing modelled response of aquitard-piezometer to (a) sustained 100mm-water pressure head equivalent one-step loading; (b) 100mm change in water table elevation; and (c) combined effects of water table and loading [i.e. (a) + (b) for corresponding (i), (ii) & (iii)]

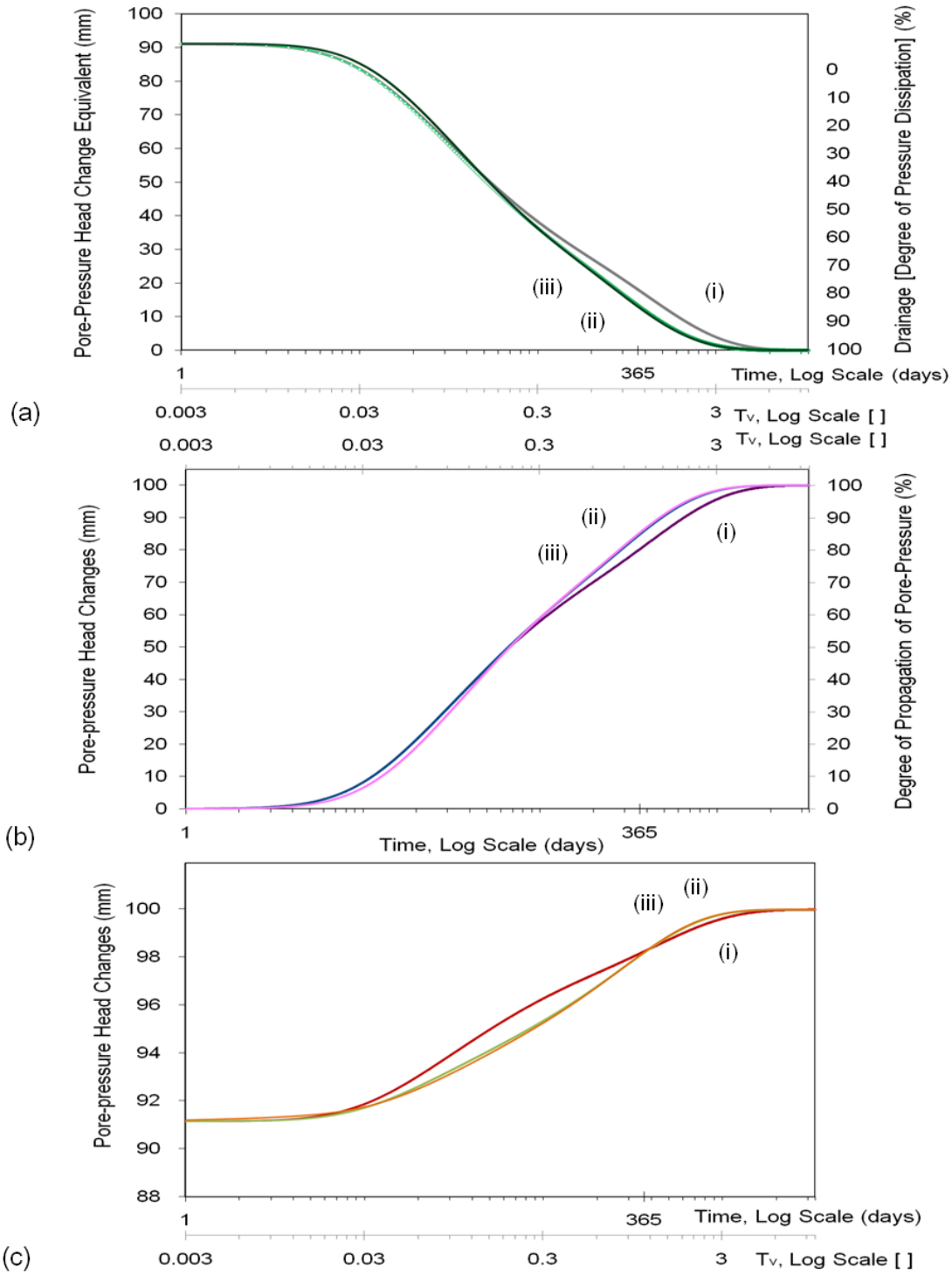

Figure 5.9. Effect of degree of linear variation of elastic properties with depth on a 60-m thick glacial till conceptual model using (i) 1-Layer- (uniform elastic-region-), (ii) 2-Layer- (2-elastic-region-) and (iii) 6-layer- (6-elastic-region-) models showing modelled response of aquitard-piezometer to (a) sustained 100mm-water pressure head equivalent one-step loading; (b) 100mm change in water table elevation; and (c) combined effects of water table and loading [i.e. (a) + (b) for corresponding (i), (ii) & (iii)]

5.3.5 Effect of Change of Hydraulic Conductivity

The vertical hydraulic conductivity, K_v, remained the major unknown material parameter prior to model calibration. Decisions on K_v and the uncertainties associated with the till depth were made after the "best fit" calibrated values of K_v of 2.1 x 10^{-5} m/day, 4.5 x 10^{-5} m/day and 7 x 10^{-5} m/day were obtained for the cases of 22.5m-, 40m- and 60m-thick models, respectively, and compared against their least fitting errors. These comparative "best-fit" calibrations are shown in Figure 5.10. The result for 40m-thick aquitard was left out for clarity of the illustration; it was poorly fit (RSME of 72mm) and with a similar trend as for the case of a 60m-thick aquitard (RMSE of 91mm). Clearly, the 22.5m thick model produced the overall best-fit (RMSE of 63mm) and was therefore adopted.

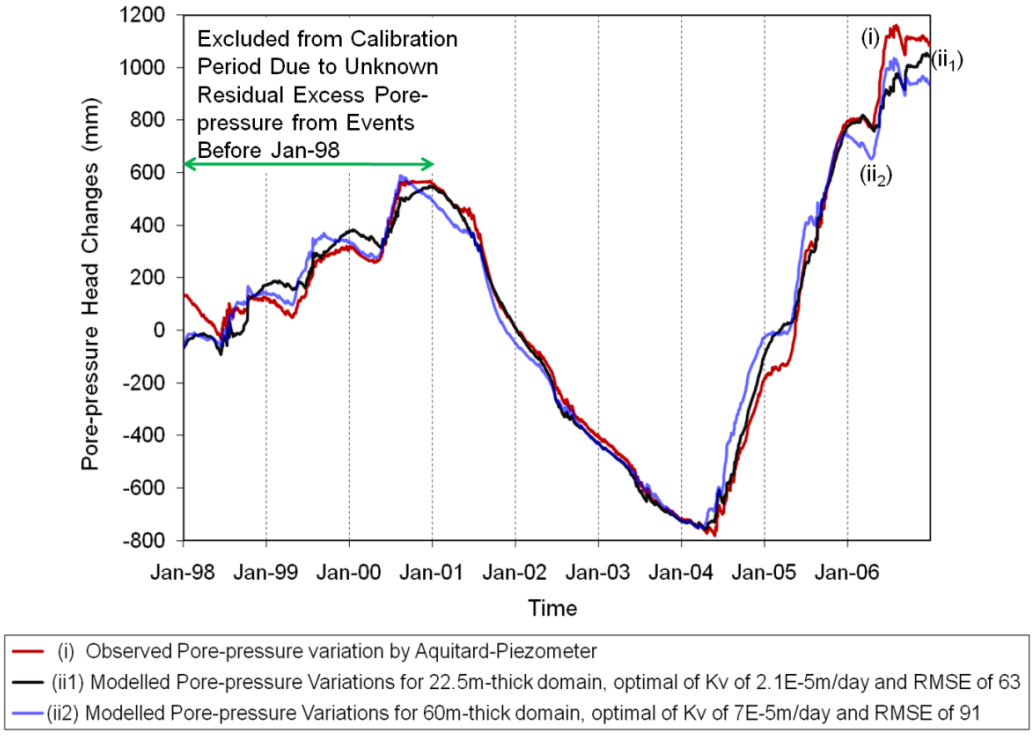

Figure 5.10. Selection of optimum K_v and Geometry through calibration "best-fit" of (i) Observed; and Modelled pore-pressure responses of aquitard-piezometer in Old Aspen Site for: (ii_1) 22.5m-thick model with K_v of 2.1x10^{-5} m/day; and (ii_2) 60m-thick model with K_v of 7x10^{-5} m/day (result of 40m-thick model with optimum K_v of 4.5x10^{-5} m/day not shown to avoid congestion)

The fitting errors (RMSE) for various values of K_v for the selected 22.5m-thick-model are shown in Figure 5.11. Only values close to the best-fit within an order of magnitude are shown. The aquitard-piezometer response of the model showed a high sensitivity to variations in K_v, even over a small range of K_v of less than a factor of 2 (Figure 5.11). On another instance, on a wider range, two different simulations using values of hydraulic conductivity one order of magnitude apart resulted in fitting errors (RMSE) of over 200%. Ultimately, the overall "best-fit" calibration of the model to field measurements was achieved with K_v of 2.07 x 10^{-5} m/day (i.e. approximately 2.4 x10^{-10} m/s) for a 22.5m-thick aquitard. In the context of the unknown full stratigraphic depth (thickness of aquitard) and the likelihood of increasing K_v with increasing thickness (Fig 5.10), the selected K_v of approximately 2.1 x 10^{-5} m/day could potential vary by as much as over a factor (multiple) of 3. The obtained hydraulic conductivity falls within the range reported in literature between a fractured and an unfractured till (Table 3.1).

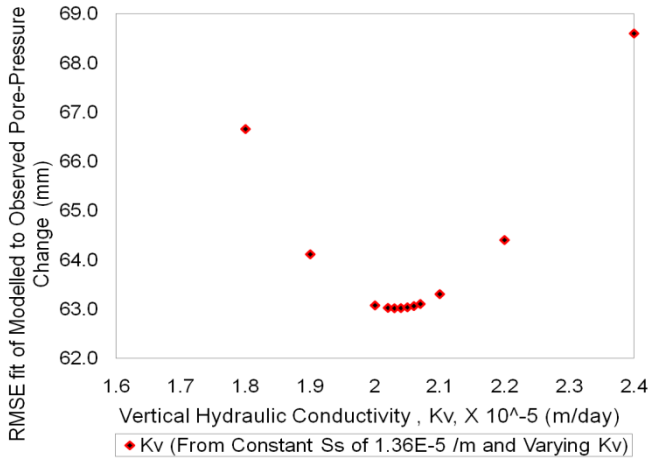

Figure 5.11. Effect of varying vertical hydraulic conductivity, K_v, on fitting error (RMSE) of modelled and observed response of aquitard-piezometer to measured water table fluctuation and loading by changing soil water balance, resulting in selection of K_v of 2.07 x 10^{-5} m/day for 22.5m-thick aquitard model

5.3.6 Summary of Sensitivity Analyses with Respect to Deficiency of Site Data

The sensitivity tests would have been more beneficial if more site information was available. This is paradoxical considering that the essence of the sensitivity testing

scheme was also to further grasp the influence of the model-parameters on the behaviour of the physical system (Barbour and Krahn 2004). However, "major" gaps open to a wide array of guesses would not be reliably bridged by sensitivity tests. For instance, the exact material behaviour of stratigraphic units below the aquitard model is not known. If the depth and material properties were better known or additional observations such as a set of nested piezometers was available, more refined results would have been obtained. Unfortunately, such ideal situation where there is sufficient site data for numerical modelling rarely occurs (Barbour and Krahn 2004).

Since the whole calibration exercise, in principle, revolved around simulating the consolidation time of the aquitard, then the fewer the unknown independent variables the more accurately the simulation of the time effect. Recall (from Equation [4.17]) that characteristic time, t_c, depends directly on square of the (drainage path) thickness of the aquitard, h_d^2, and inversely on the hydraulic diffusivity (i.e. directly on storage, S_s, and inversely on hydraulic conductivity, K_v). A variant of Equation [4.17] showing all key independent variable to t_c is:

$$t_c = \frac{S_s {h_d}^2}{K_v} \qquad [5.1]$$

If sufficient site data were available, the primary unknown variable as determined by numerical modelling would be K_v. However that was not the case in this research problem. In fact, sensitivity tests showed the aquitard pore-pressure response is sensitive to the thickness of the aquitard. Though the pore-pressure responses did not show significant sensitivity to elastic storage property, S_s, (or E) for the tested aquitard-thicknesses, the trick is that it could as well vary greatly with depth where different stratigraphic materials exist. These results imply that while there are two major unknowns (K_v and h_d) in this current problem, a subtle third unknown variation of S_s with depth compounds the situation. Finally, though the calibrated properties served for the solution of the research problem, there is still need for more field data, from a full stratigraphic depth instrumented with a set of nested piezometers, to improve the results.

5.4 Result of Modelled Aquitard-Piezometer Responses to Observed Water Table

The outcome of the modelled responses of aquitard piezometer to the water table fluctuation using the fully-field-calibrated elastic and hydraulic properties of the 22.5m-thick conceptual model is shown in Figure 5.12. These results were used to isolate the unwanted effect of transients from the water table by subtracting them from the observed pore-pressure responses of the aquitard-piezometer corrected for earth tide and barometric pressure changes (Figure 5.1 (i)). The balance of the deduction produced the drained pore-pressure response of the aquitard-piezometer to loading from total soil moisture changes, discussed in the next section.

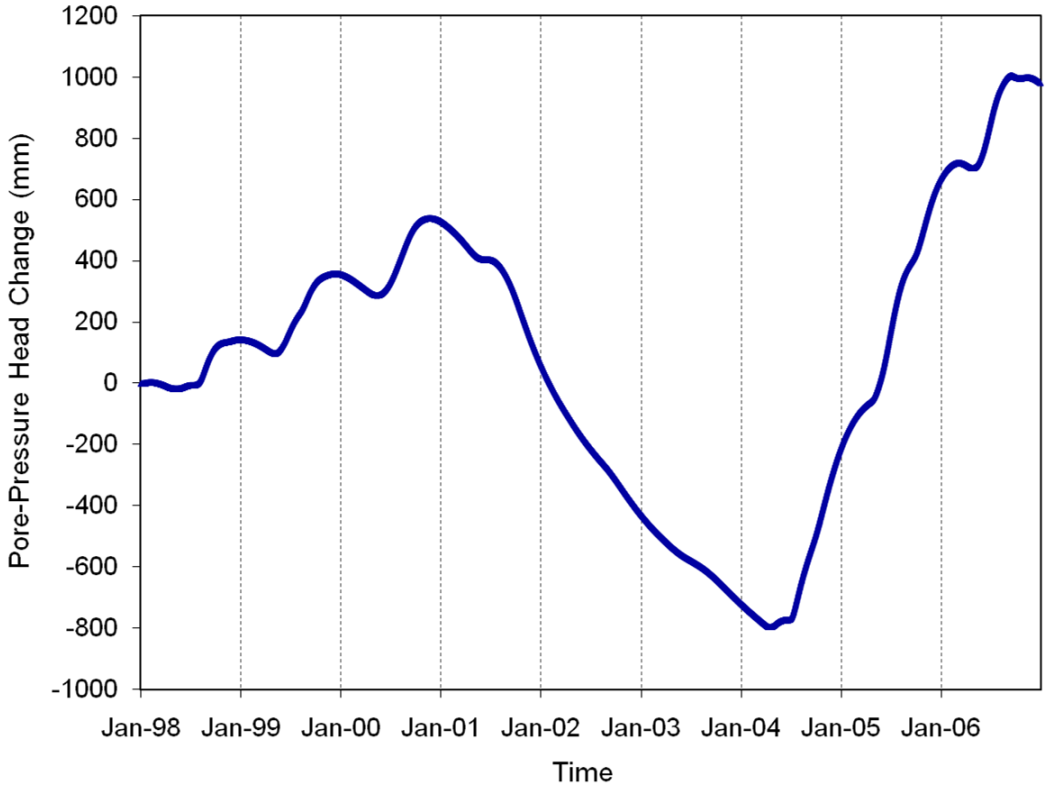

Figure 5.12. Modelled pore-pressure responses of the aquitard-piezometer to observed water table fluctuations

5.5 Result of Observed Aquitard-Piezometer Responses to Soil Moisture Changes

A key solution for the "geological weighing lysimeter" observation in this research is the long term pore-pressure responses of aquitard-piezometer to mechanical loading associated with changes in total soil moisture (site water balance) alone and the associated consolidation drainage. The resulting aquitard-piezometer- (lysimeter-) response to changes in site water balance and the modelled aquitard-piezometer-response to changes in meteorological (P – ET) water balance are shown in Fig 5.13. They are in relatively good agreement during the dry period of early 2001 to early 2004, with discrepancies occurring over some periods in 2005 and 2006 (Figure 5.13), which were particularly "wet" years.

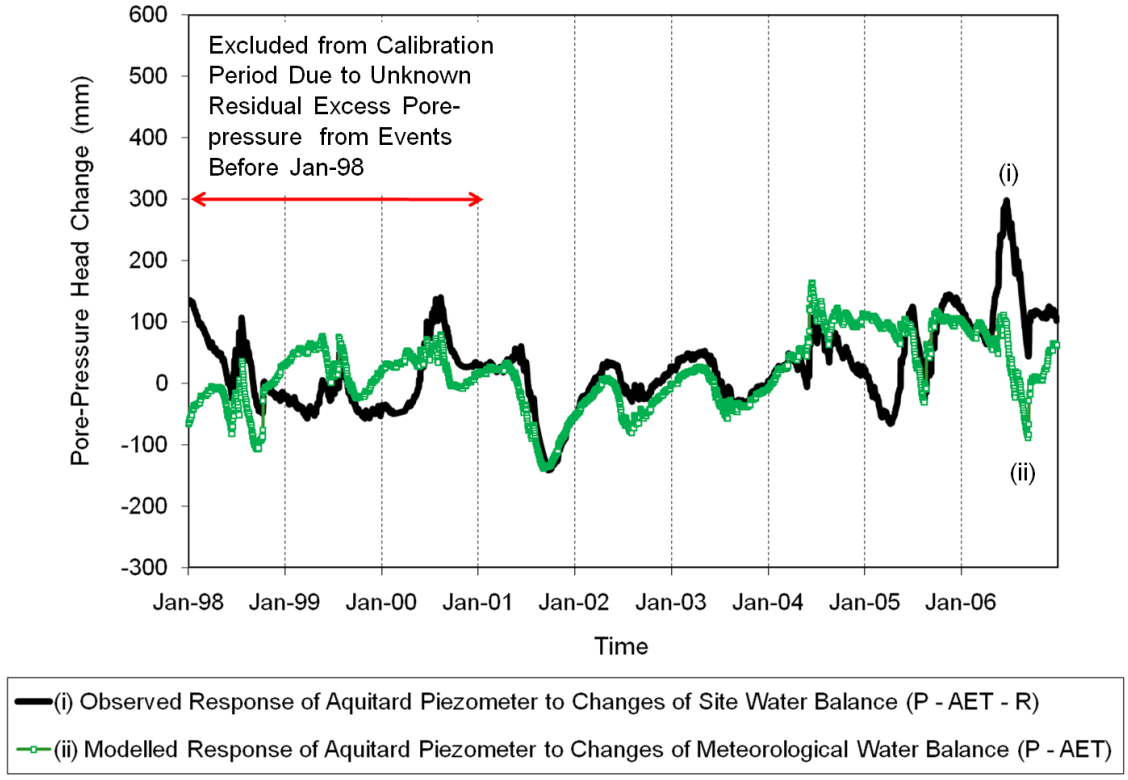

Figure 5.13. (i) Observed pore-pressure responses to changes of soil moisture as isolated using method of superposition (measured pore-pressure changes minus modelled pore-pressure responses to water table fluctuation alone); and (ii) Modelled pore-pressure responses to meteorological (vertical) water balance (using climate station data as input in the coupled model) for Old Aspen Site (considering 2001 – 2006)

5.6 Discussion of the Key Results and the Potential Applications

The assumption of insignificant runoff during the dry period (2001 to early 2004) appears valid as evident in the good agreement between the modelled and observed piezometric response to loading by water balance (Figure 5.13). If this is true, then the cause of the minor discrepancies can be further investigated. These periods could provide some insight into questions pertaining to possible errors in gauge precipitation measurements or possible misrepresentation of evapotranspiration. The agreement in results also suggest that the developed numerical modelling methodology enhances data interpretation and the potential for deployment of the piezometer-based "geological weighing lysimeter" for different applications speculated in Chapter 1 such as real-time-monitoring of site water balance and hydrological events including precipitation.

The effect of net lateral flow (runoff) may have been responsible for the discrepancy in the latter years. This arises because the modelling assumed input loading from changes in meteorological water balance due only to (vertical) net climatic fluxes (P – ET) whereas the contribution of net lateral flow could have had a significant contribution to the loading (i.e. P – ET – R) of the aquitard during the wet years (2005 and 2006). The results for the early part (winter to spring) of the year 2005 suggests that there might have been a net loss while the summer of 2005 and 2006 shows a net gain of water possibly due to runoff which was unaccounted for in the meteorological water balance. Interestingly, on the other hand, these "disparities" might even prove in future work to provide an alternative method of studying and quantifying runoff in hydrology. That is because the difference between the two results in Figure 5.13 could be considered the estimate of pore-pressure responses to loading associated with runoff (net lateral flow).

This research work also contributes a geotechnical case history of a method of using climatic and piezometric data to determine soil properties at significant depths, since in situ parameters obtained in this methodology agree with the range of values in literature for elastic and hydraulic properties of clay till (Table 3.1) determined by other methods.

6 CHAPTER 6 - CONCLUSION AND RECOMMENDATIONS

6.1 Conclusion

A methodology to isolate and identify the pore-pressure response to only loading associated with site water balance (total soil moisture variations) using finite element coupled stress-flow numerical modelling has been successfully developed in this work. The pore-pressure responses of a deep aquitard-piezometer to water table fluctuations in an overlying aquifer were modelled using finite element numerical models. These simulated pore-pressure dynamics were then deducted from the observed pore-pressure responses, cleaned of barometric and earth tide effects, to isolate the required responses.

The extracted pore-pressure responses were identified as responses to surface loading arising from the surface water balance and these pore-pressure responses were compared to modelled pore-pressure responses to an independently monitored meteorological water balance for the site. There was reasonably good agreement between the pore-pressure responses to the two water balances for a 9-year period, particularly during "dry" years, with some discrepancies during "wet" years. Consequently, the primary goal of using the numerical modelling methodology to interpret the measured pore-pressure transients to identify pore-pressure responses to surface water balance (total soil moisture) was achieved. The use of this numerical modelling methodology progresses the potential for the general adoption of the "piezometer-based geological weighing lysimeter" for a variety of hydrological applications. Even the "wet-" period disparity suggests that there is potential to advance this method so that it could be used to estimate runoff (net lateral flow) from a piezometer-based geological weighing lysimeter.

The developed method relies on accurate, large-scale, in situ estimates of hydraulic conductivity and compressibility. Elastic parameters were determined by evaluating the pore-pressure response to atmospheric pressure fluctuations, prior to embarking on the numerical modelling. The hydraulic parameters were obtained from the simulation of the observed pore-pressure responses to coupled water table fluctuations and variations in total stress generated by changes in total soil moisture. The calibration of the model to field-monitored data was used to determine the, large-scale, "equivalent" formation properties of K_v of 2.1 x 10^{-5} m/day (2.4 x 10^{-10} m/s) and S_s of 1.36 x 10^{-5} m^{-1}, using an assumed porosity of 0.26 and Skempton's $\bar{B}$ of 0.91 (i.e. drained confined compressibility, m_v, of 1.26 x 10^{-6} kPa^{-1} or drained confined elastic modulus, E_c, of 793MPa; or drained Young's modulus, E, of 528 MPa with an assumed drained Poisson's ratio, v, of 1/3). The material parameters are consistent with the reported values obtained from other in situ methods of establishing material properties. Consequently, this work also constitutes a special case history of the use of an approach for determining geotechnical (soil material) properties from detailed transient pore-pressure observations and climatic data.

6.2 Recommendations

The fully saturated model and the assumptions made in designing the boundary conditions, such as the constant stress boundary for the effect of water table variations, were such that the total stress changes associated with the water table fluctuations were considered negligible. This was based on the assumption that changes in water mass storage at the water table were due solely to the water balance already accounted for (weighed) in the meteorological water mass balance used as input to the stress boundary. Any other contribution of net lateral flow (runoff) to total stress changes was ignored. The periods of discrepancy between simulated and measured pore-pressure responses to water balance (Figures 5.13) suggest that the contributions of net lateral flow to the

"lysimeter" observations could be incorporated into the method so that the contributions of lateral flow to the total stress changes could be estimated.

This new approach would require the following additional work:

- Incorporation of the vadose zone into the model (i.e. the overlying aquifer) in such a way that the body force associated with changes in water content could be included in the applied load. This would account for the (small) changes in total stress due to changes in soil density that accompany water table fluctuations. In the case that lateral flow did occur within the aquifer then these changes would be evident in the changes in pore-pressure measured within the weighing lysimeter and could be incorporated into the model.
- A potential "add-in function" to implement this special "body force" has been developed for the SIGMA/W model by GEOSLOPE but it is yet to be fully evaluated. Additional site specific information for the aquifer may be acquired to re-simulate the problem using the alternative conceptual model with the special "body-force" function.

In order to further increase the reliability of the application of numerical modelling in estimating water balance (loading) in long-term observations, the overlapping consolidation drainage associated with loading must be recovered to derive the exact undrained pore-pressure responses (accumulations) required for the computation. Consequently, an appropriate method of recovering consolidation drainage, such as deconvolution of the pore-pressure signals, is required to fully deal with the "residual" transients in the drained pore-pressure responses to loading associated with changes of total soil moisture.

REFERENCE

Anochikwa, C.I., van der Kamp, G., and Barbour, S.L. 2009. Numerical simulation of observed pore-pressure changes in an aquitard due to changes of total soil moisture. *Proceedings of the 62nd Canadian Geotechnical Conference and 10th Joint Canadian Geotechnical Society/International Association of Hydrogeologists-Canadian National Chapter (CGS/IAH-CNC) Groundwater Conference, Halifax,* 1600 - 1606.

Barbour, S.L., and Krahn, J. 2004. Numerical modelling – Prediction or Process? *Geotechnical News*, December, 44 – 52.

Barbour, S.L. *Lecture at a Geotechnical Modelling Workshop – on fundamentals, theory and application, at Banff in* 2007.

Bardsley, W.E., and Campbell, D.I. 1994. A new method for measuring near-surface moisture budgets in hydrological systems. *Journal of Hydrology*, 154, 245 – 254.

Bardsley, W.E. and Campbell, B.I. 2000. Natural geological lysimeters: calibration tools for satellite and ground surface gravity monitoring of subsurface water-mass change. *Natural Resources Research*, 9(2), 147 – 156.

Bardsley, W.E., and Campbell, D.I. 2007. An expression for land surface water storage monitoring using a two-formation geological weighing lysimeter. *Journal of Hydrology*, 335: 240-246.

Barr, A., van der Kamp, G., Schmidt, R., and Black, T.A. 2000. Monitoring the moisture balance of a boreal aspen forest using a deep groundwater piezometer. *Agricultural and Forest Meteorology*, 102(1): 13-24.

Biot, M.A. 1941. General theory of three-dimensional consolidation. *Journal of Applied Physics*, 12: 155-164.

Bishop, A.W. 1954. The use of pore-pressure coefficients in practice. *Geotechnique*, 4 (4), 148.

Bishop, A.W. 1973. Influence of an undrained change in stress on the pore pressure in porous media of low compressibility. *Geotechnique*, 23 (3), 435 – 442.

Black, T.A., Den Hartog, G., Neumann H.H., Blanken, P.D., Yang, P.C., Russell, C., Nesic, Z., Lee, X., Chen, S.G., Staebler, R., and Novak, M.D. 1996. Annual cycles of water vapour and carbon dioxide fluxes in and above a boreal aspen forect. *Global Change Biology, 2, 219 – 229.*

Bredehoeft, J.D. 1967. Response of well-aquifer systems to earth tides. *Journal of Geophysical Research*, 72(12): 3075 – 3087.

Christiansen, E.A. 1968. Pleistocene stratigraphy of the Saskatoon area, Saskatchewan, Canada. *Canadian Journal of Earth Sciences*, 5, 1167 – 1173.

Christiansen, E.A. 1973. Geology and Groundwater Resources of the Shellbrook Area (73G). *Saskatchewan Research Council, Geology Division, Map No. 17*.

Christiansen, E.A. 1973.Geology and Groundwater Resources of the Prince Albert Area (73H). *Saskatchewan Research Council Geology Division, Map No. 15*

Christiansen, E.A. 1992. Pleistocene stratigraphy of the Saskatoon area, Saskatchewan, Canada: an update. *Canadian Journal of Earth Sciences*, 29: 1767–1778.

Conly, F.M., and van der Kamp, G. 2001. Monitoring the hydrology of Canadian prairie wetlands to detect the effect of climate change and land use changes. *Environmental Monitoring and Assessment*, 67, 195 – 215.

Dawson, C.W., Abrahart, R.J., and See, L.M. 2007. HydroTest: A web-based toolbox for evaluation matrix for standardised assessment of hydrological forecasts. *Environmental modelling and software* 22, 1034 – 1052.

DeJong, J., and Harris, M.C. 1971. Settlement of two multi-storey buildings in Edmonton. *Canadian Geotechnical Journal, 8: 217 – 235.*

Dunnicliff, J., and Green, G.E. 1993. *Geotechnical instrumentation for monitoring field performance*. NY: John Wiley.

DMTI CanMap® Parks & Recreation v2008.3 – Saskatchewan, [Database from which ArcGis Map was accessed in 2009]

Domenico, P.A., and Schwartz, F.W. 1998. *Physical and chemical hydrogeology (second edition).* John Wiley, New York, NY, USA.

Fluxnet-Canada. 2005. Eddy correlation notes in the Fluxnet-Canada carbon cycle course.

Faures, J., Goodrich, D.C., Woolhiser, D.A., and Sorooshian, S. 1995. Impact of small-scale spatial rainfall variability on runoff model. *Journal of Hydrology*, 173, 309-326.

Fluxnet-Canada. www.fluxnet-canada.ca [Accessed in 2009]

Freeze, R.A., and Cherry, J.A. 1979. *Groundwater*. NJ: Prentice Hall.

Geokon Inc. 1996. *Instrumentation manual model 4500 vibrating wire piezometer*. NH, USA.

GEO-SLOPE International Limited. 2007. *Seepage modeling with SEEP/W 2007: an engineering methodology (second edition)*. GEO-SLOPE, Calgary, Alberta, Canada.

GEO-SLOPE International Limited. 2008. *Stress-deformation modeling with SIGMA/W 2007: an engineering methodology (third edition)*. GEO-SLOPE, Calgary, Alberta, Canada.

Goodrich, D.C., Faurès , J., Woolhiser, D.A., Lane, L.J., and Sorooshian, S. 1995. Measurement and analysis of small-scale convective storm rainfall variability. *Journal of Hydrology*, 173, (1-4), 283-308.

Google Earth. www.google.earth.com [Accessed 2009]

Gray, H. 1945. Simultaneous consolidation of contiguous layers of unlike compressible soils. *Transactions of American Society of Civil Engineers*, 110, 1327 – 1344.

Grisak, G.E., and Cherry, J.A. 1975. Hydrologic characteristics of response of fractured till and clay confining a shallow aquifer. *Canadian Geotechnical Journal*, 12: 23 – 43.

Hendry. J.M. 1982. Hydraulic conductivity of glacial till in Alberta. *Ground Water*, 20(2), 162 – 169.

Huang, B.Q. 2005. Effect of subglacial shear on the geomechanical properties of glacial soil. MSc thesis, in Department of Civil and Geological Engineering, University of Saskatchewan, Canada.

Istok, J. 1989. Groundwater modelling by finite element method. *American Geophysical Union, Water Resources Monograph*, 13, 495p.

Jacob, C. 1940. On the flow of water in an artesian aquifer, *Transactions- American Geophysical, Union*, 21, 574 – 586.

Karvonen, A. 1997. Numerical modelling of region ground water system in the west Saskatoon district: implication for brine migration at the Cory and Vanscoy Potash Mine. MSc thesis in Department of Geological Sciences, University of Saskatchewan, Canada.

Keller, C.K, van der Kamp, G., and Cherry, J.A. 1986. Fracture permeability and groundwater flow in a clayey till near Saskatoon, Saskatchewan, *Canadian Geotechnical Journal*, 23: 229-240.

Keller, C.K., van der Kamp, G., and Cherry, J.A. 1988. Hydrogeology of two Saskatchewan tills, I. fractures, bulk permeability, and spatial variability of downward flow, *Journal of Hydrogeology*, 101, 97-121.

Keller, C. K., van der Kamp, G., and Cherry, J.A. 1989. A multi-scale study of permeability of thick clayey till, *Water Resources Research,* 25 (11): 2299-2317.

Klohn, E.J. 1965. The elastic properties of a dense glacial till deposit, *Canadian Geotechnical Journal,* 11 (2): 116 – 128.

Lee, P.K.K., Xie, K.H., and Cheung, Y.K. 1992. A study of one-dimensional consolidation of layered systems. *International Journal for Numerical and Analytical Methods in Geomechanics*, 16, 815 – 831.

Marin, S., van der Kamp, G., Pietroniro, A., Davison, B., and Toth, B. 2009. Use of geological weighing lysimeter to calibrate a distributed hydrological model for the simulation of land-atmosphere moisture exchange. *Journal of Hydrology,* Accepted subject to minor revisions, September 2009.

Matheson, D.S., Morgenstern, N.R., and Nussbaum, H. 1987. Design and performance of Nipawin dams. *40th Canadian Geotechnical Conference, Regina, Saskatchewan, Canada*, 141-170.

Mercer, J.W., and Faust, C.R. 1981. Ground-water modeling. *National Water Well Association*.

Mesri, G. 1973. One-dimensional consolidation of clay layer with impeded drainage boundaries. *Water Resources Research*, 9 (4), 1090 – 1093.

Millard, M.J. 1990. Geology and ground water resources of Prince Albert area (73H) Saskatchewan. *Saskatchewan Research Council Report R-1210-8-E-90*. (www.swa.ca/WaterManagement/Documents/R1210-8E90%20Prince%20Albert.pdf)

Millard, M.J. 1994. Geology and groundwater resources of Shellbrook area (73G) Saskatchewan. *Saskatchewan Research Council Report R-1210-9-E-94.* (www.swa.ca/WaterManagement/Documents/R1210-9E94%20Shellbrook.pdf)

Poulos, H.G., and Davis, E.H. 1974. *Elastic solutions for soil and rock mechanics.* John Wiley & Sons, New York, NY, USA.

Rojstaczer, S. 1988. Determination of fluid flow properties from the response of water levels in wells to atmospheric loading. *Water Resources Research*, 24 (11), 1927 – 1938.

Rojstaczer, S., and Agnew, D.C. 1989. The influence of formation material properties on the response of water levels in wells to earth tide and atmospheric loading. *Journal of Geophysical Research*, 94 (B9), 12403-12411.

Santucci de Magistris, F., Sato, T., Koseki, J., and Tasuoka, F. 1998. Effects of strain rate and ageing on small strain behaviour of compacted silty sand. In: Evangelista, A., and Picarelli, L (editors) *The geotechnics of hard soils – soft rocks, Proceedings of Second International Symposium on Hard Soils-Soft Rock in Naples*, Italy: Balkemma, Rotterdam, 2: 843 – 853.

Sauer, E.K., Egeland, A.K., and Christiansen, E.A. 1993. Compression characteristics and index properties of till and intertill clays in southern Saskatchewan, Canada. *Canadian Geotechnical Journal*, 30: 257-275.

Saskatchewan Watershed Authority (SWA). [Accessed 2009: www.swa.ca/WaterManagement/Groundwater.asp?type=Mapping]

Schiffman, R.L., and Stein, J.R. 1970. One-dimensional consolidation of layered systems, *Journal of Soil Mechanics and Foundation, ASCE*, 96: 1499 – 1504.

Schulze, K.C., Kümpel, H.-J., and Huenges, E. 2000. In situ petrohydraulic parameters from tidal and barometric analysis of fluid level variations in deep wells: some results from KTB. In: Stober, I. and Bucher, K. (editors), *Hydrogeology of Crystalline Rocks*, 79-104.

Shaw, R.J., and Hendry, M.J. 1998. Hydrogeology of a thick clay till and Cretaceous clay sequence, Saskatchewan, Canada. *Canadian Geotechnical Journal*, 35, 1041-1052.

Skempton, A. 1954. The pore-pressure coefficients A and B. *Géotechnique*, 4, 143-147.

Sophocleous, M., Bardsley, W.E., and Healey, J. 2006. A rainfall loading response recorded at 300 m depth: Implications for geological weighing lysimeters. *Journal of Hydrology*, 319: 237–244.

Taylor, D.W. 1948. *Fundamentals of Soil Mechanics*. John Wiley & Sons, New York, NY, USA.

Terzaghi, K. 1923. Die Berechnung des Durchlassigkeitsziffer des tones aus dem verlauf der hydrodynamiischen spannungserscheinungen, Sitz. Akad. Wiss. Wein, Abt. IIa, 132, 125-138. [English translation by Clayton et al, 1995**:** A method of calculating the coefficient of permeability of clay from the variation of hydrodynamic stress with time**.** As cited in Clayton, C.R.I., Steinhagen, H.M., and Powrie, W. 1995. Terzaghi's theory of consolidation, and the discovery of effective stress. *Proceedings of the Institution of Civil Engineers, Geotechnical engineering*, 113(4), 191-205.]

Terzaghi, K. 1925. *Erdbaumechanik auf bodenphysikalischer Grundlage.* Leipzig and Wien: Franz Deuticke.

Terzaghi, K., and Frohlich, K. O. 1936. *Theorie der Setzung von Tonshichten: eine einfuhrung in die analytische Tonmechanil*, Leipzig, Franz Deuticke. [As cited in

Terzaghi, K., Peck, R. B., and Mesri, G. 1996. *Soil mechanics in engineering practice (third edition),* John Wiley and Sons, New York. NY, USA.]

Terzaghi, K. 1943. Theoretical soil mechanics. *John Wiley and Sons*, New York.

Terzaghi, K., Peck, R. B., and Mesri, G. 1996. *Soil mechanics in engineering practice (third edition),* John Wiley and Sons, New York. NY, USA.

van der Kamp, G. and Gale, J.E. 1983. Theory of Earth tide and barometric effects in porous formations with compressible grains. *Water Resources Research,* 19(2): 538–544.

van der Kamp, G., and Maathuis, H. 1985. Excess hydraulic head in aquitards under solid waste emplacement. *Memoirs of the 17th International Association of Hydrogeologists*, 2, 118-128.

van der Kamp, G., and Maathuis, H. 1991. Annual fluctuations of ground water levels as a result of loading by surface moisture. *Journal of Hydrology*, 127, 137-152.

van der Kamp, G., and Schmidt, R. 1997. Monitoring of total soil moisture on a scale of hectares using groundwater piezometers. *Geophysical Research Letters*, 24(6): 719-722.

van der Kamp, G. 2001. Methods for determining the in situ hydraulic conductivity of shallow aquitards – an overview. *Hydrogeology Journal*, 9: 5-16.

van der Kamp, G., Barr, A., Granger, R., and Schmidt, R. 2003. Use of deep piezometers in aquitards for continuous monitoring of hectare-scale soil moisture balance. *In the 56th Canadian Geotechnical and 4th Joint IAH-CNC/CGS Conference, Winnipeg,* 4p.

Vuez, A., and Rahal, A. 1994. Cyclic loading for the measuring of soil consolidation parameters. *Proceedings of Settlement 94, Geotechnical Special Publications, ASCE,* 1(40), 760 – 774.

Vuez, A., and Rahal, A. 1998. Analysis of settlement and pore-pressure induced by cyclic loading of silo. *Journal of Geotechnical and Geoenvironmental Engineering,* 124(12), 1208 – 1210.

Wang, H.F., and Anderson, M.P. 1982. Introduction to groundwater modelling: Finite difference and finite element methods. W.H. Freeman, 237p.

Woods, D. M. 2007. *Soil behaviour and critical state soil mechanics*. Cambridge University Press, Cambridge.

Zienkiewicz, O. C., and Taylor, R. L. 2000. *Finite element method fifth edition volume 1: the basis*. Butterworth Heinmann, Oxford.

APPENDIX A

A1. Site Borehole Logs Relative to the Adopted Conceptual Model

Three bore holes were drilled at the Old Aspen Forest site prior to the installation of the piezometers. The site lithological and hydrogeological profiles obtained from the bore holes labelled Bore holes 9601, 9602 and 9603 are shown in Figures A1, A2 and A3 respectively (Environment Canada, 1996 and 1997 weighing lysimeter construction information).

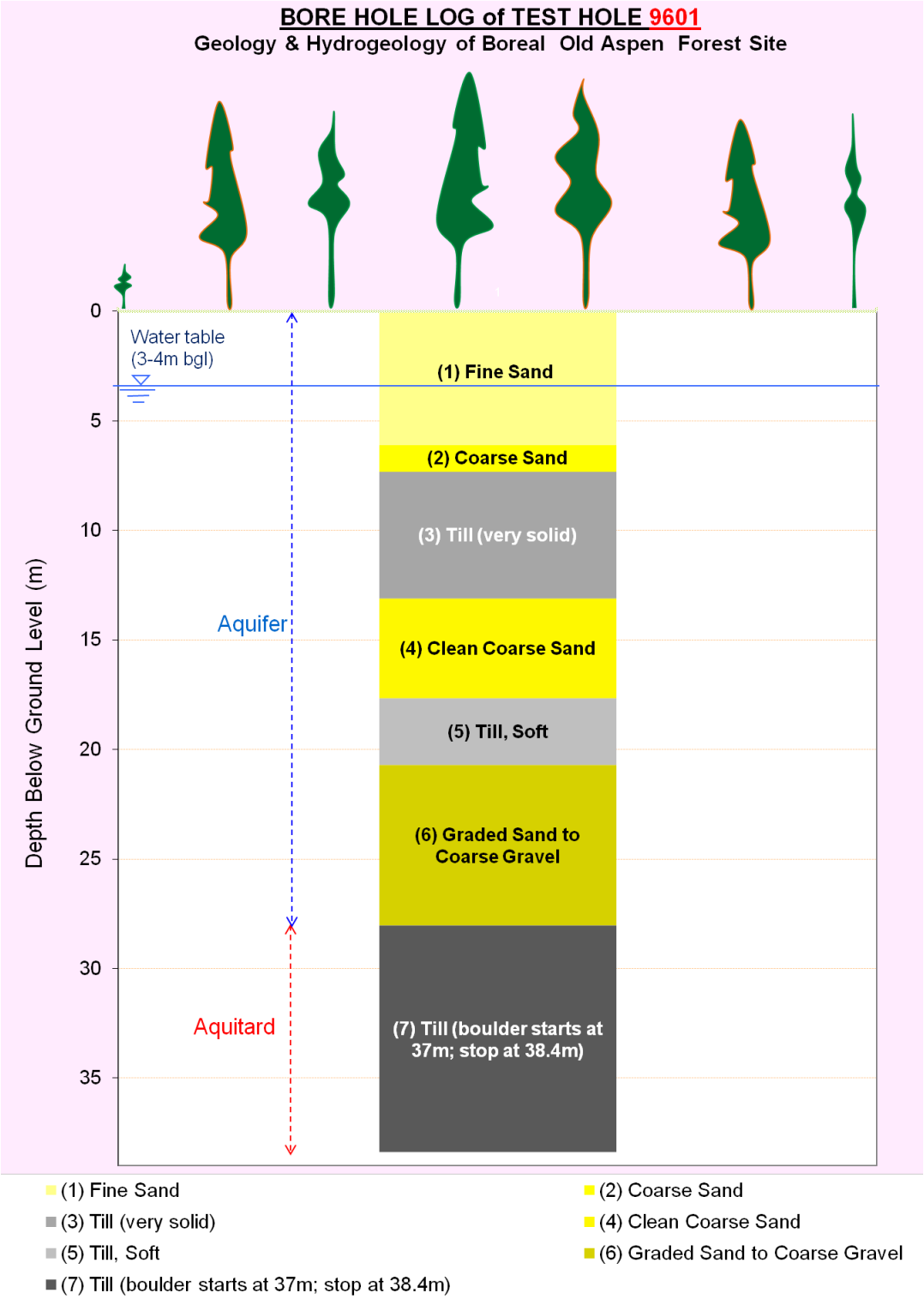

Figure A1. The log of Bore Hole 9601 at the Old Aspen Forest Site

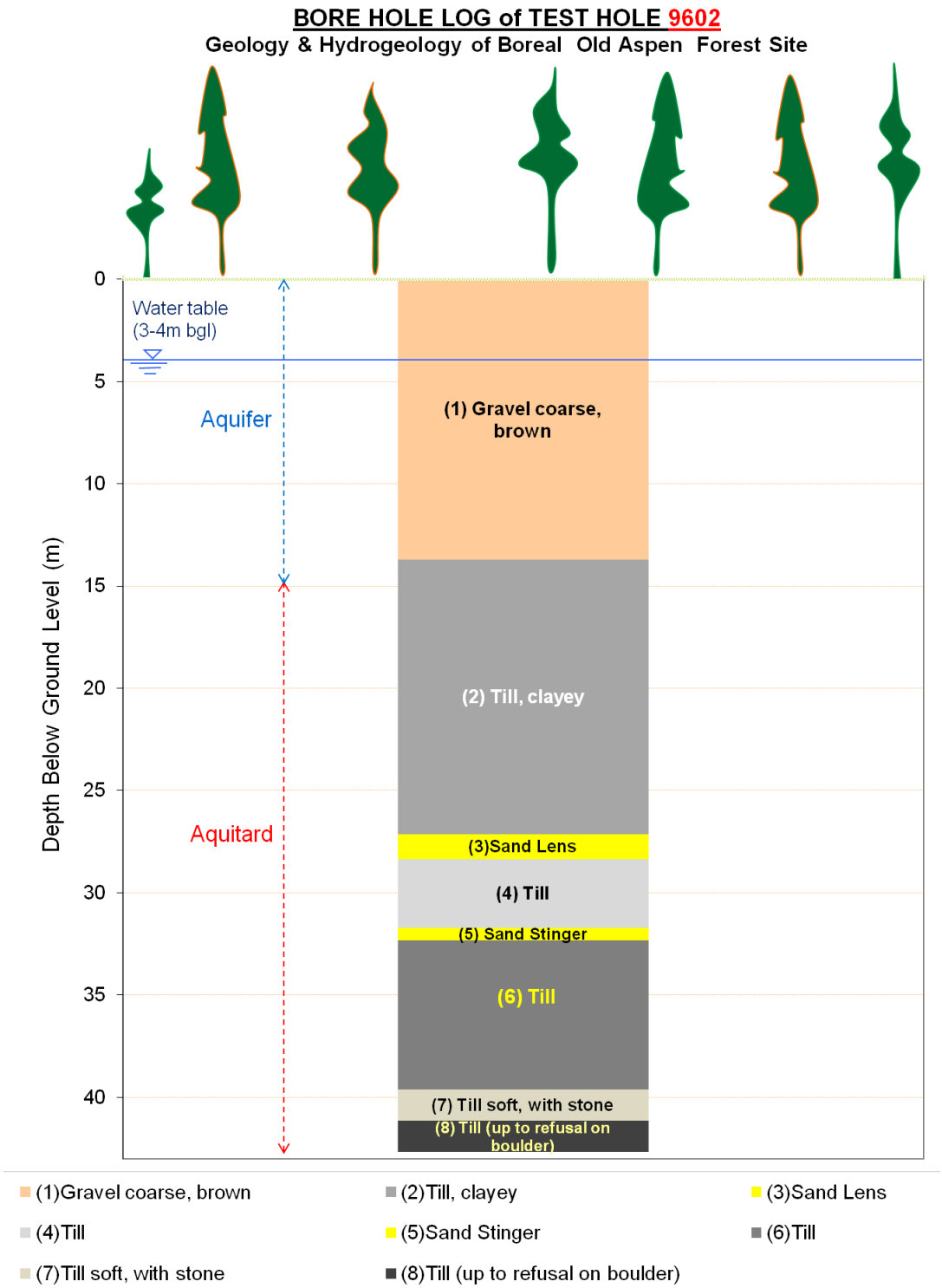

Figure A2. The log of Bore Hole 9602 at the Old Aspen Forest Site

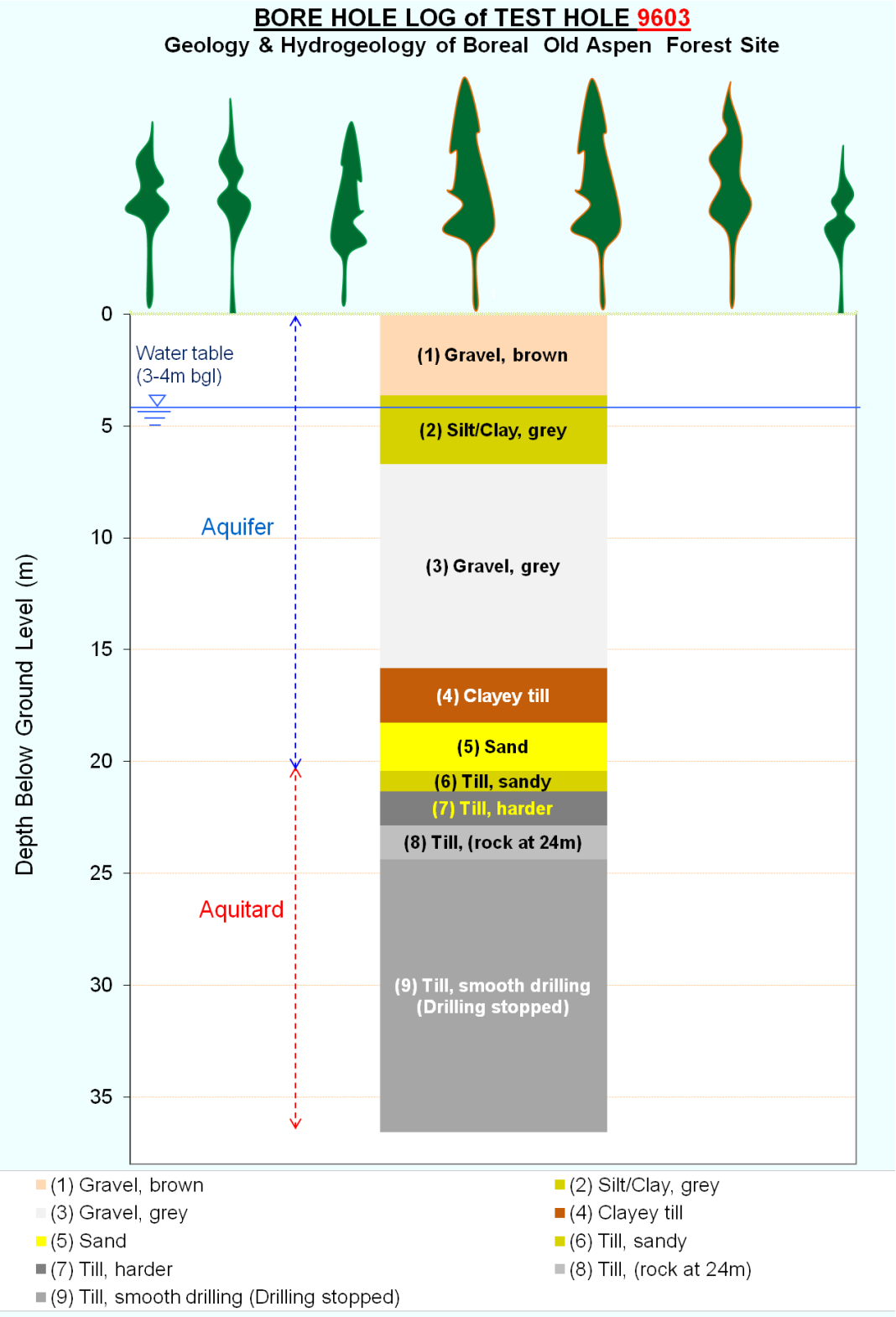

Figure A3. The log of Borehole 9603 at the Old Aspen Forest Site

On the “micro” borehole scales observed for the three borehole logs, the site profile shows heterogeneous layers of stratigraphic units. Gravel and sand were predominant with some pockets of silt and till in the top layer (to depth of about 14m to 28m below ground level). The underlying deposit comprises mainly clayey glacial till with some sand lenses up to where drilling stopped, the furthest being about 42.5m where drilling met refusal on what might have been a boulder. The water table fluctuation averages about 3 and 4m below ground level (Barr et al. 2000).

On a large scale (extending beyond the individual boreholes) the top layer was conceptualised, for the purpose of numerical modelling, as laterally extensive stratigraphic (aquifer) unit comprising a blend of gravel and sand with some silt. This was under the assumption that the other smaller layers of glacial till are not laterally extensive. The 20m-thick top sand and gravel aquifer (Barr et al. 2000) with some silt was adopted as a reasonable extensive profile of the site which falls within the observed range of the aquifer formation in the three borehole logs. Similarly, the underlying formation was conceptualised as another laterally extensive single stratigraphic (aquitard) unit of glacial till which ignores the pockets of embedded sand lenses assuming them not as extensive as the till. The known thickness of the glacial till aquitard is about 22.5m; however, the actual thickness (depth) of the glacial till at the site was not known due to difficulties with drilling.

Reference (for Appendix A)

Barr, A., van der Kamp, G., Schmidt, R., and Black, T.A. 2000. Monitoring the moisture balance of a boreal aspen forest using a deep groundwater piezometer, *Agricultural and Forest Meteorology*, 102(1): 13-24.

Environment Canada, Saskatoon. Documentation of the (1996 and 1997) construction of the Old Aspen weighing lysimeter.

APPENDIX B

B1. Elastic Properties from Correction of Barometric Effects

In order to determine the elastic properties of the formation (in which a piezometer is completed) laboratory mechanical (loading) tests of material or in situ mechanical tests are required. Laboratory testing of overconsolidated materials (e.g. glacial till) have been reported to underestimate the stiffness (overestimates compressibility) of the formation due to eased off stress and the associated structural disturbance in handling samples (Klohn 1965; Radhakrishna and Klym 1974). In situ elastic properties are therefore considered more realistic (e.g. van der Kamp 2001).

In situ load-deformation testing of (soil) formations can be carried out either by anthropogenic loading (as in pressure meter tests (Radhakrishna and Klym 1974), plate load test and field observation of settlement/rebound at construction sites (Klohn 1965)) or by observation of responses of pore-fluid level in fluid (liquid)-saturated geological formation to continuous natural "forcing" in the environment (e.g. Jacob 1940; van der Kamp 1983; Schulze et al. 2000). The natural "forcing" includes pressure/stresses generated by (atmospheric) barometric pressure, (earth and/or ocean) tidal strain (Jacob 1940; van der Kamp 1983; Rojstaczer and Agnew 1989), changes in soil moisture associated with water balance (P–ET–R) (e.g. van der Kamp and Maathuis 1991; van der Kamp and Schmidt 1997) and seismic waves (Schulze et al. 2000). While the first two "stressing sources" are the commonly discussed with high frequency, soil moisture changes also occur continuously but become pronounced during precipitation events (e.g. Barr et al. 2000) and the latter may be relevant in earthquake-prone regions.

The effects of barometric pressure changes generally produce significantly higher amplitudes in observed pore-pressure changes than produced by the earth tides even in deep wells (as much as 4km, confined formation) where tidal effects are expected to be high (Schulze et al. 2000) due to strain sensitivity associated with high stiffness and low porosity (Rojstaczer and Agnew 1989). It is important to note while accounting for observable tidal forcing, that ocean tides have also been monitored in inland bore holes in Germany (about 500km from the ocean) (Schulze et al. 2000). However, in the case of Old Aspen Forest in Saskatchewan ocean tides may not contribute to the tidal waves in the pore-pressure considering the relatively shallow depth (34.6m) of glacial till formation which may not have continuous connection through the large distance (over 1000km) to outcrops to the oceans. Therefore, for the site under consideration, only earth tides are considered the likely contributors to any observed tides in site data.

Vertically upward and/or downward gravitational motions of the atmospheric mass are required in this "natural" in situ load-deformation test. The ground-loading motion occurs generally as interplay of both global and local scale effects; for instance, local topography-related circulations driven by balancing of solar-heating effects and frictional-turbulence could occur and on the global scale includes the balancing of solar-radiation-induced global air circulation with rotary motion of the earth (e.g. Hamilton et al. 2008), and/or tidal solar-lunar gravitational pull on the (earth's) atmosphere (e.g. Ivanon 2007). The radius of influence for continental scale atmospheric loading has been reported to be in order of 1000km (Rabbel and Zschau 1985). Atmospheric pressure fluctuations have also been noted to vary with seasons of the year as temperature varies (Ivanon 2007).

The critical aspects of application of barometric response of pore-pressure in the determination of elastic properties are (i) the response mechanics of the type of piezometer (and the pressure transducer), (ii) data processing and (iii) the timing of the tests. Open (stand pipe) piezometers (e.g. open well) and piezometers with sealed-in

(non-vented) pressure transducer respond differently to atmospheric pressure such that while the open piezometers display inverse barometric response (e.g. Tuinzaad 1954; Bear 1972, pp. 211, 212), the sealed-in piezometers respond directly to barometric pressure (e.g. also observed in Old Aspen piezometric data) even where the piezometers are completed in, say, the same confined formation. Barometric and piezometric data are processed as changes, and not absolute pressures, similar to the incremental loading required for incremental deformation-responses in typical testing for elastic-property. Finally, the test performed through different periods would accommodate the spectrum of loading intensities associated with seasonal variations in atmospheric pressure. In addition, periods of intense precipitation may be excluded to avoid the overlapping response to the loading from such large fluctuations in changes of total soil moisture.

B1.1 Mechanics and Correction of Barometric Effects in Piezometric Data

Loading on soil surface is equilibrated by the pore water pressure response and the effective (solid soil structure) stresses on any horizontal plane in the soil profile underlying the loading which is known as effective stress principle (Terzaghi 1923). The same principle applies to atmospheric loading on soil. Consequently, barometric loading transmitted through the overlying formation is shared by the pore-pressure and the soil structure in the semi-confined aquitard. These barometric pressure changes are assumed to occur rapidly such that pore-pressure responds under static, no-flow (undrained), condition (e.g. Jacob 1940, van der Kamp and Gale 1983; Domenico and Schwartz 1998) especially under low permeability or confined conditions.

The mechanical equilibrium of the “active” barometric loading with the barometric reactions at the horizontal plane of the sealed-in pressure transducer of a piezometer in an aquitard is illustrated in Figure B1.

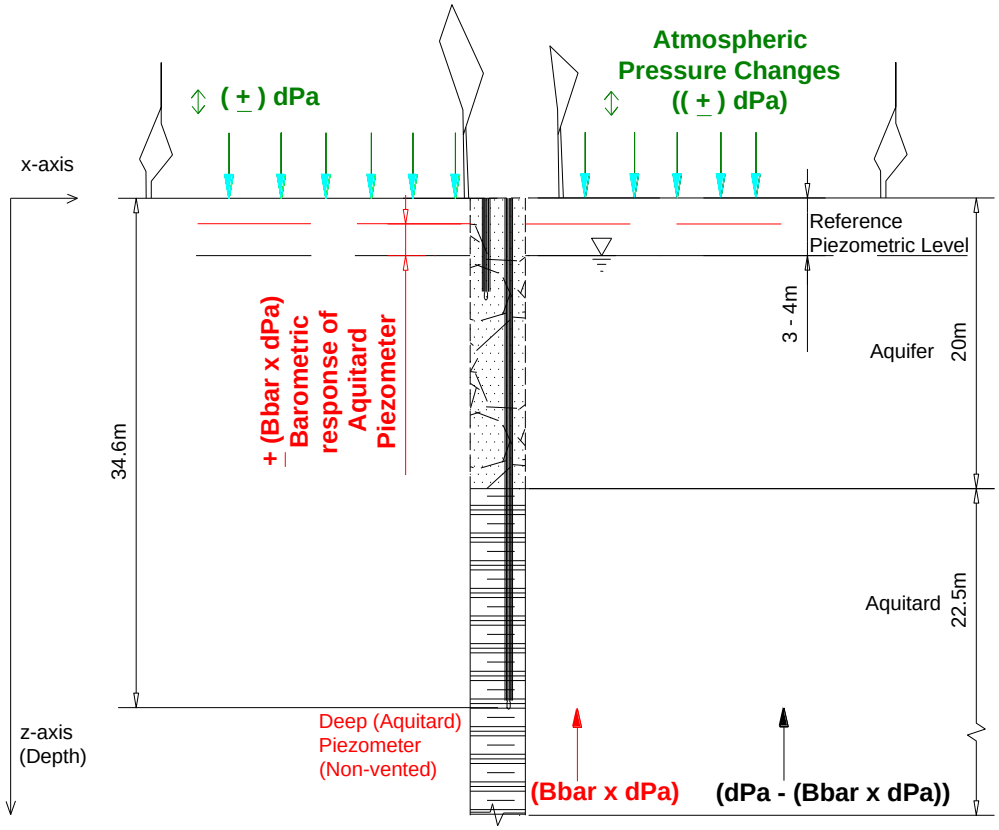

Figure B1. Barometric responses of a (semi-confined) aquitard-piezometer; showing the loading (meaning (+) downward and (–) upward) from atmospheric pressure changes on the ground surface; pore-pressure and effective stress responses at intake level of aquitard piezometer are also shown [N.B. Only incremental stresses are shown]

The equilibrium at the horizontal plane at intake level of the aquitard-piezometer in terms of effective stress principle (Terzaghi 1923) adopted using only the incremental stresses from Jacob (1940) is:

$$dP_a = \bar{B}dP_a + (dP_a - \bar{B}dP_a) \quad [B1]$$

such that:

$$u_{P_a} = \bar{B}dP_a \quad [B2]$$

where the $\bar{B}dP_a$ represents the change in aquitard pore-pressure u_{Pa}, which is referred to as the barometric response, while $(dP_a - \bar{B}dP_a)$ is the corresponding change in effective

stress; $\bar{B}$ is often referred to as the Skempton's B-bar coefficient (Skempton 1954) and is also known as tidal efficiency or loading efficiency defined as the ratio of the pore-pressure response to the applied load (Skempton 1954; Jacob 1940; van der Kamp and Gale 1983).

Equation [B2] is used to evaluate the barometric response of the piezometer which shows up as "noise" (fluctuations) in the data. In order to correct the "noisy" piezometric data, barometric responses (Equations [B2]) are (reversed) eliminated from the piezometric data by simple mathematical subtraction from the observed pore-pressure change corrected for earth tide, u_e. Consequently, the pore-pressure change of the pressure transducer in the sealed-in aquitard-piezometer corrected for (earth tide and) barometric response, u, (e.g. Barr et al. 2000) is:

$$u = u_e - \bar{B} dP_a \qquad [B3]$$

For consistency with the incremental (change) formulation, all raw piezometric and barometric data are processed to obtain only change rather than absolute measurements by deducting their respective average values for the periods of interest (as reference). The barometric corrections for various periods, across seasons, in different years are presented in Figure B2. The pore-pressure changes corrected for barometric and earth tide effects still show some residual "noisy" spikes for April to June and July to September (i.e. plot (iii) in Figures B2 (a) and (b) respectively) which can be attributed to loading associated with changes of total soil moisture (site water balance), particularly due to precipitation events. Therefore, in the barometric correction of pore-pressure changes by varying the Skempton's $\bar{B}$, precaution was taken to avoid "forcing" the smoothening to eliminate the existing spikes due to soil moisture changes. Therefore visual inspection was adopted in achieving "good-fit" corrected pore-pressure changes rather than statistically (minimal root mean squared error (RMSE)) fitting the corrected pore-pressure change to an arbitrary zero pressure change line (on Figure B2).

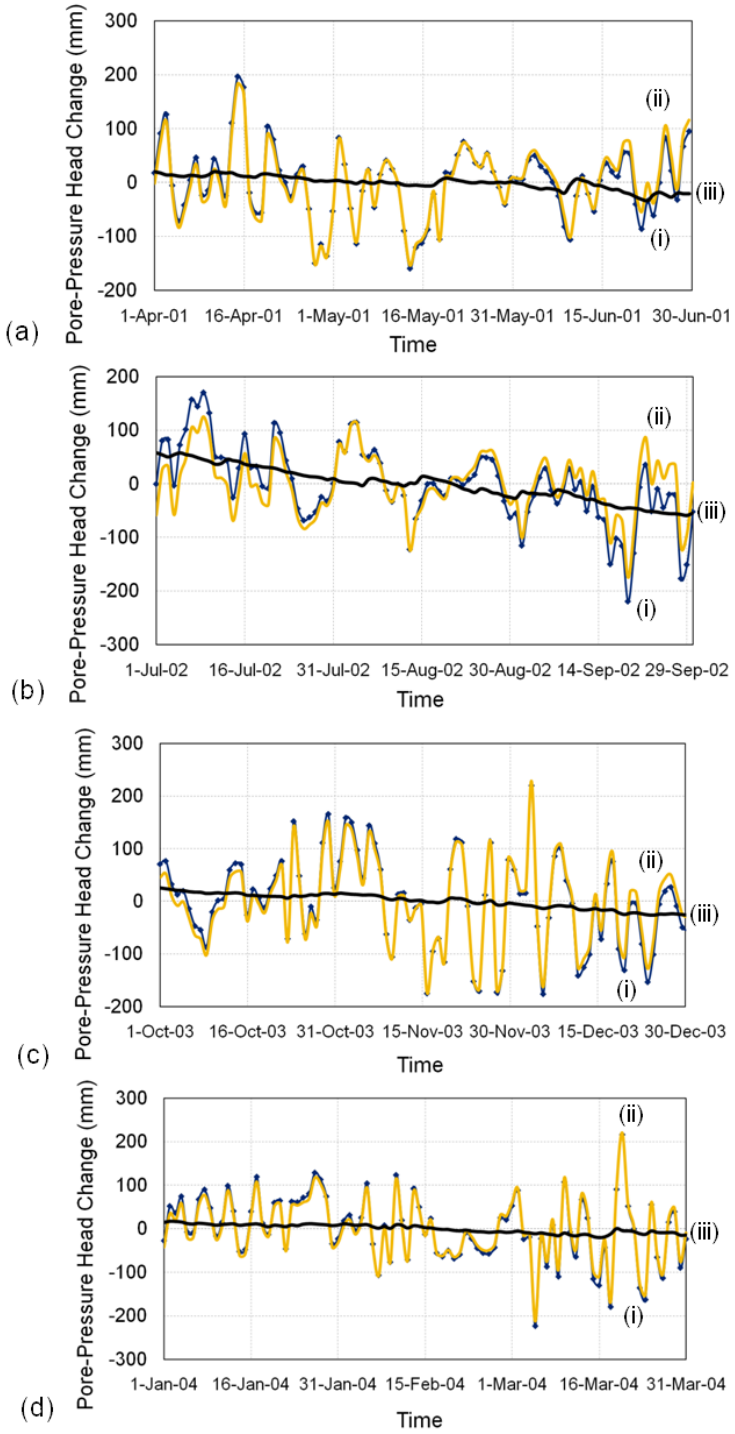

Figure B2. Barometric effects and corrections on pore-pressure head changes from which Skempton's $\bar{B}$ of 0.91 was determined (at depth of 34.6m for Old Aspen Site) for 4 different quarters (a) April-June 2001; (b) July – Sept 2002; (c) Oct-Dec 2003; and (d) Jan-Mar 2004 showing for each: (i) Observed pore-pressure head changes corrected only for earth tide; (ii) Measured barometric pressure head change x 0.91; and (iii) Pore-pressure head changes corrected for earth tide minus measured barometric pressure head change x 0.91 [i.e. (i) – (ii)]

B1.1.1 Recommendation on Refinement of Barometric Correction

In cases where precipitation and evapotranspiration (P and AET) data for soil moisture changes are available, it is being recommended that the effect of soil moisture changes be eliminated from the pore-pressure change data prior to the barometric correction. This could be achieved through the use of numerical modelling of soil moisture, and possibly transients from water table fluctuation, as discussed in this research. This may sound paradoxical since the barometric correction is first required to obtain the input elastic parameters for any modelling. The suggested workable approach would be iterative. That is, the effect of soil moisture, and possibly transients from water table fluctuation, would be modelled using input elastic parameters obtained from the "conventional" barometric correction as initial trials with reasonable hydraulic conductivity and eliminated from pore-pressure change data.

Subsequently, the barometric correction should be carried out on pore-pressure change data corrected for effects of both earth tide and soil moisture changes (and possibly transients from water table fluctuation) to obtain smooth "spike" free (and level) corrected pore-pressure changes. Indeed, the ultimate test of the precision of the elastic parameters (Skempton's $\bar{B}$ and drained Young's Modulus, E, or drained constrained compressibility, m_v) obtained from the barometric correction would be the successful numerical simulation of the undrained barometric response of the pore-pressure (dP_a x $\bar{B}$) in the "semi-confined" glacial till aquitard.

B1.2 Earth-Tide-Correction Relative to Barometric Correction

Prior to the barometric correction, aquitard pore-pressure responses to earth tide dilation (van der Kamp and Gale 1983; Bredehoeft 1967; Jacob 1940) are identified and

corrected using TSOFT[8] software. Cyclic (van der Kamp and Gale 1983) residual "noise" observed in pore-pressure data after preliminary barometric corrections would suggest response to earth tide, if pore-pressure data and timing are free from other cyclic loading sources. Where earth tides are identified, they are corrected in the pore-pressure data followed by the barometric correction; otherwise, only barometric correction would apply. Earth tides in pore-pressure of confined aquifers are usually as small as 10mm to 20mm in magnitude (Bredehoeft 1967) (e.g. crest-to-crest amplitudes of up to about 13mm (Schulze et al. 2000) and even less than 4mm identified in Old Aspen forest Site).

Conversely, high magnitudes (crest-to-crest amplitudes) of barometric responses of pore-pressure have been observed to be over 300mm in a 4km-deep formation (Schulze et al. 2000) and up to approximately 500mm for 34.6m deep aquitard in Old Aspen Forest Site in the 9 year-observation period used in this research. This implies, in the case of Old Aspen site, that the earth tides in the pore-pressures are less than 1% of the barometric response of the same pore-pressure, in total amplitude. Since the magnitude (amplitude) of the earth tide responses is so small relative to that of barometric responses of pore-pressure, in such a case, the earth tide correction prior to barometric correction could even be omitted, if high resolution of pore-pressure is not critical in the analysis.

B1.3 Derivation of Elastic Parameters from Barometric Correction

Elastic properties determined by correction of barometric response is applicable to the case of confined formations (e.g. aquitard in Figure B1) where the elastic parameter of the formation gets involved in defining the barometric response (e.g. Equation [B1] and [B3]). The barometric correction and the determination of the constrained elastic pore-

[8] TSOFT is a software package for the analysis of time series and earth tide. [Accessed online in 2008 and 2009 at: http://seismologie.oma.be/TSOFT/tsoft.html]

pressure coefficient (Skempton $\bar{B}$) were achieved simultaneously through varying $\bar{B}$ by trial-and-error (Equations [B3]) to smoothen the "noisy" plot of pore-pressure changes.

Key elastic parameters required for geotechnical modelling were then derived from the measured Skempton $\bar{B}$ coefficient. First, using the relationship between the constrained elastic pore-pressure coefficient (Skempton's $\bar{B}$), modulus of elasticity of water, E_w, porosity, n, and the drained constrained elastic modulus of soil structure, E_c, (van der Kamp and Gale 1983):

$$\bar{B} = \frac{1/E_c}{1/E_c + n/E_w} \quad [B4]$$

the drained, constrained elastic modulus of soil structure, E_c, was then obtained:

$$E_c = \frac{E_w - \bar{B}E_w}{\bar{B}n} \quad [B5]$$

where n is the porosity of the formation; $1/E_c$ is the drained constrained compressibility of the soil structure, m_v; and E_w is the elastic modulus of water, such that $1/E_w$ is the compressibility of water taken as 4.8×10^{-7} kPa^{-1} at the temperature of 25°C (Domenico and Schwartz 1998). The porosity was assumed to be 0.26 in this study with reference to a range of reported n values for similar tills of 0.26 – 0.36 in Saskatchewan (Keller et al. 1986, 1988).

Elastic storage (specific storage) of laterally constrained soil, S_s, was then obtained using the drained constrained elastic modulus of soil structure, E_c, the compressibility of water, $1/E_w$ and porosity (Jacob 1940):

$$S_s = \rho_w g\left(\frac{1}{E_c} + \frac{n}{E_w}\right) \quad [B6]$$

The drained elastic Young's modulus, E, used as input in the numerical model was established from the relationship with the drained constrained elastic modulus, E_c, and drained Poisson's ratio, ν (Poulos and Davis 1974; van der Kamp and Gale 1983):

$$E = \frac{E_c(1+\nu)(1-2\upsilon)}{(1-\nu)} \qquad [B7]$$

which becomes:

$$E = \frac{2}{3}E_c \qquad [B8]$$

if v is assumed to be 1/3 (i.e. E becomes $0.67E_c$).

Reference (for Appendix B)

Barr, A., van der Kamp, G., Schmidt, R., and Black, T.A. 2000. Monitoring the moisture balance of a boreal aspen forest using a deep groundwater piezometer. *Agricultural and Forest Meteorology*, 102(1): 13-24.

Bear, J. 1972. *Dynamics of fluids in porous media*. Courier Dover publication, New York. (Googlebook accessed in 2009: http://books.google.com/books?id=lurrmlFGhTEC&pg=PA211&dq=barometric+efficiency+%2BBear&ei=ZiuUR63VD4qqswPj19RJ&sig=c-JVdu3BVB4-0gMg1BzDhLopqtY#PPA211,M1)

Bredehoeft, J.D. 1967. Response of well-aquifer systems to earth tides. *Journal of Geophysical Research*, 72(12): 3075 – 3087.

Hamilton, K., Ryan, S.C., and Ohfuchi, W. 2008. Topographic effects on the solar semidiurnal surface tide simulated in a very fine resolution general circulation model. Journal of Geophysical Research. D117114. [Accessed in 2009 at: http://www.agu.org/journals/jd/jd0817/2008JD010115/]

Ivanov, V.V. 2007. Seasonal and diurnal variation in atmospheric pressure. *Izvestiya Atmospheric and Oceanic Physics*, 43(3), 358 – 372.

Jacob, C. 1940. On the flow of water in an artesian aquifer. *Transactions- American Geophysical, Union*, 21, 574 – 586.

Klohn, E.J. 1965. The elastic properties of a dense glacial till deposit, *Canadian Geotechnical Journal*, 11 (2): 116 – 128.

Poulos, H.G., and Davis, E.H. 1974. *Elastic solutions for soil and rock mechanics.* John Wiley & Sons, New York, NY, USA.

Rabbel, W., and Zachau, Z. 1985. Static deformation and gravity changes at the Earth's surface due to atmospheric loading. *Journal of Geophysics*, 56, 81-99. [As cited in Rojstaczer, S., and Agnew, D.C. 1989. The influence of formation properties on the response of water level in wells to earth tides and atmospheric loading. *Journal of Geophysical Research*, 94, 12403 – 12411.]

Radhakrishna, H.S. and Klym, T.W. 1974. Geotechnical properties of very dense glacial till. *Canadian Geotechnical Journal*, 11, 396 – 408.

Rojstaczer, S., and Agnew, D.C. 1989. The influence of formation properties on the response of water level in wells to earth tides and atmospheric loading. *Journal of Geophysical Research*, 94, 12403 – 12411.

Schulze, K.C., Kümpel, H.-J., and Huenges, E. 2000. In situ petrohydraulic parameters from tidal and barometric analysis of fluid level variations in deep wells: some results from KTB. Stober, I. and Bucher, K. (eds.) *Hydrogeology of Crystalline Rocks*, 79-104.

Skempton, A. 1954. The pore-pressure coefficients A and B. *Géotechnique*, 4, 143-147.

Terzaghi, K. 1923. Die Berechnung des Durchlassigkeitsziffer des tones aus dem verlauf der hydrodynamiischen spannungserscheinungen, Sitz. Akad. Wiss. Wein, Abt. IIa, 132, 125-138. [English translation by Clayton et al, 1995**:** A method of calculating the coefficient of permeability of clay from the variation of hydrodynamic stress with time**.** As cited in Clayton, C.R.I., Steinhagen, H.M., and Powrie, W. 1995. Terzaghi's theory of consolidation, and the discovery of effective stress. Proceedings of the Institution of Civil Engineers. Geotechnical engineering, 113(4), 191-205.]

Tuinzaad, H. 1954. Influence of atmospheric pressure on the head of artesian water and phreatic water. *International Symposium of Hydrologists, Rome*, 32-37.

van der Kamp, G., and Gale, J.E. 1983. Theory of Earth tide and barometric effects in porous formations with compressible grains. *Water Resources Research*, 19(2): 538–544.

van der Kamp, G. 2001. Methods for determining the in situ hydraulic conductivity of shallow aquitards – an overview. *Hydrogeology Journal*, 9: 5-16.

APPENDIX C

C1. Skempton's $\bar{B}$, Compressibility and Porosity Relationship of Soil Formation

In general, the pore-pressure coefficients (unconstrained Skempton's B coefficient and, by direct inference, the constrained Skempton's $\bar{B}$ coefficient) are sensitive to the degree of saturation (Skempton 1954; Black and Lee 1973), the compressibility of soil structure relative to the compressibility of pore fluid (Bishop 1973; Terzaghi et al. 1996) and the porosity of soil (Bishop 1973; Skempton 1954). The elastic pore-pressure coefficient appears to be highly sensitive to the first factor, the degree of saturation, particularly in stiff soil. For instance, Black and Lee (1973) illustrated that very stiff soil (of B coefficient of about 0.91 at full saturation) experienced a wide drop of about 80% in the value of B coefficient (from 0.91 to 0.2) for just less than 0.5% de-saturation (>99.5% saturation). Wet soil formations located at substantial depth (tens of metres) below the water table aquifer remote from the amplitude of water table fluctuation can be assumed fully saturated as in the case of the aquitard in the Old Aspen forest. Consequently, the relationship of Skempton's $\bar{B}$ pore-pressure coefficient with the remaining two factors, relative compressibility of the soil structure and porosity, were treated as the case of a fully saturated soil assumed for the semi-confined glacial till aquitard in the Old Aspen Forest problem.

The relationship between Skempton's $\bar{B}$ (B-bar) coefficient and constrained soil structure compressibility for soil types of various porosities are shown in Figure C1.

.

A similar plot was shown by Bishop (1973) but for Skempton's B coefficient (the unconstrained condition). Reported porosity range of 0.26 to 0.36 for glacial till in Saskatchewan (Keller et al. 1986; 1988) is represented in the figure. The plots were generated using the expression of Skempon's $\bar{B}$ (Skempton 1954) as presented by van der Kamp and Gale (1983) in Equation [B4] as the term loading efficiency, which is also referred to as tidal efficiency expressed by Jacob (1940).

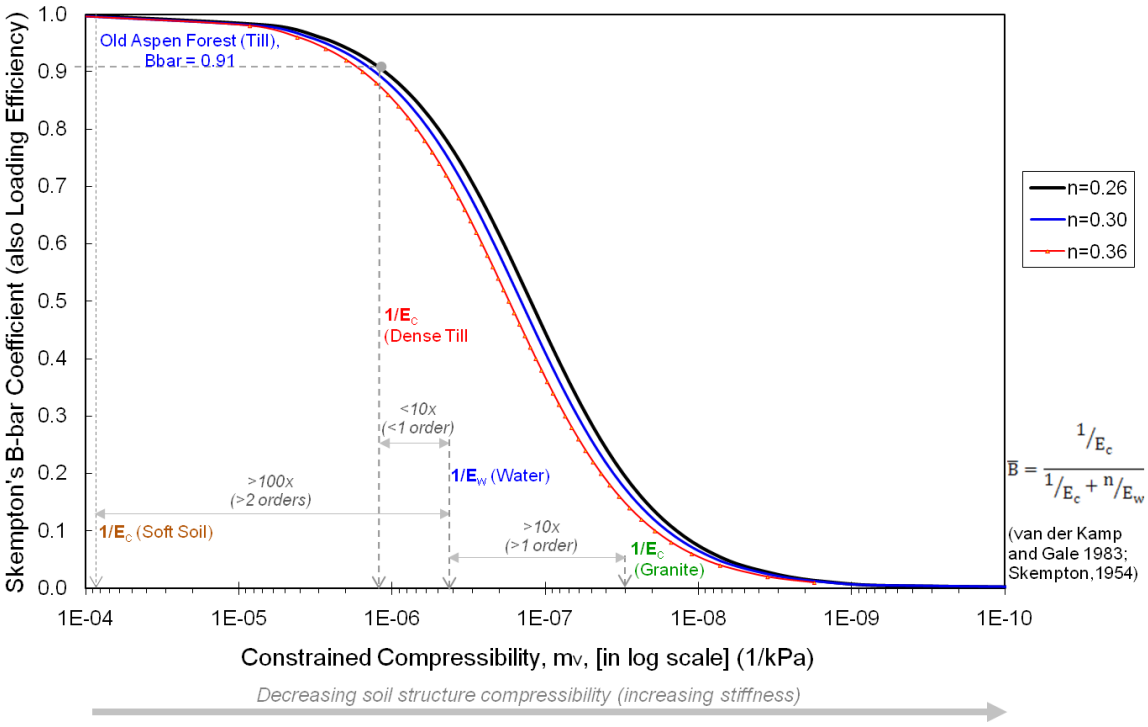

Figure C1. Skempton's $\bar{B}$ (B-bar) coefficient and drained constrained compressibility for soil of porosity values of 0.26, 0.3 and 0.36 showing compressibility values for overconsolidated glacial till at Old Aspen forest site, soft soil and granite (rock) relative to the compressibility of water

The seemingly convergent trend of the three plots (Figure C1) for the highly compressible soil (compressibility range greater than 1 x 10^{-5} kPa^{-1} or Skempton's $\bar{B}$ of over 0.99) suggests that soft soil types are not as sensitive to porosity (range of 0.26 to 0.36) as the stiffer soil types. The sensitivity of such stiff formations to porosity, however, drops in cases of highly stiff geological formations, which are significantly

stiffer than water, as can be observed for the convergent trend at such a range of low compressibility (Skempton's $\bar{B}$ of less than 0.1) on Figure C1.

The glacial till in Old Aspen Forest site with Skempton's $\bar{B}$ of 0.91 (between the two extreme "convergent zones") cuts across the soil formation types, for compressibility range, sensitive to porosity values though not significantly sensitive (Figure C1). Since the exact porosity was not measured, any reasonable value of porosity, within the given range, still satisfies the model calibration to transient pore-pressure observation as long as the arising combination of specific storage and hydraulic conductivity (diffusivity) simulates the consolidation time (rate). Porosity of 0.26 which falls within the reported range was adopted for the entire numerical modelling.

Reference (for Appendix C)

Bishop, A.W. 1973. Influence of an undrained change in stress on the pore pressure in porous media of low compressibility. *Geotechnique*, 23 (3), 435 – 442.

Black, D.K., and Lee, L.L. 1973. Saturated laboratory samples by back pressure. *Journal of the Soil Mechanics and Foundation Division*, ASCE(SM1): 75-93. [As cited in Eigenbrod, K., and Wurmnest, W.H. 1991. Effective stress paths and pore-pressure responses during undrained shear along the bedding planes of varved Fort William clay. *Canadian Geotechnical Journal*, 28(6), 804-811.]

Jacob, C. 1940. On the flow of water in an artesian aquifer, *Transactions- American Geophysical, Union*, 21, 574 – 586.

Keller, C.K, van der Kamp, G. and Cherry, J.A. 1986. Fracture permeability and groundwater flow in a clayey till near Saskatoon, Saskatchewan. *Canadian Geotechnical Journal*, 23: 229-240.

Keller, C.K., van der Kamp, G. and Cherry, J.A. 1988. Hydrogeology of two Saskatchewan till, I fractures, bulk permeability, and spatial variability of downward flow. *Journal of Hydrogeology*, 101, 97-121.

Skempton, A. 1954. The pore-pressure coefficients A and B, *Géotechnique,* 4, 143-147.

Terzaghi, K., Peck, R. B., and Mesri, G. 1996. *Soil mechanics in engineering practice (third edition),* John Wiley and Sons, New York. NY, USA.

van der Kamp, G. and Gale, J.E. 1983. Theory of Earth tide and barometric effects in porous formations with compressible grains, *Water Resources Research,* 19(2): 538–544.